

On the Fusion Algebras of Bimodules Arising from Goodman-de la Harpe-Jones Subfactors

By Satoshi GOTO

Abstract. By using Ocneanu’s result on the classification of all irreducible connections on the Dynkin diagrams, we show that the dual principal graphs as well as the fusion rules of bimodules arising from any Goodman-de la Harpe-Jones subfactors are obtained by a purely combinatorial method. In particular we obtain the dual principal graph and the fusion rule of bimodules arising from the Goodman-de la Harpe-Jones subfactor corresponding to the Dynkin diagram E_8 . As an application, we also show some subequivalence among A - D - E paragroups.

1. Introduction

Since V. F. R. Jones initiated the index theory for subfactors in [15], intensive studies on the classification of subfactors have been made by many people. The classification of subfactors of the AFD type II_1 factor with index less than 4 has been completed by many people’s contribution ([2, 13, 14, 15, 16, 21], see also [9]) after A. Ocneanu’s announcement [18].

Goodman-de la Harpe-Jones subfactors (abbreviated as GHJ subfactors) [11] are known as a series of interesting non-trivial examples of irreducible subfactors with indices greater than 4, though some of them have indices less than 4. The indices of all GHJ subfactors are given in [11]. They are constructed from the commuting squares arising from the embeddings of type A string algebras into other string algebras of type ADE . (See [9, Chapter 11] for the construction of GHJ subfactors from a viewpoint of string algebra embedding.) The principal graphs of these subfactors are easily obtained by a simple method but the dual principal graphs as well as their fusion rules are much more difficult to compute. (Okamoto first computed their principal graphs in [20].)

One of the most important examples of GHJ subfactor has index $3 + \sqrt{3}$ and it is constructed from the embedding of the string algebra of A_{11} into

that of E_6 . In this particular case it happens that it is not very difficult to compute the dual principal graph (see [17], [9, Section 11.6]). But it is more difficult to determine its fusion rules. Actually D. Bisch has tried to compute the fusion rule just from the graph but there were five possibilities and it turned out that the fusion rule cannot be determined from the graph only [3]. Some more information is needed and Y. Kawahigashi obtained the fusion rule as an application of paragroup actions in [17].

In his lectures at The Fields Institute A. Ocneanu introduced a new algebra called *double triangle algebra* by using the notion of essential paths and extension of Temperley-Lieb recoupling theory of Kauffman-Lins [19]. He also announced a solution to the problem of determining the dual principal graphs and their fusion rules of the GHJ subfactors as one of some applications of his theory. But the details have not been published.

After A. Ocneanu's works, F. Xu and J. Böckenhauer-D. E. Evans have revealed a relation between the GHJ subfactors and conformal inclusions ([22], [5], [6], [7]) and J. Böckenhauer, D. E. Evans and Y. Kawahigashi ([8]) obtained essentially the same fusion algebras of GHJ subfactors of type D_{2n}, E_6, E_8 by using conformal field theory and the Cappelli-Itzykson-Zuber's classification of modular invariant [10].

In this paper we give detailed computations of the dual principal graphs and the fusion rules for any GHJ subfactors by a purely combinatorial method. For this purpose we will make the most use of Ocneanu's result on the classification of all irreducible connections on the Dynkin diagrams (See [19]. Our method here is based on the observation in [12]). Especially we will make use of Figures 21~36, which were first found by A. Ocneanu [19]. Our result does not rely on either conformal field theory or the classification of modular invariant.

2. Correspondence between System of Connections and System of Bimodules

Let K and L be two connected finite bipartite graphs. A bi-unitary connection on four graphs is called a K - L *bi-unitary connection* if it has the graph K as an upper horizontal graph and the graph L as a lower horizontal graph as in Figure 1.

If we have a K - L connection, we can construct a subfactor $N \subset M$ by choosing a distinguished vertex $*_K$ of the upper graph K and applying

string algebra construction to the connection. (See [9, Section 11].) This construction seems to depend on the choice of the vertex $*_K$. But it is well-known that the subfactors constructed from this connection does not depend on the choice of the vertex $*_K$, that is, they become all isomorphic because of the relative McDuff property [4].

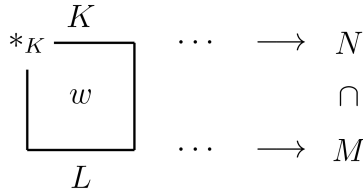


Figure 1.

On the one hand as a paragroup of the subfactor $N \subset M$ obtained from the connection w as above, we obtain the system of 4-kinds of bimodules, i.e. N - N , N - M , M - N , M - M bimodules, by taking irreducible decomposition of alternating relative tensor products of ${}_N M_M$ and its conjugate bimodule ${}_M M_N$ as usual. (See [9] for details.)

On the other hand we also get the system of 4-kinds of connections, i.e. K - K , K - L , L - K , L - L bi-unitary connections, by taking irreducible decomposition of alternating compositions of the connection w and its conjugate L - K connection \bar{w} .

Now the problem is the relation between the system of bimodules and the system of connections obtained as above. We can easily see that those two systems become the same paragroup for $N \subset M$ if the subfactor $N \subset M$ has finite depth.

To see this it is enough to see the relation among a usual paragroup based on bimodules, a system of generalized open string bimodules and a system of bi-unitary connections. The details of these relations are found in [1]. Note that when we consider a system of bi-unitary connections forms a paragroup, we need the notion of intertwiners between two connections. For this purpose, we need to fix distinguished vertices $*_K$ and $*_L$ of both even and odd part of the graphs K and L , then we identify all the bi-unitary connections of the system as the generalized open string bimodules constructed from those connections. Then we define the intertwiners between two connections by those between the corresponding two generalized open

string bimodules. Now from the argument in [1], the intertwiners between two connections can naturally be identified with the intertwiners between the corresponding 4 kinds of bimodules, i.e. N - N , N - M , M - N , M - M bimodules arising from the usual paragrroup. See Theorem 4 in [1] for more details.

Hence we obtain the following theorem.

THEOREM 2.1. *If the subfactor $N \subset M$ constructed from a K - L connection ${}_K w_L$ has finite depth, the system of 4-kinds of connections obtained from ${}_K w_L$ and the system of 4-kinds of bimodules obtained from the subfactor $N \subset M$ have the same fusion rules. Moreover these two systems defines the same paragrroup for $N \subset M$ via the correspondence between connections and generalized open string bimodules.*

REMARK 2.2. As we mentioned above, the subfactor constructed from a connection ${}_K w_L$ does not depend on the choice of the distinguished vertex $*_K$. In the same way we need to fix two vertices $*_K$ and $*_L$ in order to construct a generalized open string bimodule from a connection. But the above theorem holds true for arbitrary choice of two distinguished vertices $*_K$ and $*_L$ of the graphs K and L respectively.

The above theorem provide us a purely combinatorial method to compute fusion rules for the subfactor obtained from a connection ${}_K w_L$. Actually we can compute the fusion rules of a system of connections by looking at the composition and decomposition of their vertical graphs.

3. The (Dual) Principal Graphs and Their Fusion Rules of the Goodman-de la Harpe-Jones Subfactor

Let A be the Dynkin diagram A_n and K one of the ADE Dynkin diagrams with the same Coxeter number. The subfactors constructed from the commuting square as in Figure 2 are called the Goodman-de la Harpe-Jones subfactors (abbreviated as GHJ subfactors). Here the construction depends only on the graph K and the vertex $*_K = x$. (See [11] for details.) We denote this subfactor $\text{GHJ}(K, *_K = x)$. We remark that the vertical graphs G and G' as in Figure 2 are easily obtained from the dimension of essential paths on the graph K (Figures 21~30). Here we note that the graphs G and G' may be disconnected.

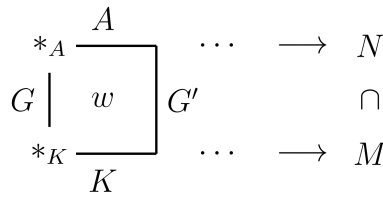


Figure 2.

We use the next two propositions to compute the fusion rule of the Goodman-de la Harpe-Jones subfactors.

PROPOSITION 3.1 ([12, Proposition 5.6]). *Let A, K, G and G' be the four graphs connected as in Figure 3. Suppose there is a bi-unitary connection on the four graphs. Then the connecting vertical graphs G and G' are uniquely determined by the initial condition, i.e., the condition of edges connected to the distinguished vertex of the graph A (see Figure 4). Moreover such a connection is unique up to vertical gauge choice.*

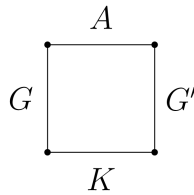


Figure 3.

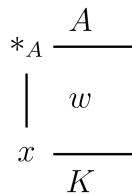


Figure 4.

PROPOSITION 3.2 (**Frobenius reciprocity**) ([12, Proposition 3.21]).
 Let K, L and M be three connected finite bipartite graphs with the same Perron-Frobenius eigenvalue. Let ${}_K\alpha_L, {}_L\beta_M$ and ${}_K\gamma_M$ be three irreducible bi-unitary connections which are K - L , L - M and K - M respectively. If γ appears n times in the composite connection $\alpha\beta$, then α appears n times in $\gamma\beta$ and β appears n times in $\bar{\alpha}\gamma$.

3.1. The fusion rules of four kinds of connections arising from GHJ subfactors

The system of connections arising from a GHJ subfactor consists of four kinds of connections, i.e. A - A , A - K , K - A and K - K connections. So the fusion rules consist of the following 8 kinds of multiplication table.

- (1) A - $A \times A$ - $A \longrightarrow A$ - A
- (2) A - $A \times A$ - $K \longrightarrow A$ - K
- (2)' K - $A \times A$ - $A \longrightarrow K$ - A (2)'' A - $K \times K$ - $A \longrightarrow A$ - A
- (3) A - $K \times K$ - $K \longrightarrow A$ - K
- (3)' K - $K \times K$ - $A \longrightarrow K$ - A (3)'' K - $A \times A$ - $K \longrightarrow K$ - K
- (4) K - $K \times K$ - $K \longrightarrow K$ - K

Among these multiplication tables, (2)' and (3)' are obtained by taking conjugation of (2) and (3) respectively. The tables (2)'' and (3)'' are also obtained from (2) and (3) respectively by Frobenius reciprocity. So it is enough to determine four multiplication table (1), (2), (3) and (4).

3.1.1 *The fusion rules of (1) A - $A \times A$ - $A \longrightarrow A$ - A and (2) A - $A \times A$ - $K \longrightarrow A$ - K and the principal graphs*

We put the labels $0, 1, 2, \dots, m - 1$ of vertices of the Dynkin diagram A_m as in Figure 5. We denote the unique irreducible A - A connection with the “initial edge” connected to the vertex n in the lower graph A_m by A^n_A (Figure 6). We also denote the unique irreducible A - K connection with

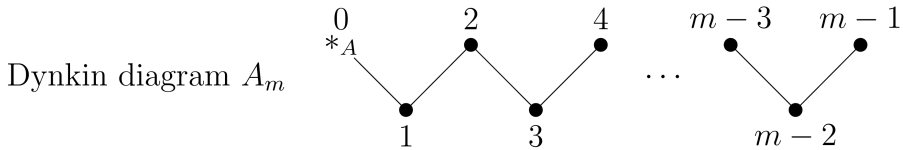


Figure 5. The label of vertices of the Dynkin diagram A_m .

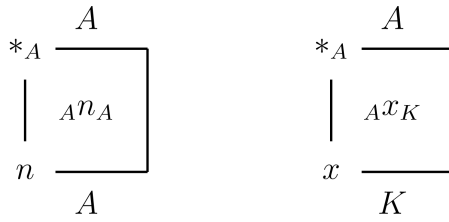


Figure 6.

the “initial edge” connected to the vertex x in the lower graph K by Ax_K (Figure 6).

Then the fusion rules of (1) $A-A \times A-A \rightarrow A-A$ and (2) $A-A \times A-K \rightarrow A-K$ can be obtained by composition and decomposition of the (left) vertical edges of the two connections An_A and Ax_K as in Figure 7. So we have only to count the vertical edges of the connection Ax_K in order to determine the fusion tables of (1) and (2).

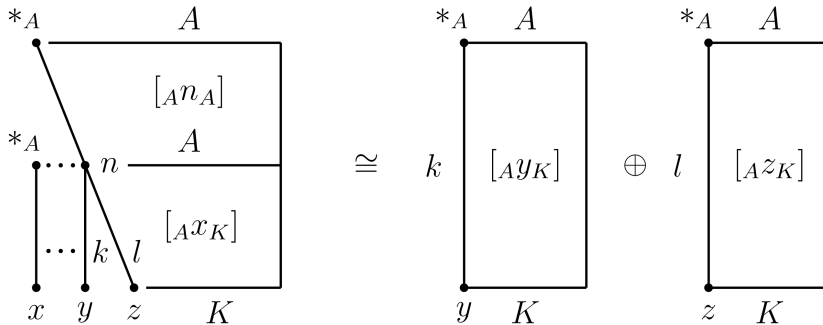


Figure 7. The fusion rule of $A-A \times A-K \rightarrow A-K$.

Because we need the notion of essential paths on graphs in order to describe these fusion rules, we review the definition here for readers convenience. Please see [19, section 32.2, page 254–256] for more details and the proof of the moderated Pascal rule.

DEFINITION 3.3. A space of essential paths of a graph G with length n is defined by $\text{EssPath}^{(n)}G = p_n \cdot \text{HPath}^{(n)}G$. Here $p_n = 1 - e_1 \vee e_2 \vee \dots \vee e_{n-1}$ is the Wenzl projector and e_k is the k -th Jones projection. We denote the

space of essential paths of a graph G with length n , with starting point x and end point y by $\text{EssPath}_{x,y}^{(n)}G$.

The dimensions of spaces of essential paths of length n is easily obtained by using the following *moderated Pascal rule*.

$$\begin{aligned} \dim \text{EssPath}_{a,x}^{(n+1)}G &= \sum_{\xi \in \text{Edge } G, r(\xi)=x} \dim \text{EssPath}_{a,s(\xi)}^{(n)}G \\ &\quad - \dim \text{EssPath}_{a,x}^{(n-1)}G \end{aligned}$$

Now we continue the description of the fusion rules (1) and (2). Because the connection ${}_A x_K$ comes from the inclusion of the string algebras $\text{String}_* A \subset \text{String}_x K$, the number of vertical edges of this inclusion coincides with the dimension of essential paths from the vertex x to y of K with length n . (See Figures 21~30 for the dimension of essential paths.) Hence we get the fusion tables of (1) and (2) as follows.

$$\begin{aligned} {}_A n_A \cdot {}_A x_K &\cong \bigoplus_{y \in \text{Vert } K} (\dim \text{EssPath}_{x,y}^{(n)}K) {}_A y_K \\ K \bar{x}_A \cdot {}_A n_A &\cong \bigoplus_{y \in \text{Vert } K} (\dim \text{EssPath}_{x,y}^{(n)}K) K \bar{y}_A \\ {}_A y_K \cdot K \bar{x}_A &\cong \bigoplus_{n \in \text{Vert } A} (\dim \text{EssPath}_{x,y}^{(n)}K) {}_A n_A \end{aligned}$$

Since the principal graph is obtained from the fusion rule of $A-A \times A-K \longrightarrow A-K$, we can easily see that the principal graph of $\text{GHJ}(K, *_K = x)$ coincides with the connected component of the vertical edges of the connection ${}_A x_K$ including the distinguished vertex $*_A$. This principal graph can be obtained easily by counting the dimension of essential path. It follows from this fact that the even vertices of the the principal graph of $\text{GHJ}(K, *_K = x)$ coincides with (possibly a subset of) the even vertices of the Dynkin diagram A_m .

3.1.2 *The fusion rules of (3) $A-K \times K-K \longrightarrow A-K$ and the dual principal graphs*

We denote the unique irreducible $A-K$ connection with the “initial edge” connected to the vertex x in the lower graph K by ${}_A x_K$ as before and an irreducible $K-K$ connection by ${}_K w_i K$ (Figure 8). Here ${}_K w_i K$ is one of the

connections of all K - K connection system (Figures 31~36). (See [12, section 5.3, pages 244–252] for details.) In this case the fusion rule of (3) A - $K \times K$ - $K \rightarrow A$ - K is also obtained by composition and decomposition of the (left) vertical edges of the two connections Ax_K and Kw_iK as in Figure 9. We can get the fusion table of (3) by counting the vertical edges of the connection Kw_iK in the same way as subsection 3.1.1.

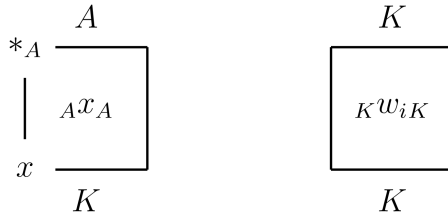


Figure 8.

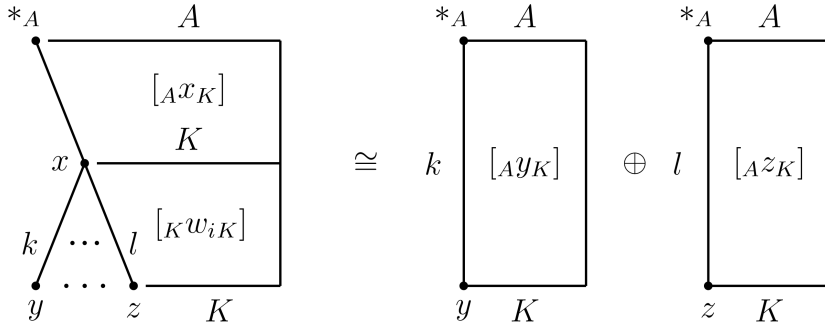


Figure 9. The fusion rule of A - $K \times K$ - $K \rightarrow A$ - K .

This time the method of counting dimensions of essential paths does not work in order to get the vertical edges of the connection Kw_iK . But we can compute them by using Ocneanu’s classification of all irreducible K - K connections and their fusion rules ([12, section 5.3, pages 244–252]).

For example, the vertical edges of all K - K connections are given in Figures 37~47 in the case of $K = A_3, A_4, A_5, A_6, D_4, D_5, D_6, E_6, E_7, E_8$. Here in the case of E_6, E_7, E_8 , we give list of incidence matrices of vertical graphs instead of graphs themselves because it is complicated to draw them

all.

Now we get the fusion rule of $A\text{-}K \times K\text{-}K \longrightarrow A\text{-}K$ as follows.

$$\begin{aligned} Ax_K \cdot {}_K w_i K &\cong \bigoplus_{y \in \text{Vert} K} n(w_i)_{x,y} Ay_K \\ {}_K w_i K \cdot K \bar{x}_A &\cong \bigoplus_{y \in \text{Vert} K} n(w_i)_{x,y} K \bar{y}_A \\ K \bar{x}_A \cdot Ay_K &\cong \bigoplus_{w_i \in {}_K Z_K} n(w_i)_{x,y} {}_K w_i K \end{aligned}$$

Here ${}_K Z_K$ represents the system of all $K\text{-}K$ connections which is isomorphic to the fusion algebras of the center of $K\text{-}K$ double triangle algebra ([12, Theorem 4.1, Corollary 4.5]). And $n(w_i)_{x,y}$ means the number of vertical edges of the $K\text{-}K$ connection ${}_K w_i K$ connecting the vertices x and y .

Now we can get the dual principal graph from the fusion rule of (3) $A\text{-}K \times K\text{-}K \longrightarrow A\text{-}K$. It is the connected component of the fusion graph of (3) which contains the connection Ax_K .

3.1.3 The fusion rules of (4) $K\text{-}K \times K\text{-}K \longrightarrow K\text{-}K$

This is the fusion rule of the system of all $K\text{-}K$ connections obtained by Ocneanu (Figures 31~36, [12, section 5.3, pages 244–252]). It is isomorphic to the fusion algebras of the center of $K\text{-}K$ double triangle algebra $({}_K Z_K, \cdot)$ with dot product (vertical product) “ \cdot ”. We know that this fusion algebra $({}_K Z_K, \cdot)$ is generated by chiral left part and chiral right part which are isomorphic to the fusion algebra of connections arising from corresponding ADE subfactor and that the chiral left and right part are relatively commutative [12, Theorem 5.16]. So we can compute the fusion rule of $({}_K Z_K, \cdot)$ from the above facts.

We remark that the commutativity of the chiral left and right part is proved at the same time when we draw the diagrams of all $K\text{-}K$ connections (Figures 31~36). The proof is based on coset decomposition, fusion rules of chiral left (right) part and indices of irreducible connections. We refer readers to [12, section 5.3, pages 244–252] for details.

The fusion tables of $({}_K Z_K, \cdot)$, i.e. the system of all $K\text{-}K$ connections for $K = E_6, E_7$ and (a part of) E_8 is given in Figures 48~50. We note that these fusion tables is expressed in product form. For example in the table 49, we can read $(3) \cdot 4 = (1)^2(3)^3(5)$, which means the fusion rule $w_{(3)} \cdot w_4 = 2w_{(1)} + 3w_{(3)} + w_{(5)}$ holds.

3.2. The fusion rules of even vertices of the (dual) principal graphs of $\text{GHJ}(K, *_K = x)$

Let $N \subset M$ be the Goodman-de la Harpe-Jones subfactor $\text{GHJ}(K, *_K = x)$. Here we will compute the fusion rules of even vertices of the (dual) principal graphs of $\text{GHJ}(K, *_K = x)$, that is, the fusion rules of N - N bimodules and M - M bimodules of the subfactor $N \subset M$.

The system of N - N bimodules are isomorphic to the system of A - A connections generated by ${}_A x_K$ and this is the same as ${}_A Z_A^{\text{even}}$, i.e. the fusion algebra of even part of ${}_A Z_A$. So the fusion algebra of N - N bimodules are isomorphic to the fusion algebra A^{even} , i.e. the fusion algebra of even vertices of the Jones' type A subfactor. Hence it turns out that the fusion algebra of N - N bimodules are always commutative for any GHJ subfactors.

The system of M - M bimodules are similarly isomorphic to the system of K - K connections generated by ${}_A x_K$ and this is the same as (a part of) ${}_K Z_K^{\text{even}}$, i.e. the fusion algebra of even part of ${}_K Z_K$. So we have only to compute the fusion rule of ${}_K Z_K^{\text{even}}$.

Here the fusion rule of ${}_K Z_K^{\text{even}}$ and the vertical edges of irreducible K - K connections can be summarized as in the Table 1. As we mentioned above, we can compute the fusion rule of ${}_K Z_K^{\text{even}}$ in detail from the fusion graph of all K - K connections as in Figures 31~36 and 48~50.

In the following table, ε represents the index 1 D_{2n} - D_{2n} connection which corresponds to the flip of two tails of D_{2n} . Because ${}_{D_{2n}} Z_{D_{2n}}$ has coset decomposition $D_{2n} \cup D_{2n} \cdot \varepsilon$ and $\varepsilon^2 = id$ as shown in Figures 32, 41 and 43, we can easily compute the fusion rule for ${}_{D_{2n}} Z_{D_{2n}}$.

Table 1. The fusion rule of ${}_K Z_K^{\text{even}}$ and vertical edges of K - K connections.

Graph K	fusion rule of ${}_K Z_K^{\text{even}}$	vertical edges of K - K connections
A_n	commutative	$\text{EssPath}A_n$ (Figures 37~40)
D_{2n}	non-commutative	$\text{EssPath}D_{2n} + \varepsilon$ (Figures 41 and 43)
D_{2n+1}	commutative	$\text{EssPath}D_{2n+1}$ (Figure 42)
E_6	commutative	Figure 44
E_7	commutative	Figure 45
E_8	commutative	Figures 46, 47

4. The Structure of Goodman-de la Harpe-Jones Subfactors

4.1. Goodman-de la Harpe-Jones subfactors of type A_n

Let $N \subset M$ be the Jones' subfactor of type A_n and $N \subset M \subset M_1 \subset M_2 \subset \dots \subset M_k \subset$ be the Jones tower. We label the vertices of the Dynkin diagram A_n by a_0, a_1, \dots, a_{n-1} as in Figure 10. Then the Goodman-de la Harpe-Jones subfactor $\text{GHJ}(A_n, * = a_m)$ is isomorphic to $pN \subset pM_{m-1}p$, where p is a minimal projection in $\text{Proj}(N' \cap M_{m-1})$ corresponding to the vertex a_m . Hence in this case the principal graph and the dual principal graph coincide and fusion rule of even vertices of both graphs becomes A_n^{even} .

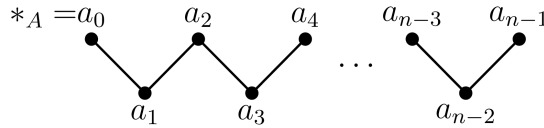


Figure 10. The label of vertices of the Dynkin diagram A_n .

4.2. Goodman-de la Harpe-Jones subfactors of type D_{2n+1}

We label the vertices of the Dynkin diagram D_{2n+1} by $d_0, d_1, d_2, \dots, d_{2n-2}, d_{2n-1}, d'_{2n-1}$ as in Figure 11.

The Goodman-de la Harpe-Jones subfactor $\text{GHJ}(D_{2n+1}, *_K = d_0)$ is isomorphic to the unique index 2 subfactor $N \subset N \rtimes \mathbf{Z}_2$.

If the vertex $*_K \neq d_0, d_{2n-1}, d'_{2n-1}$, $\text{GHJ}(D_{2n+1}, *_K)$ has nontrivial intermediate subfactor as in Figure 12 because we have the decomposition of connections ${}_A d_k D = {}_A d_0 D \cdot {}_D [k] D$ for $k = 1, 2, \dots, 2n - 2$. Here ${}_D [k] D$ is the D_{2n+1} - D_{2n+1} connection corresponding to the vertex $[k]$ as in Figures 33 and 42.

The (dual) principal graphs of $\text{GHJ}(D_{2n+1}, *_K)$ are given in Figures 51~73 for $n = 2, 3, 4, 5$.

The incidence matrices of the (dual) principal graphs of $\text{GHJ}(D_{\text{odd}}, *_K)$ are also given in Figure 102.

4.3. Goodman-de la Harpe-Jones subfactors of type D_{2n}

We label the vertices of the Dynkin diagram D_{2n} by $d_0, d_1, d_2, \dots, d_{2n-3}, d_{2n-2}, d'_{2n-2}$ as in Figure 13.

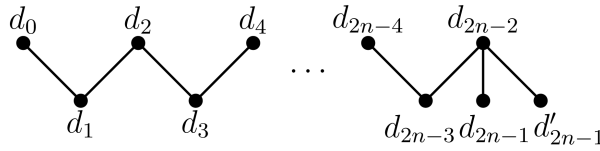


Figure 11. The label of vertices of the Dynkin diagram D_{2n+1} .

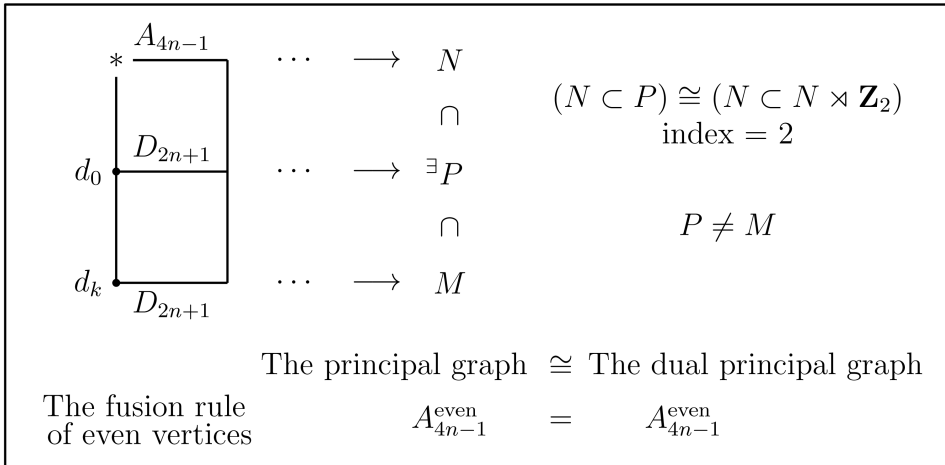


Figure 12.

The Goodman-de la Harpe-Jones subfactor $\text{GHJ}(D_{2n}, *K = d_0)$, $\text{GHJ}(D_4, *K = d_2)$ and $\text{GHJ}(D_4, *K = d'_2)$ are isomorphic to the unique index 2 subfactor $N \subset N \rtimes \mathbf{Z}_2$.

If $n > 2$ and the vertex $*K \neq d_0$, $\text{GHJ}(D_{2n}, *K)$ has nontrivial intermediate subfactor as in Figure 12 because we have the decomposition of connections $A d_k D = A d_0 D \cdot D[k]_D$ for $k \neq 0$. Here $D[k]_D$ is the $D_{2n} - D_{2n}$ connection corresponding to the vertex $[k]$ as in Figures 32 and 43.

The (dual) principal graphs of $\text{GHJ}(D_{2n}, *K)$ are given in Figures 74~101 for $n = 3, 4, 5, 6$.

The incidence matrices of the (dual) principal graphs of $\text{GHJ}(D_{\text{even}}, *K)$ are also given in Figures 103 and 104.

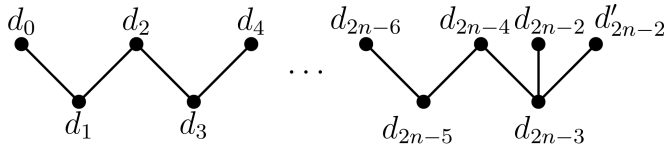


Figure 13. The label of vertices of the Dynkin diagram D_{2n} .

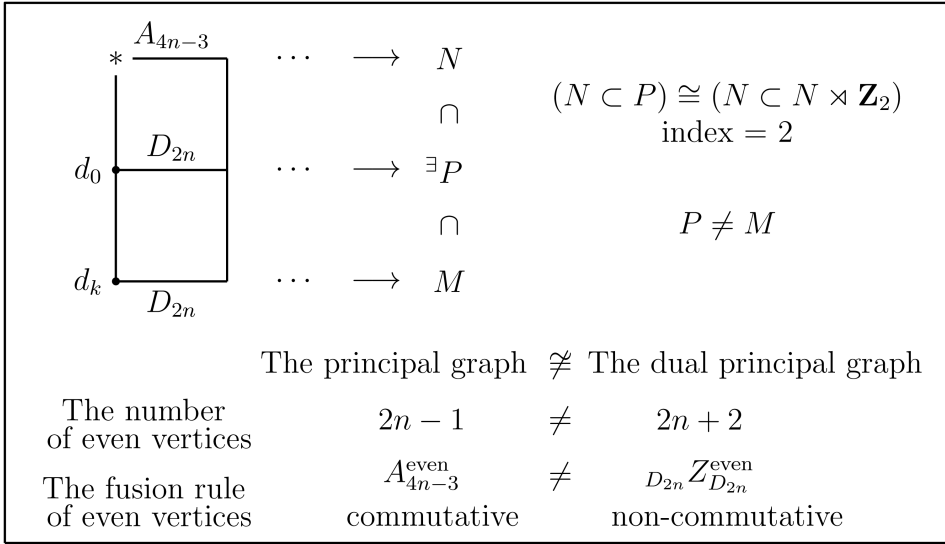


Figure 14.

Example 4.1. From these computations for $\text{GHJ}(D_n, *_K)$ as above, the (dual) principal graphs of $\text{GHJ}(D_n, * = \text{triple point})$ can be obtained for general n as in Figure 105.

4.4. Goodman-de la Harpe-Jones subfactors of type E_6

We label the vertices of the Dynkin diagram E_6 by $e_0, e_1, e_2, \dots, e_5$ as in Figure 15.

The Goodman-de la Harpe-Jones subfactor $\text{GHJ}(E_6, *_K = e_0)$, has index $3 + \sqrt{3}$ and it has the same principal and dual principal graph. But the fusion rules of the two graphs are different. This subfactor is known as the example

which has the smallest index among such subfactors. The (dual) principal graphs of $\text{GHJ}(E_6, *K)$ are given in Figures 106~109.

If the vertex $*K \neq e_0, e_4$, $\text{GHJ}(E_6, *K)$ has nontrivial intermediate subfactor as in Figure 16 because we have the decomposition of connections ${}^A e_k E = {}^A e_0 E \cdot {}_E [w_k]_E$ for $k = 1, 2, 3, 5$. Here ${}_E [w_k]_E$ is the E_6 - E_6 connection corresponding to the vertex $[k]$ as in Figures 34 and 44.

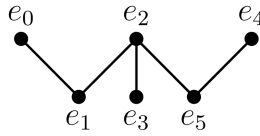


Figure 15. The label of vertices of the Dynkin diagram E_6 .

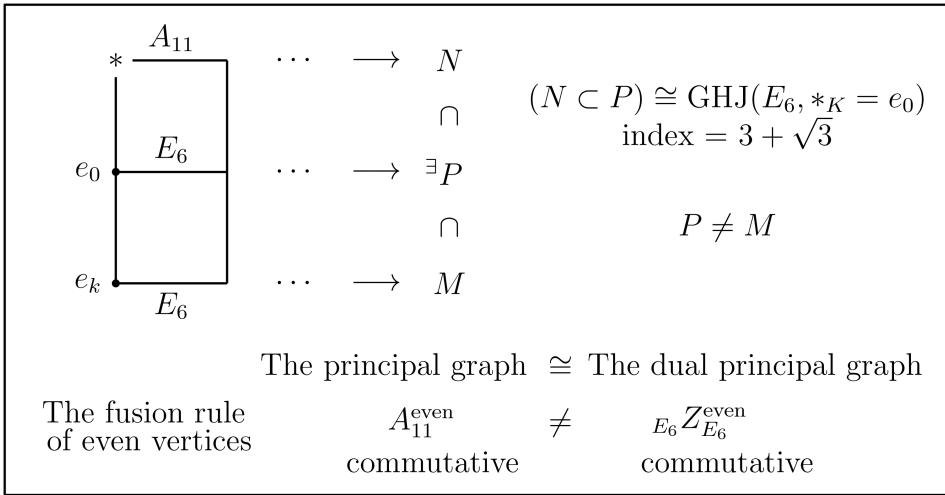


Figure 16.

4.5. Goodman-de la Harpe-Jones subfactors of type E_7

We label the vertices of the Dynkin diagram E_7 by $e_0, e_1, e_2, \dots, e_6$ as in Figure 17.

The Goodman-de la Harpe-Jones subfactor $\text{GHJ}(E_7, *K = e_0)$, has index

$\frac{|A_{17}|}{|E_7|}$ which is approximately 7.759. Here $|A_{17}|$ and $|E_7|$ represents the “total mass” of the graph A_{17} and E_7 respectively, i.e. the sum of squares of normalized Perron-Frobenius eigenvalues over all the vertices of the graph. The (dual) principal graphs of $\text{GHJ}(E_7, *K)$ are given in Figures 110~116.

If the vertex $*K \neq e_0, e_4, e_5$, $\text{GHJ}(E_7, *K)$ has nontrivial intermediate subfactor as in Figure 18 because we have the decomposition of connections $Ae_{kE} = Ae_{0E} \cdot E[w_k]_E$ for $k = 1, 2, 3$ and $Ae_{6E} = Ae_{0E} \cdot E[w_{(5)}]_E$. Here $E[w_k]_E$ is the E_7 - E_7 connection corresponding to the vertex $[k]$ ($k = 1, 2, 3$) and (5) as in Figures 35 and 45.

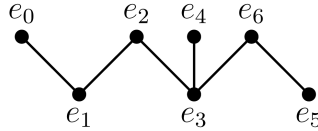


Figure 17. The label of vertices of the Dynkin diagram E_7 .

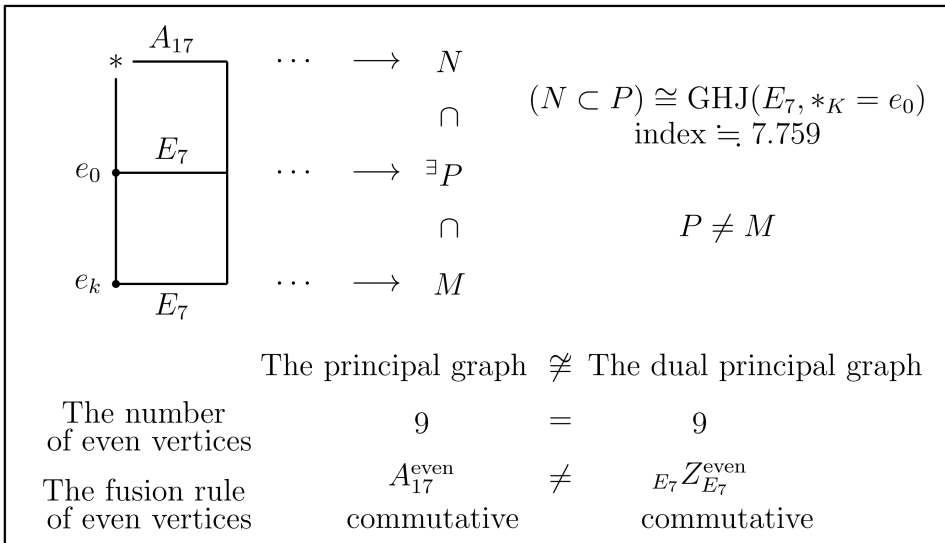


Figure 18.

4.6. Goodman-de la Harpe-Jones subfactors of type E_8

We label the vertices of the Dynkin diagram E_8 by $e_0, e_1, e_2, \dots, e_7$ as in Figure 19.

The Goodman-de la Harpe-Jones subfactor $\text{GHJ}(E_8, *K = e_0)$, has index $\frac{|A_{29}|}{|E_8|}$ which is approximately 19.48. Here $|A_{29}|$ and $|E_8|$ represents the “total mass” of the graph A_{29} and E_8 respectively. The (dual) principal graphs of $\text{GHJ}(E_8, *K)$ are given in Figures 117~124.

If the vertex $*K \neq e_0$, $\text{GHJ}(E_7, *K)$ has nontrivial intermediate subfactor as in Figure 20 because we have the decomposition of connections

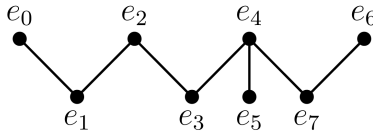


Figure 19. The label of vertices of the Dynkin diagram E_8 .

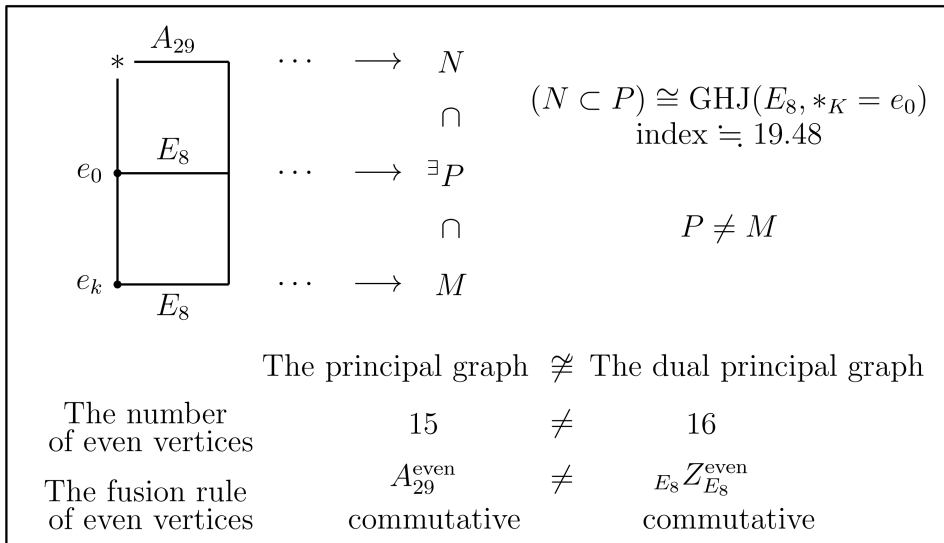


Figure 20.

$Ae_kE = Ae_{0E} \cdot E[w_k]_E$ for $k \neq 0$. Here $E[w_k]_E$ is the E_8 - E_8 connection corresponding to the vertex $[k]$ as in Figures 36, 46 and 47.

5. An Application to Subequivalence on Paragroups

Let K be one of the Dynkin diagrams $D_{2n}(n \geq 3), E_6, E_8$ and A_l the Dynkin diagram of type A with the same Perron-Frobenius eigenvalue as K . We can choose the vertex $*_K$ so that the GHJ subfactor $\text{GHJ}(K, *_K)$ does not have index 2. Let $N \subset M$ be the GHJ subfactor $\text{GHJ}(K, *_K)$ chosen as above, then the fusion algebra of N - N bimodules is isomorphic to A_l^{even} and the fusion algebra of M - M bimodules is isomorphic to ${}_K Z_K^{\text{even}}$. Because ${}_K Z_K^{\text{even}}$ contains K^{even} as its strict fusion subalgebra, the paragroup of type K becomes a *strictly subequivalent* to that of type A_l . Here we use the terminology *strictly subequivalent* in the sense that a fusion algebra \mathcal{A} is subequivalent but not equivalent to \mathcal{B} . And in such a case, we denote $\mathcal{A} \succ \mathcal{B}$.

In the case of D_4 , we can choose the direct sum of 3 connections for $\text{GHJ}(D_4, *_K)$ ($*_K = d_0, d_2, d'_2$) as a connection for subequivalence between A_5 and D_4 paragroups.

Hence we get the following subequivalence of paragroups.

THEOREM 5.1. *The paragroups of Jones' type A subfactors have the following strictly subequivalent paragroups.*

$$A_{4n-3} \succ D_{2n} \ (n \geq 2), \quad A_{11} \succ E_6, \quad A_{29} \succ E_8.$$

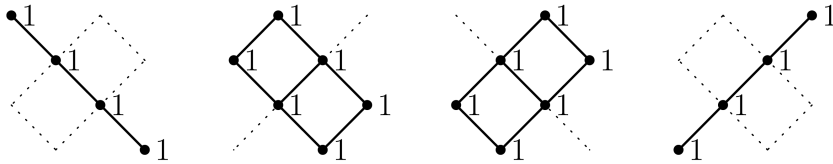


Figure 21. Essential paths on the Coxeter graph A_4 .

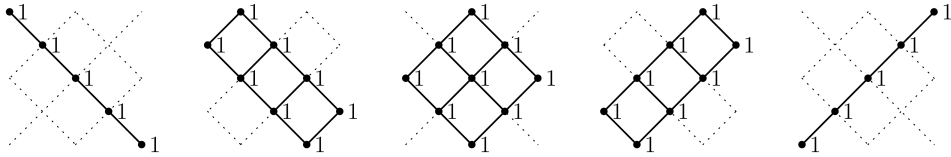


Figure 22. Essential paths on the Coxeter graph A_5 .

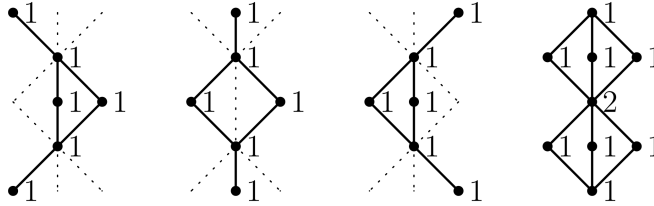


Figure 23. Essential paths on the Coxeter graph D_4 .

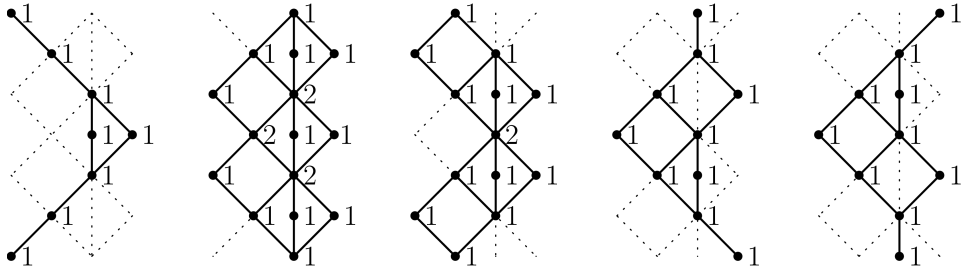
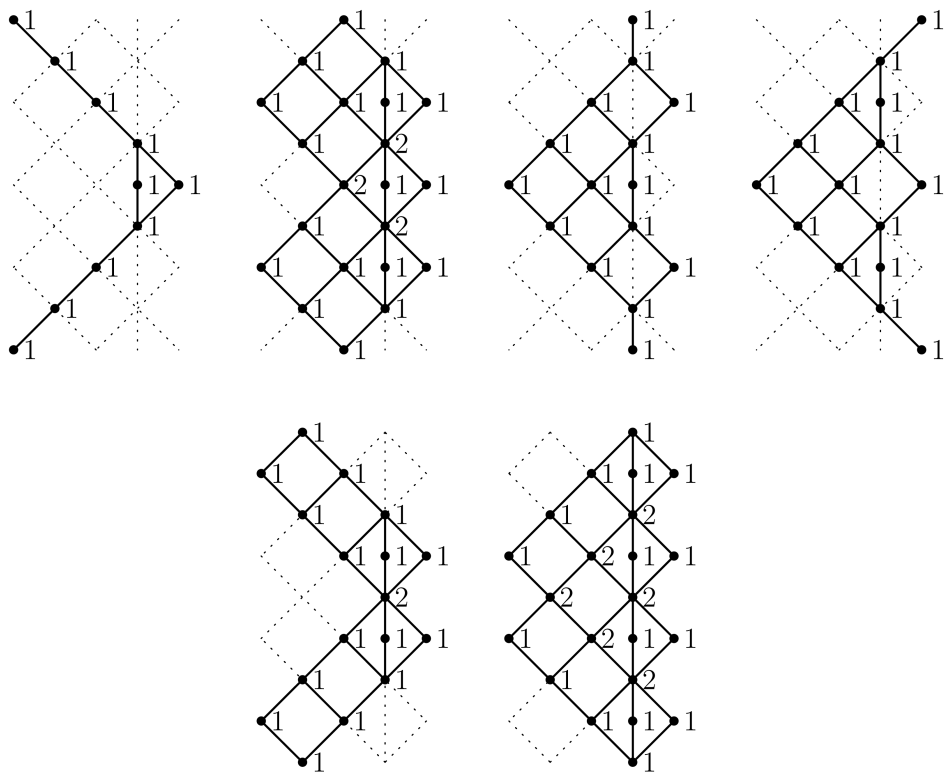


Figure 24. Essential paths on the Coxeter graph D_5 .

Figure 25. Essential paths on the Coxeter graph D_6 .

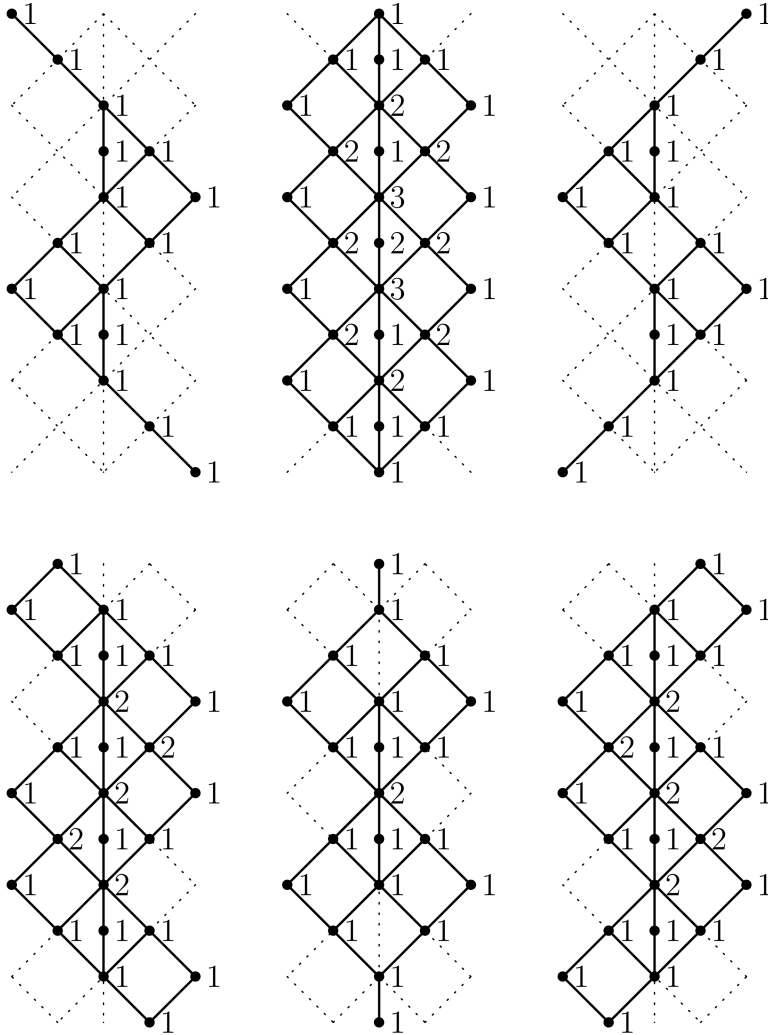


Figure 26. Essential paths on the Coxeter graph E_6 .

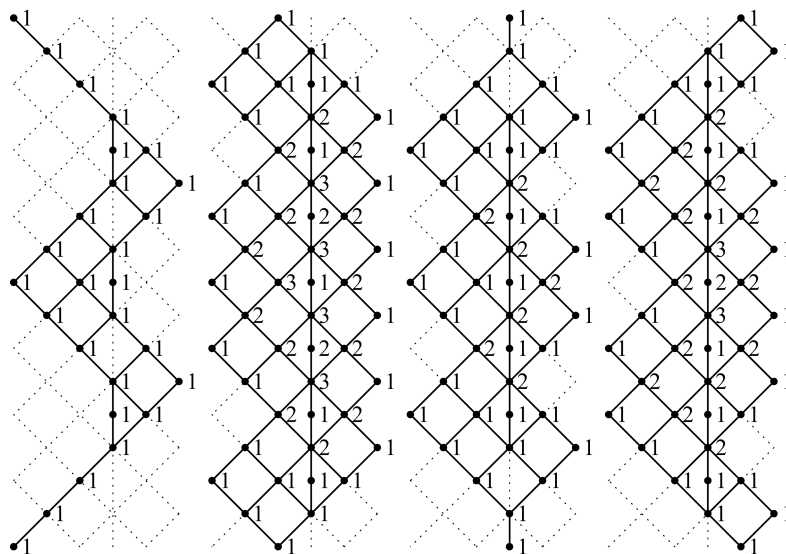


Figure 27. Essential paths on the Coxeter graph E_7 (1).

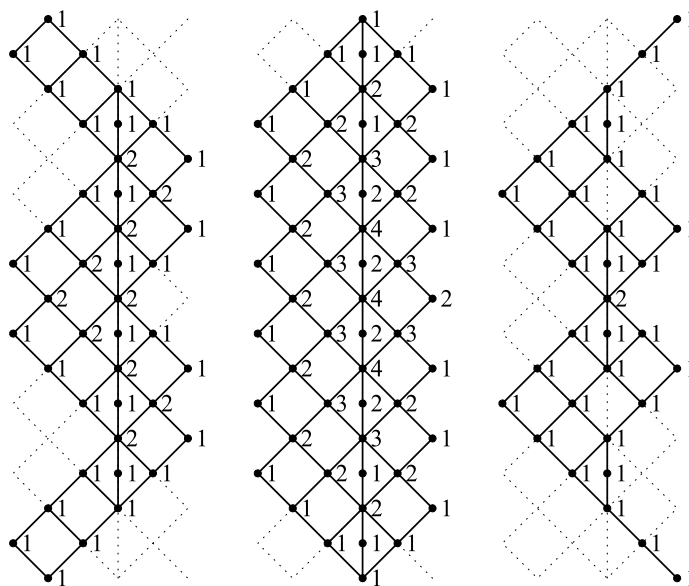


Figure 28. Essential paths on the Coxeter graph E_7 (2).

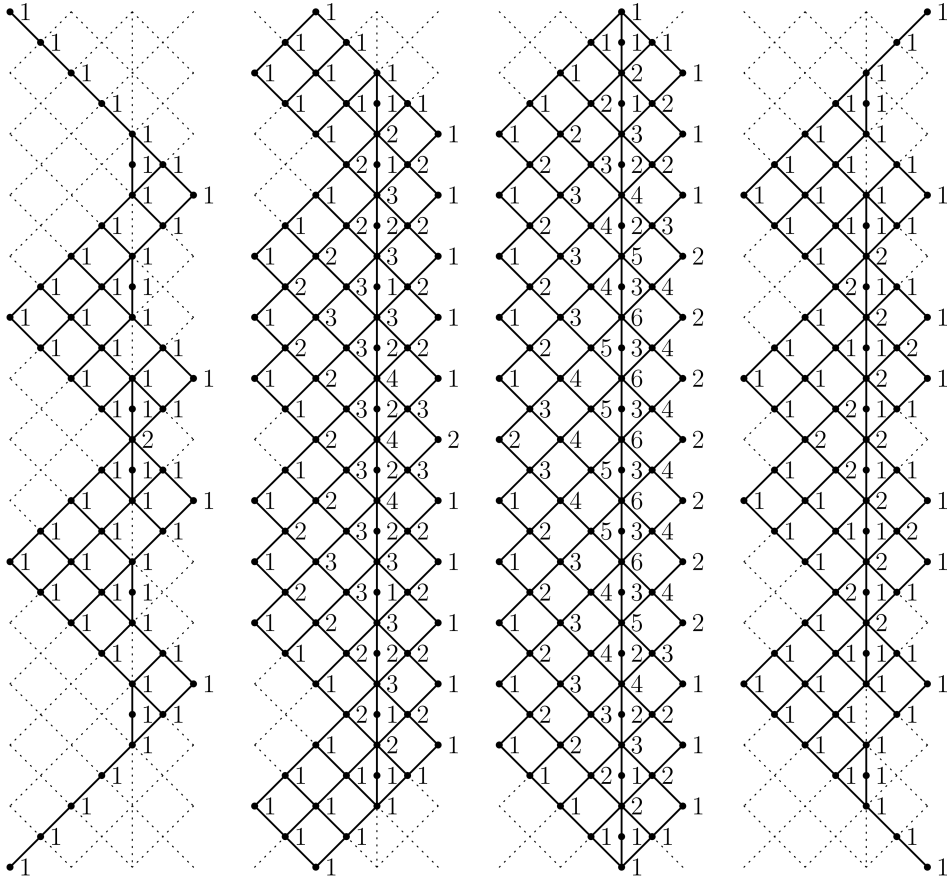
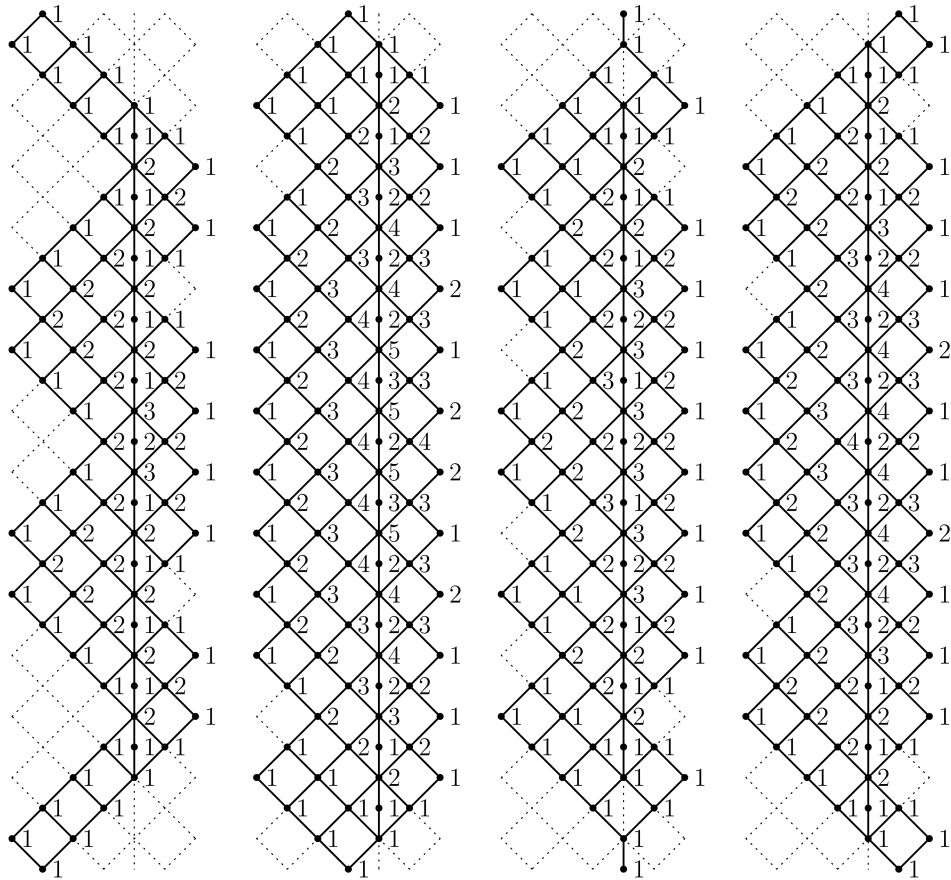


Figure 29. Essential paths on the Coxeter graph E_8 (1).

Figure 30. Essential paths on the Coxeter graph $E_8(2)$.

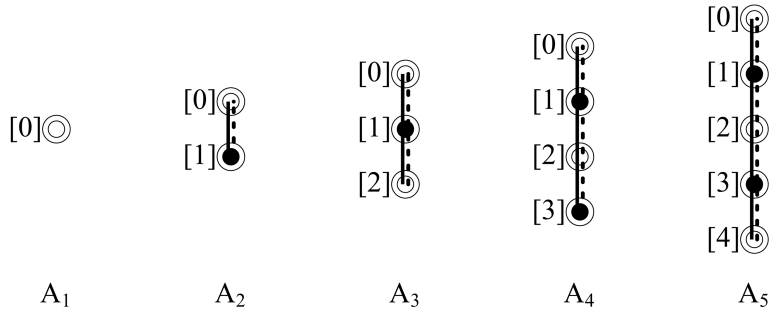


Figure 31. Chiral symmetry for the Coxeter graph A_n .

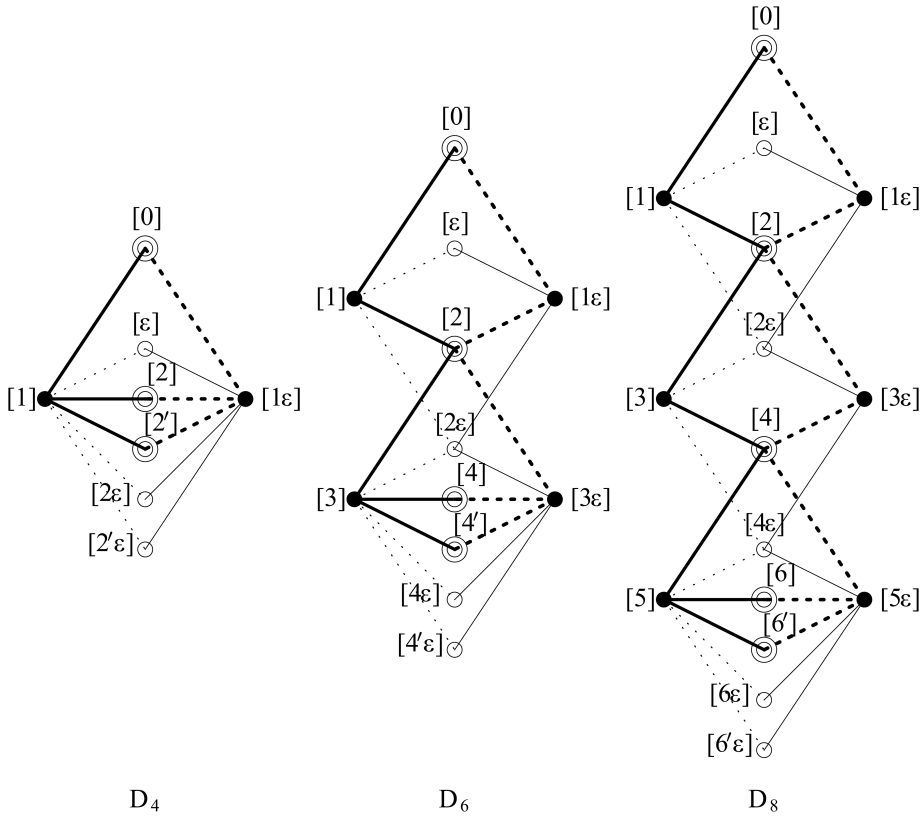


Figure 32. Chiral symmetry for the Coxeter graph D_{even} .

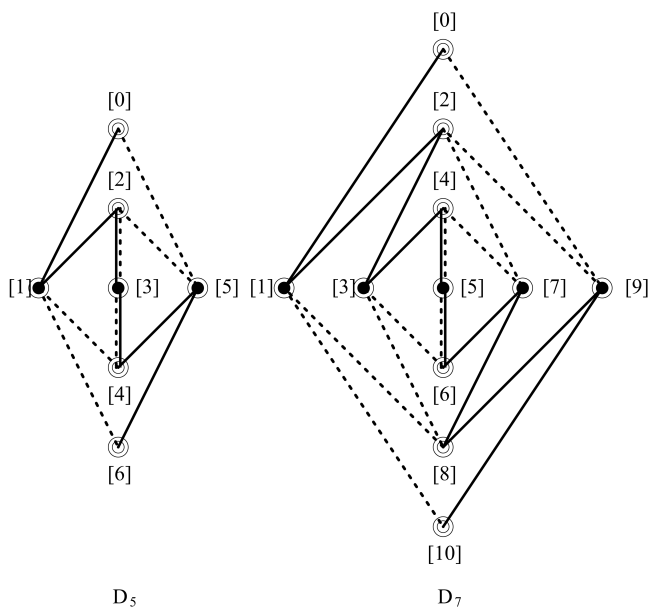


Figure 33. Chiral symmetry for the Coxeter graph D_{odd} .

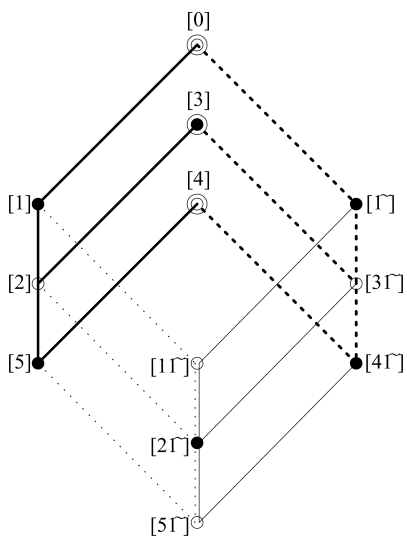


Figure 34. Chiral symmetry for the Coxeter graph E_6 .

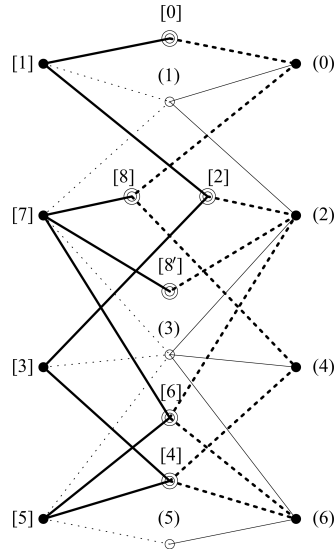


Figure 35. Chiral symmetry for the Coxeter graph E_7 .

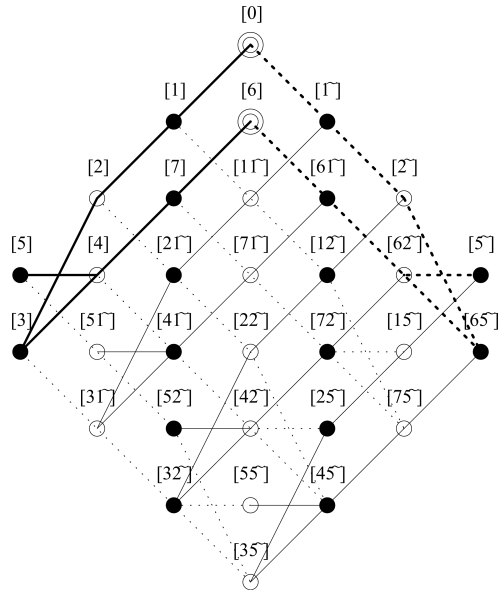


Figure 36. Chiral symmetry for the Coxeter graph E_8 .

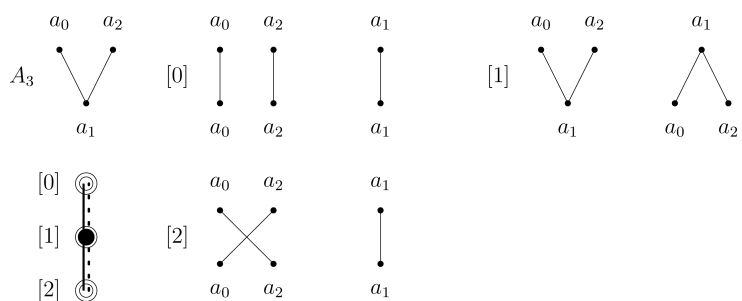


Figure 37. Vertical graphs for connections on the Coxeter graph A_3 .

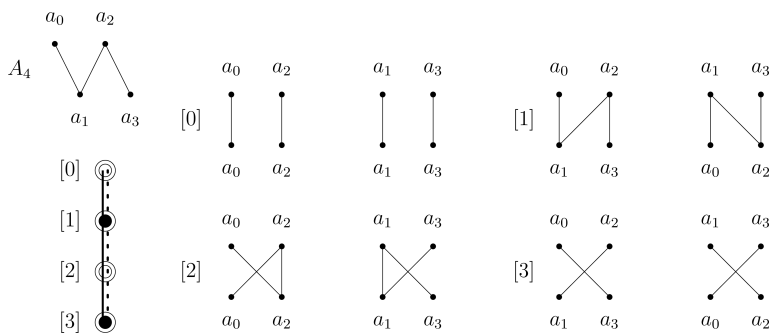


Figure 38. Vertical graphs for connections on the Coxeter graph A_4 .

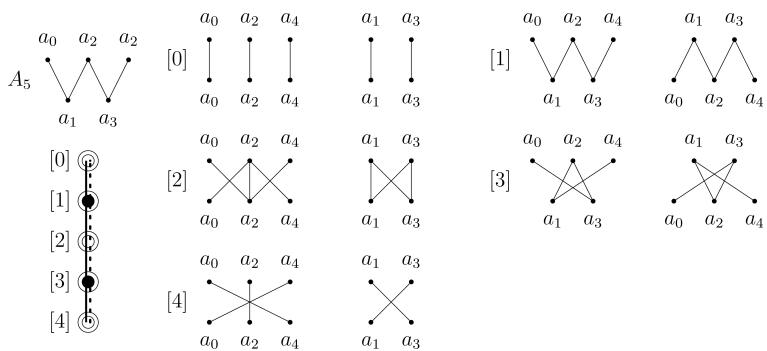


Figure 39. Vertical graphs for connections on the Coxeter graph A_5 .

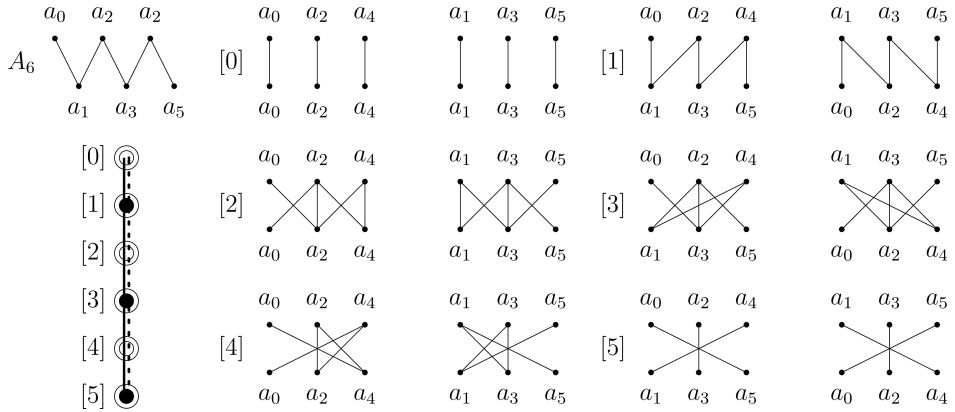


Figure 40. Vertical graphs for connections on the Coxeter graph A_6 .

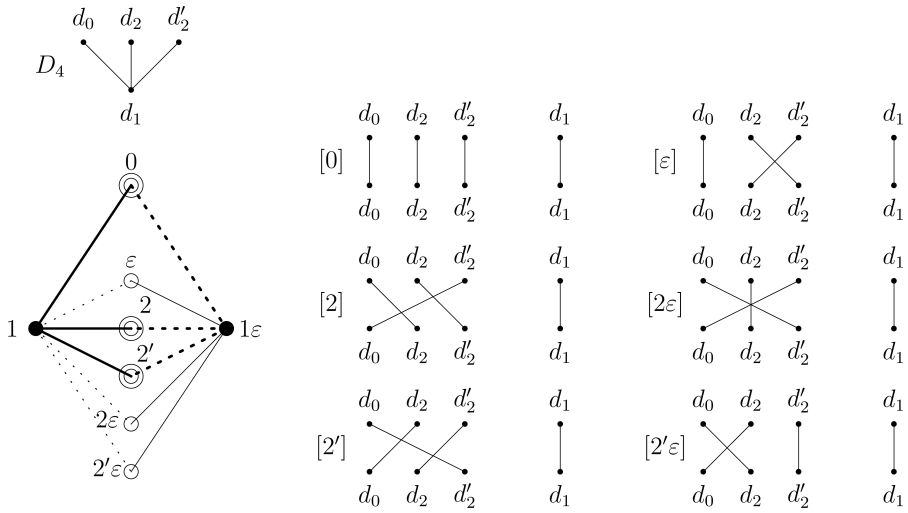


Figure 41. Vertical graphs for connections on the Coxeter graph D_4 .

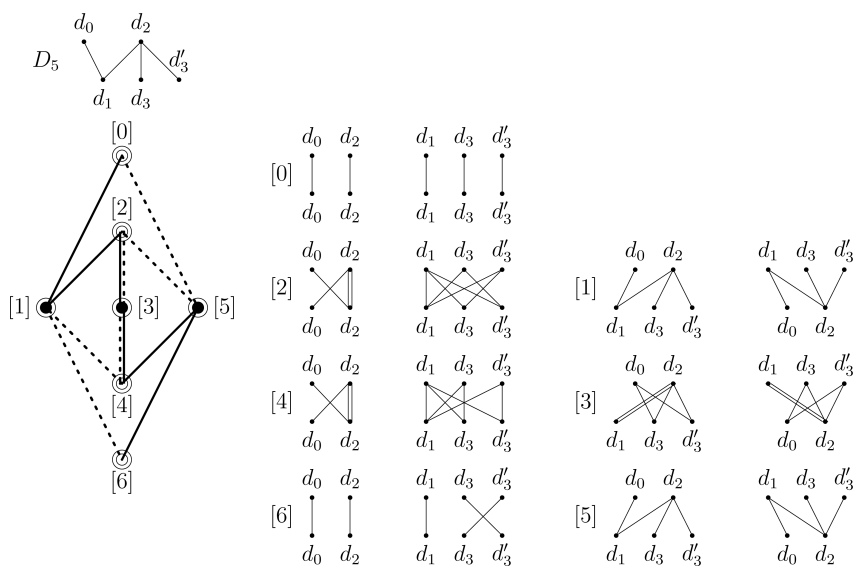


Figure 42. Vertical graphs for connections on the Coxeter graph D_5 .

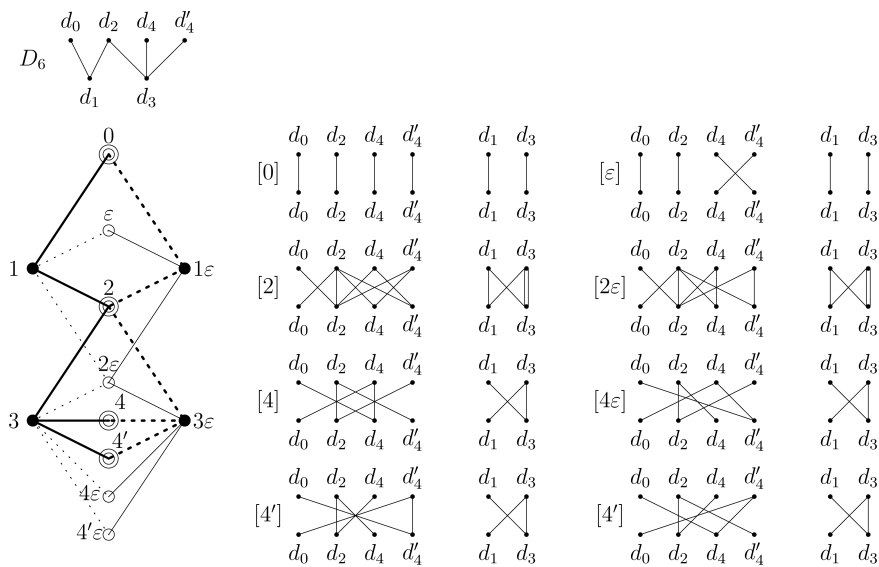
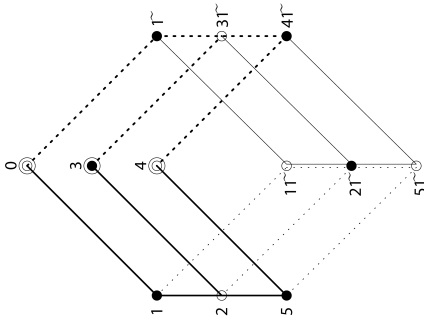


Figure 43. Vertical graphs for connections on the Coxeter graph D_6 .

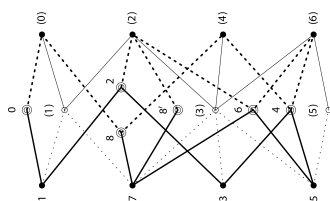
$$\begin{array}{cc}
\begin{array}{c} [w_1] \\ \begin{array}{c} e_1 \ e_3 \ e_5 \ e_7 \\ e_0 \begin{pmatrix} 1 & 0 & 0 & 0 \\ 1 & 1 & 0 & 0 \\ 0 & 1 & 1 & 1 \\ 0 & 0 & 0 & 1 \end{pmatrix} \end{array} \end{array} & \begin{array}{c} \begin{array}{c} e_0 \ e_2 \ e_4 \ e_6 \\ e_1 \begin{pmatrix} 1 & 1 & 0 & 0 \\ 0 & 1 & 1 & 0 \\ 0 & 0 & 1 & 0 \\ 0 & 0 & 1 & 1 \end{pmatrix} \end{array} \end{array} \\
\begin{array}{c} [w_5] \\ \begin{array}{c} e_1 \ e_3 \ e_5 \ e_7 \\ e_0 \begin{pmatrix} 0 & 0 & 1 & 0 \\ 0 & 1 & 0 & 1 \\ 1 & 1 & 1 & 1 \\ 0 & 1 & 0 & 0 \end{pmatrix} \end{array} \end{array} & \begin{array}{c} \begin{array}{c} e_0 \ e_2 \ e_4 \ e_6 \\ e_1 \begin{pmatrix} 0 & 0 & 1 & 0 \\ 0 & 1 & 1 & 1 \\ 1 & 0 & 1 & 0 \\ 0 & 1 & 1 & 0 \end{pmatrix} \end{array} \end{array} \\
\begin{array}{c} [w_{\bar{1}}] \\ \begin{array}{c} e_1 \ e_3 \ e_5 \ e_7 \\ e_0 \begin{pmatrix} 1 & 0 & 0 & 0 \\ 1 & 1 & 0 & 0 \\ 0 & 1 & 1 & 1 \\ 0 & 0 & 0 & 1 \end{pmatrix} \end{array} \end{array} & \begin{array}{c} \begin{array}{c} e_0 \ e_2 \ e_4 \ e_6 \\ e_1 \begin{pmatrix} 1 & 1 & 0 & 0 \\ 0 & 1 & 1 & 0 \\ 0 & 0 & 1 & 0 \\ 0 & 0 & 1 & 1 \end{pmatrix} \end{array} \end{array} \\
\begin{array}{c} [w_{4\bar{1}}] \\ \begin{array}{c} e_1 \ e_3 \ e_5 \ e_7 \\ e_0 \begin{pmatrix} 0 & 1 & 1 & 1 \\ 1 & 3 & 2 & 3 \\ 3 & 5 & 3 & 4 \\ 1 & 2 & 1 & 1 \end{pmatrix} \end{array} \end{array} & \begin{array}{c} \begin{array}{c} e_0 \ e_2 \ e_4 \ e_6 \\ e_1 \begin{pmatrix} 0 & 1 & 3 & 1 \\ 1 & 3 & 5 & 2 \\ 1 & 2 & 3 & 1 \\ 1 & 3 & 4 & 1 \end{pmatrix} \end{array} \end{array} \\
\begin{array}{c} [w_{1\bar{2}}] \\ \begin{array}{c} e_1 \ e_3 \ e_5 \ e_7 \\ e_0 \begin{pmatrix} 1 & 1 & 0 & 0 \\ 2 & 2 & 1 & 1 \\ 1 & 3 & 2 & 3 \\ 0 & 1 & 1 & 1 \end{pmatrix} \end{array} \end{array} & \begin{array}{c} \begin{array}{c} e_0 \ e_2 \ e_4 \ e_6 \\ e_1 \begin{pmatrix} 1 & 2 & 1 & 0 \\ 1 & 2 & 3 & 1 \\ 0 & 1 & 2 & 1 \\ 0 & 1 & 3 & 1 \end{pmatrix} \end{array} \end{array} \\
\begin{array}{c} [w_{5\bar{2}}] \\ \begin{array}{c} e_1 \ e_3 \ e_5 \ e_7 \\ e_0 \begin{pmatrix} 0 & 1 & 0 & 1 \\ 1 & 2 & 2 & 2 \\ 2 & 4 & 2 & 3 \\ 1 & 1 & 1 & 1 \end{pmatrix} \end{array} \end{array} & \begin{array}{c} \begin{array}{c} e_0 \ e_2 \ e_4 \ e_6 \\ e_1 \begin{pmatrix} 0 & 1 & 2 & 1 \\ 1 & 2 & 4 & 1 \\ 0 & 2 & 2 & 1 \\ 1 & 2 & 3 & 1 \end{pmatrix} \end{array} \end{array} \\
\begin{array}{c} [w_5] \\ \begin{array}{c} e_1 \ e_3 \ e_5 \ e_7 \\ e_0 \begin{pmatrix} 0 & 0 & 1 & 0 \\ 0 & 1 & 0 & 1 \\ 1 & 1 & 1 & 1 \\ 0 & 1 & 0 & 0 \end{pmatrix} \end{array} \end{array} & \begin{array}{c} \begin{array}{c} e_0 \ e_2 \ e_4 \ e_6 \\ e_1 \begin{pmatrix} 0 & 0 & 1 & 0 \\ 0 & 1 & 1 & 1 \\ 1 & 0 & 1 & 0 \\ 0 & 1 & 1 & 0 \end{pmatrix} \end{array} \end{array} \\
\begin{array}{c} [w_{4\bar{5}}] \\ \begin{array}{c} e_1 \ e_3 \ e_5 \ e_7 \\ e_0 \begin{pmatrix} 1 & 1 & 1 & 1 \\ 2 & 4 & 2 & 3 \\ 3 & 6 & 4 & 5 \\ 1 & 2 & 1 & 2 \end{pmatrix} \end{array} \end{array} & \begin{array}{c} \begin{array}{c} e_0 \ e_2 \ e_4 \ e_6 \\ e_1 \begin{pmatrix} 1 & 2 & 3 & 1 \\ 1 & 4 & 6 & 2 \\ 1 & 2 & 4 & 1 \\ 1 & 3 & 5 & 2 \end{pmatrix} \end{array} \end{array}
\end{array}
\end{array}$$

Figure 47. The incidence matrices of the vertical edges of E_8 - E_8 odd connections.



E_6	0	2	4	$[11]$	$[31]$	$[51]$	1	3	5	$[1]$	$[21]$	$[41]$
0	0	2	4	$[11]$	$[31]$	$[51]$	1	3	5	$[1]$	$[21]$	$[41]$
2	2	02^2_4	2	$[11][31][51]$	$[11][51]$	$[11][31][51]$	135	15	135	$[21]$	$[1][21]^2[41]$	$[21]$
4	4	2	0	$[51]$	$[31]$	$[11]$	5	3	1	$[41]$	$[21]$	$[1]$
$[11]$	$[11]$	$[11][31][51]$	$[51]$	$02[11][31][51]$	$2[11][51]$	$24[11][31][51]$	$[1][21]$	$[21]$	$[21][41]$	$1[21]$	$135[1-][21-]^2[41-]$	$5[21]$
$[31]$	$[31]$	$[11][51]$	$[31]$	$2[11][51]$	$04[31]^2$	$2[11][51]$	$[21]$	$[1][41]$	$[21]$	$3[1][41]$	$15[21-]^2$	$3[1][41]$
$[51]$	$[51]$	$[11][31][51]$	$[11]$	$24[11][31][51]$	$2[11][51]$	$02[11][31][51]$	$[21][41]$	$[21]$	$[1][21]$	$5[21]$	$135[1-][21-]^2[41-]$	$1[21]$
1	1	135	5	$[1][21]$	$[21]$	$[21][41]$	02	2	24	$[11]$	$[11][31][51]$	$[51]$
3	3	15	3	$[21]$	$[1][41]$	$[21]$	2	04	2	$[31]$	$[11][51]$	$[31]$
5	5	135	1	$[21][41]$	$[21]$	$[1][21]$	24	2	02	$[51]$	$[11][31][51]$	$[11]$
$[21]$	$[21]$	$1[21]^2[41]$	$[21]$	$135[1-][21-]^2[41-]$	$15[21-]^2$	$3[1][41]$	$[11][31][51]$	$[11][51]$	$0[31]$	$2[11][51]$	$2[11][51]$	$4[31]$
$[41]$	$[41]$	$[21]$	$[1]$	$5[21]$	$3[1][41]$	$1[21]$	$[51]$	$[31]$	$[11]$	$4[31]$	$2[11][51]$	$0[31]$

Figure 48. The fusion table of E_6 - E_6 connections.



EH	0	2	4	6	8	8'	(1)	(3)	(5)	1	3	5	7	(0)	(2)	(4)	(6)
0	0	2	4	6	8	8'	(1)	(3)	(5)	1	3	5	7	(0)	(2)	(4)	(6)
2	0	024	246	4688'	68'	68	(1)(3)	(1)(3)(5)	(3)	13	135	357	57 ²	(2)	(0)(2)(4)(6)	(2)(6)	(2)(4)(6)
4	2	246	024688'	246'88'	468'	468'	(3)(5)	(1)(3)(5)(6)	(1)(3)	35	1357	1357 ²	35 ² 7 ²	(4)(6)	(2)(4)(6)	(0)(2)(4)(6)	(0)(2)(4)(6)
6	4	4688'	246'88'	024'6'88'	2468'	2468'	(1)(3)(5)	(1)(3)(5)(6)	(1)(3)(5)	57	357 ²	135 ² 7 ²	13 ² 5 ² 7 ²	(2)(6)	(0)(2)(4)(6)	(2)(4)(6)	(0)(2)(4)(6)
8	8	68'	468'	468'	048	26	(1)(3)	(1)(3)(5)(6)	(3)	7	57	357	1357	(0)(4)	(2)(6)	(0)(4)(6)	(2)(4)(6)
8'	8'	68	468'	2468	26	048'	(1)(3)	(1)(3)(5)(6)	(3)	7	57	357	1357	(2)	(0)(2)(4)(6)	(2)(6)	(2)(4)(6)
(1)	(1)	(1)(3)	(3)(5)	(1)(3)(5)	(1)(3)	(1)(3)	02688'	24'6'88'	46	(0)(2)	(2)(4)(6)	(2)(4)(6) ²	(0)(2)(4)(6)	17	1357 ²	357	35 ² 7
(3)	(3)	(1)(3)(5)	(1)(3)(5)	(1)(3)(5)	(1)(3)(5)(6)	(1)(3)(5)(6)	24'6'88'	02'4'6'8'8'	2468	(2)(4)(6)	(0)(2)(4)(6) ²	(0)(2)(4)(6) ³	(0)(2)(4)(6) ³	357	13 ² 5 ² 7 ³	135 ² 7 ²	13 ² 5 ² 7 ⁴
(5)	(5)	(3)	(1)(3)	(1)(3)(5)	(3)	(3)	46	2468	068'	(6)	(2)(4)	(0)(2)(6)	(2)(4)(6)	5	357	37	157
1	1	13	35	57	7	7	(0)(2)	(2)(4)(6)	(6)	02	24	46	688'	(1)	(1)(3)	(3)	(3)(5)
3	3	135	1357	357 ²	57	57	(2)(4)(6)	(0)(2)(4)(6) ³	(2)(4)	24	0246	24688'	46'88'	(3)	(1)(3)(5)	(1)(3)(5)	(1)(3) ²
5	5	357	1357 ²	135 ² 7 ²	357	357	(2)(4)(6) ²	(0)(2)(4)(6) ²	(0)(2)(6)	46	24688'	024'6'88'	24'6'88'	(3)(5)	(1)(3)(5)	(1)(3) ²	(1) ² (3)(5)
7	7	57 ²	35 ² 7 ²	13 ² 5 ² 7 ²	1357	1357	(0)(2)(4)(6)	(0)(2)(4)(6) ³	(2)(4)(6)	688'	46'88'	24'6'88'	02'4'6'88'	(1)(3)	(1)(3)(5)	(1)(3)(5) ²	(1)(3)(5)
(0)	(0)	(2)	(4)(6)	(2)(6)	(0)(4)	(2)	17	357	5	(1)	(3)	(3)(5)	(1)(3)	08	268'	48	46
(2)	(2)	(0)(2)(4)(6)	(2)(4)(6) ²	(0)(2)(4)(6) ²	(2)(6)	(0)(2)(4)(6)	1357 ²	13 ² 5 ² 7 ²	357	(1)(3)	(1)(3)(5)	(1)(3)(5)	(1)(3)(5)	268'	024'6'8'8'	246 ² 8'	24'6'88'
(4)	(4)	(2)(6)	(0)(2)(4)(6)	(2)(4)(6)	(2)(6)	(2)(6)	357	135 ² 7 ²	37	(3)	(1)(3)(5)	(1)(3) ²	(1)(3)(5)	48	246'8'	0468	24688'
(6)	(6)	(2)(4)(6)	(0)(2)(4)(6)	(0)(2)(4)(6) ²	(2)(4)(6)	(2)(4)(6)	35 ² 7	13 ² 5 ² 7 ³	157	(3)(5)	(1)(3) ²	(1) ² (3)(5)	(1)(3)(5)	46	24'6'88'	24688'	0246'88'

Figure 49. The fusion table of E_7 - E_7 connections.

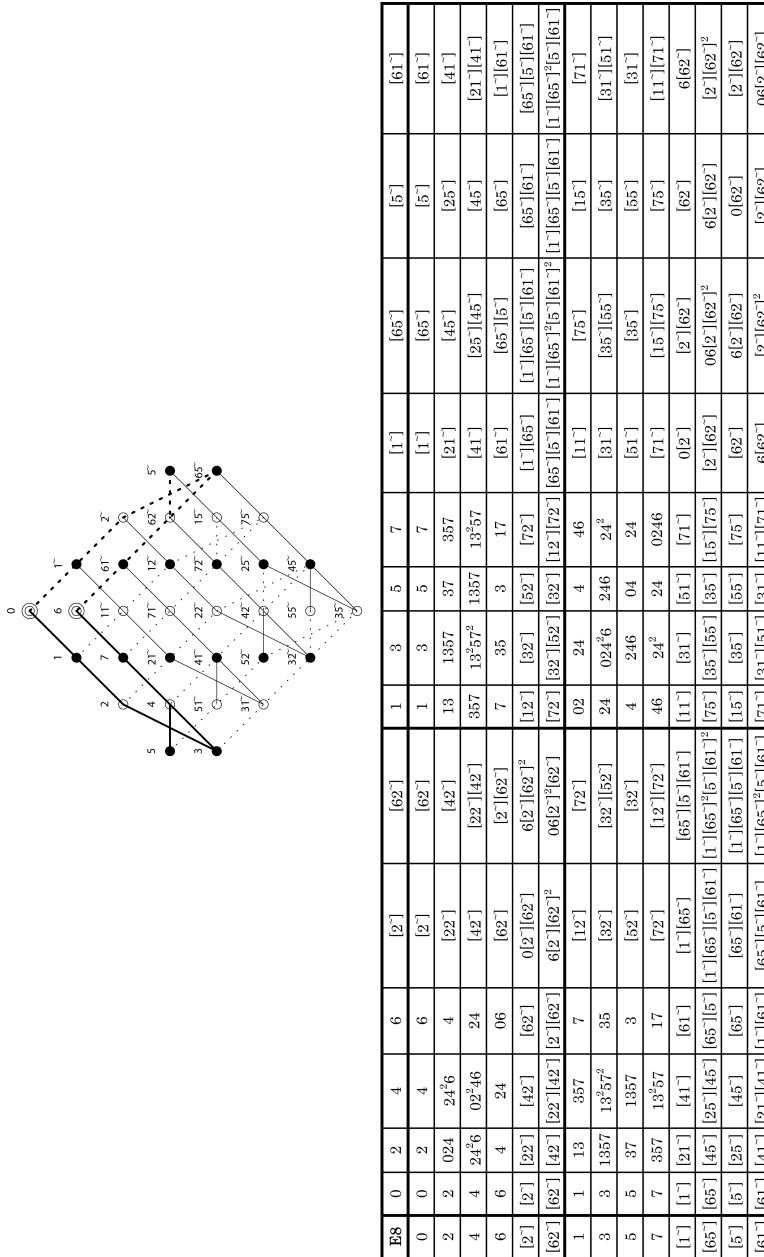


Figure 50. A part of the fusion table of E_8 - E_8 connections.

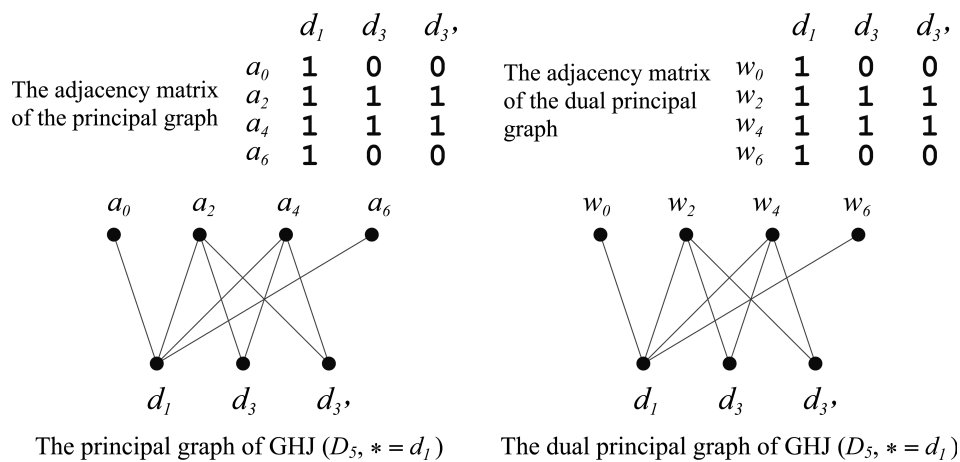


Figure 51. The (dual) principal graph of GHJ($D_5, * = d_1$).

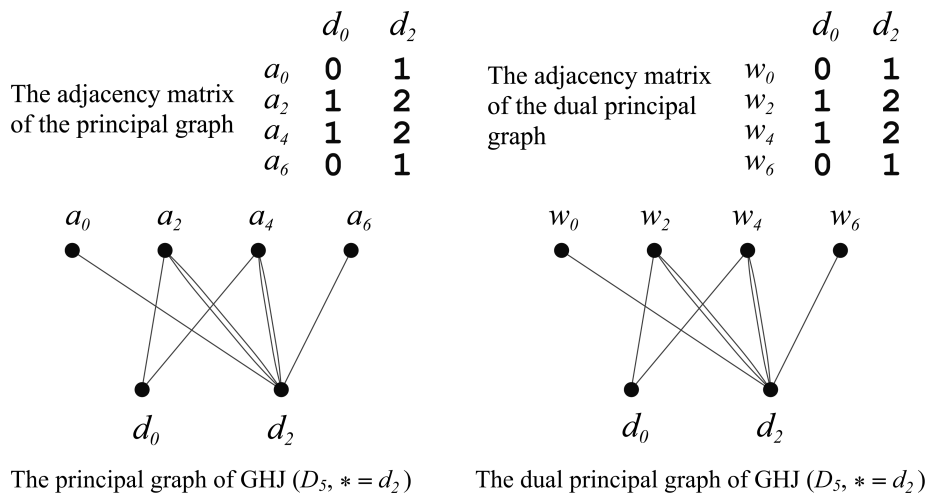


Figure 52. The (dual) principal graph of GHJ($D_5, * = d_2$).

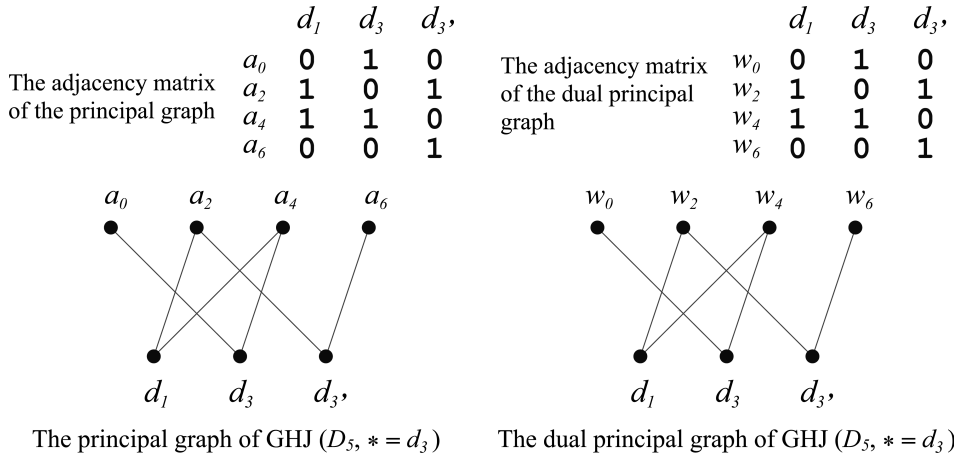


Figure 53. The (dual) principal graph of GHJ($D_5, * = d_3$).

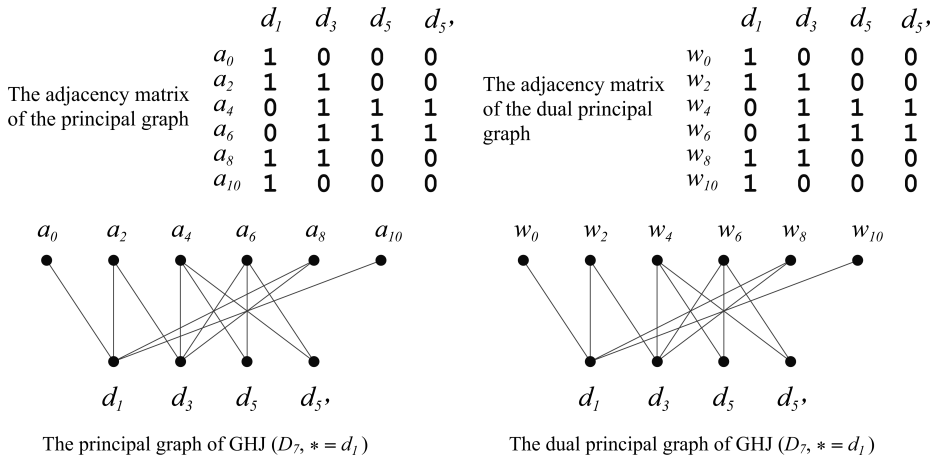


Figure 54. The (dual) principal graph of GHJ($D_7, * = d_1$).

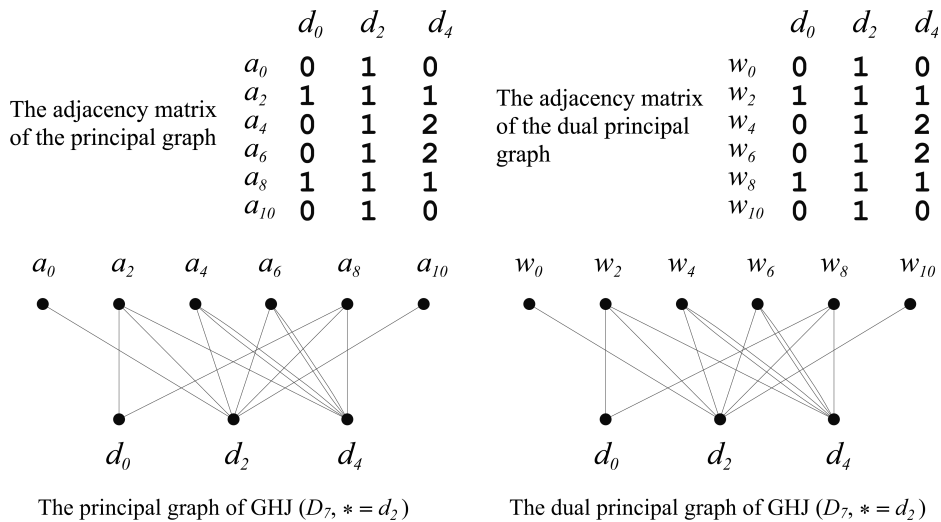


Figure 55. The (dual) principal graph of GHJ($D_7, * = d_2$).

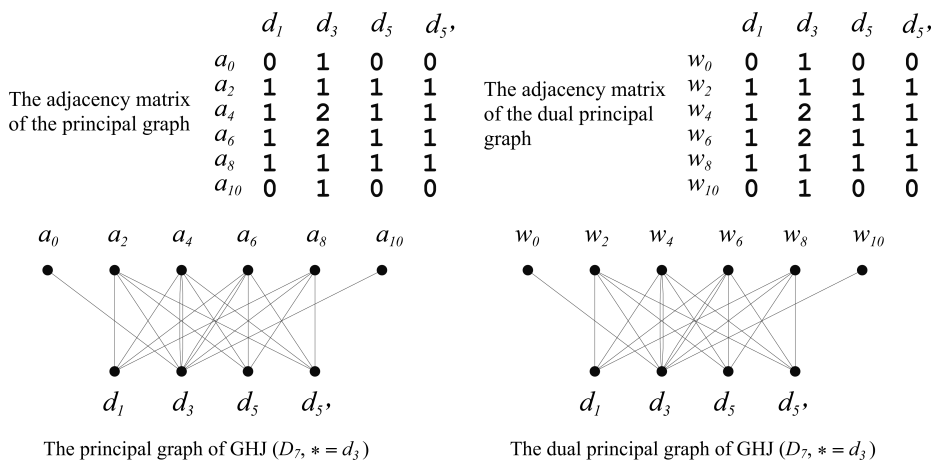


Figure 56. The (dual) principal graph of GHJ($D_7, * = d_3$).

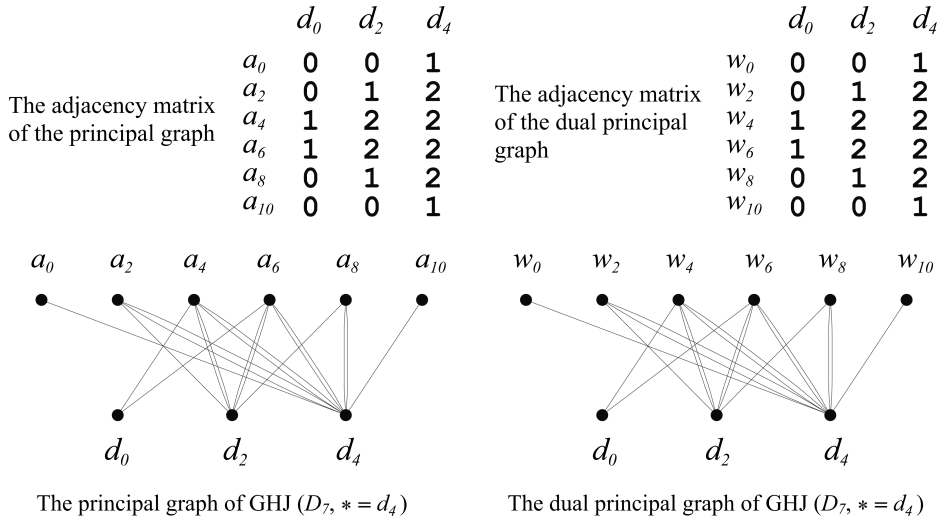


Figure 57. The (dual) principal graph of GHJ($D_7, * = d_4$).

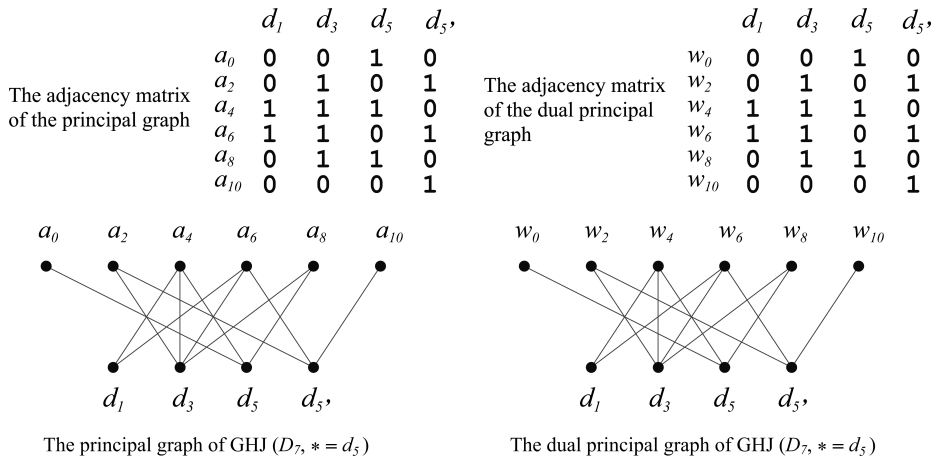


Figure 58. The (dual) principal graph of GHJ($D_7, * = d_5$).

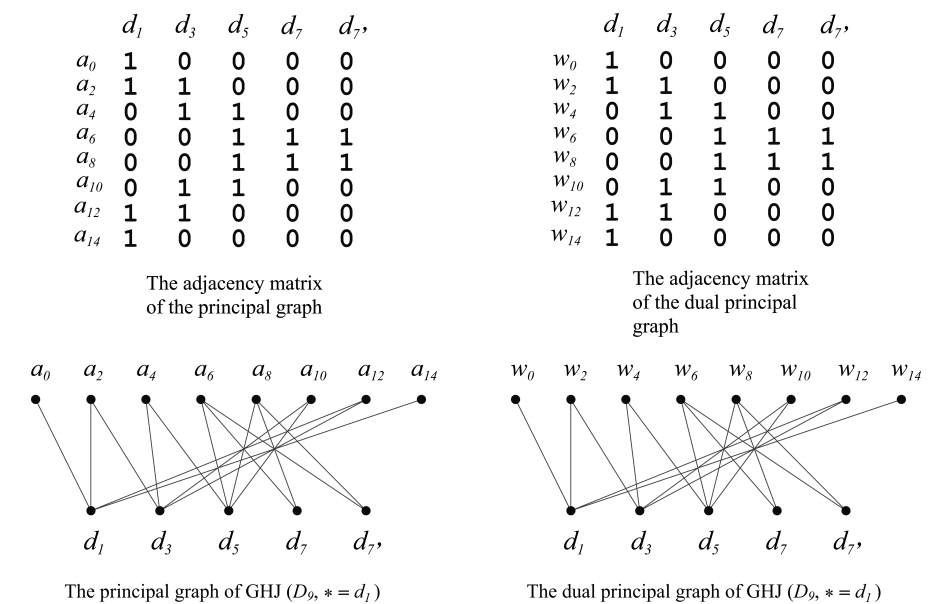


Figure 59. The (dual) principal graph of GHJ($D_9, * = d_1$).

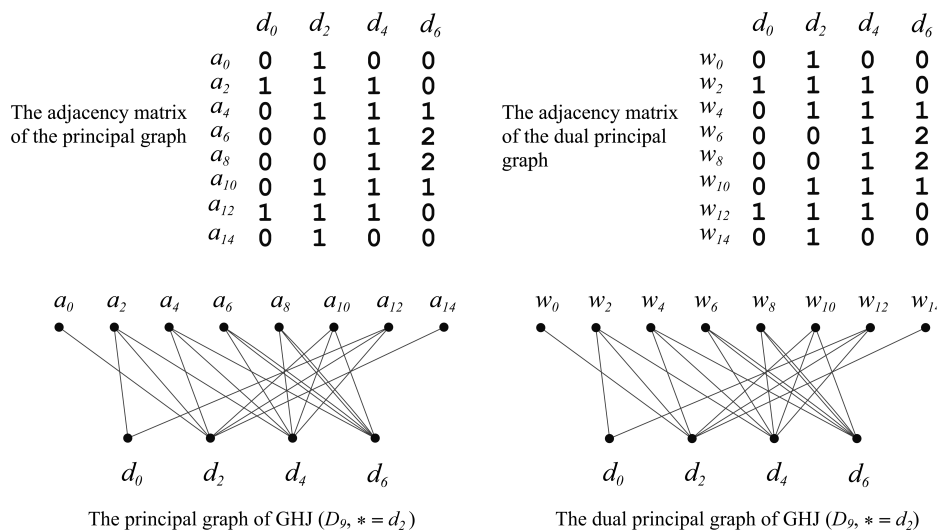


Figure 60. The (dual) principal graph of GHJ($D_9, * = d_2$).

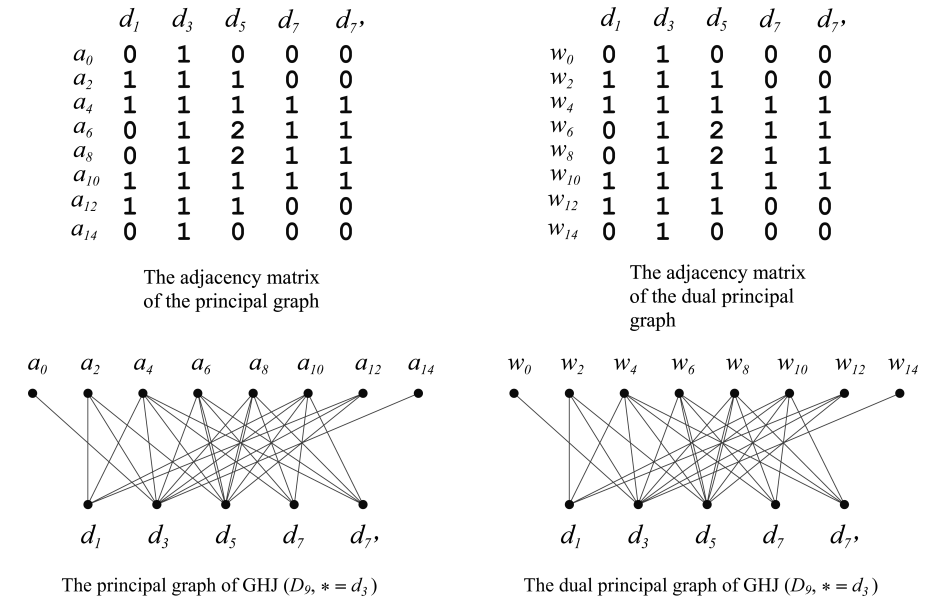


Figure 61. The (dual) principal graph of GHJ($D_9, * = d_3$).

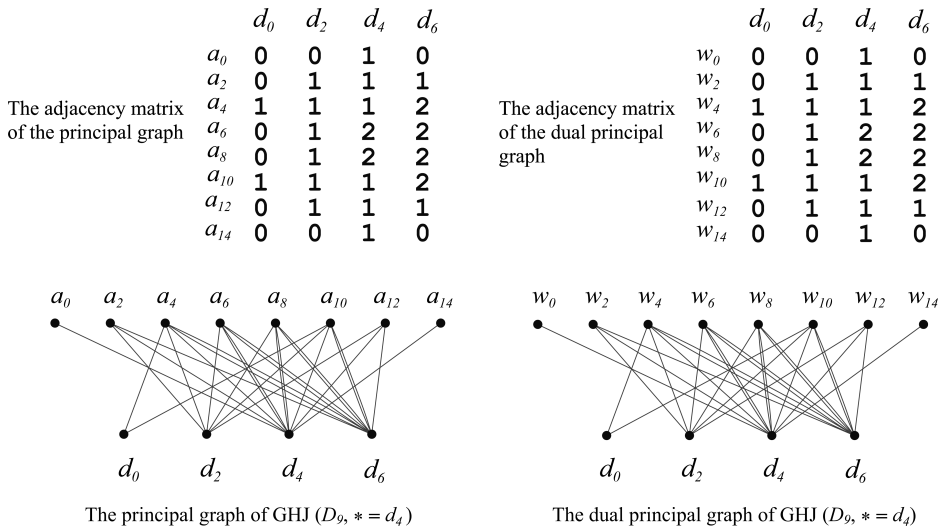


Figure 62. The (dual) principal graph of GHJ($D_9, * = d_4$).

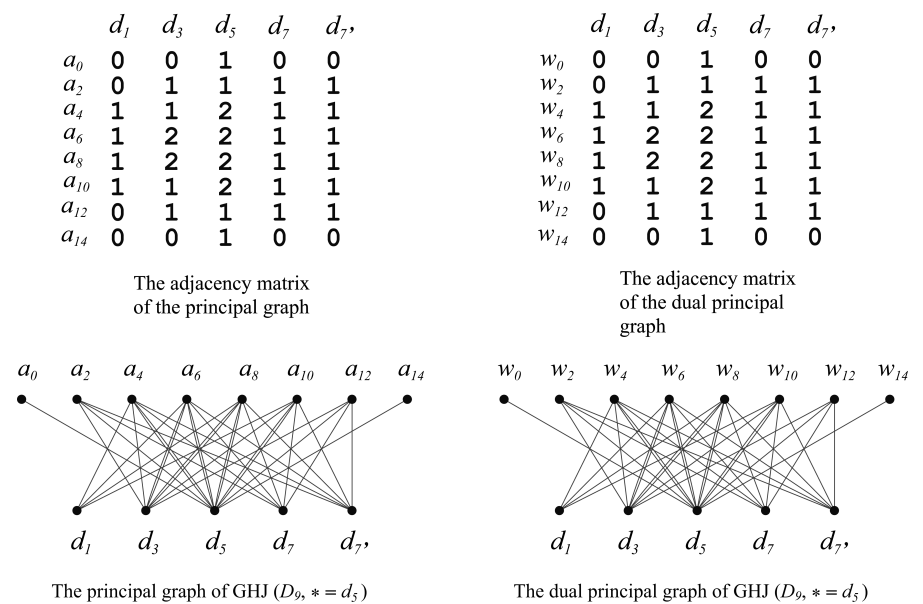


Figure 63. The (dual) principal graph of GHJ($D_9, * = d_5$).

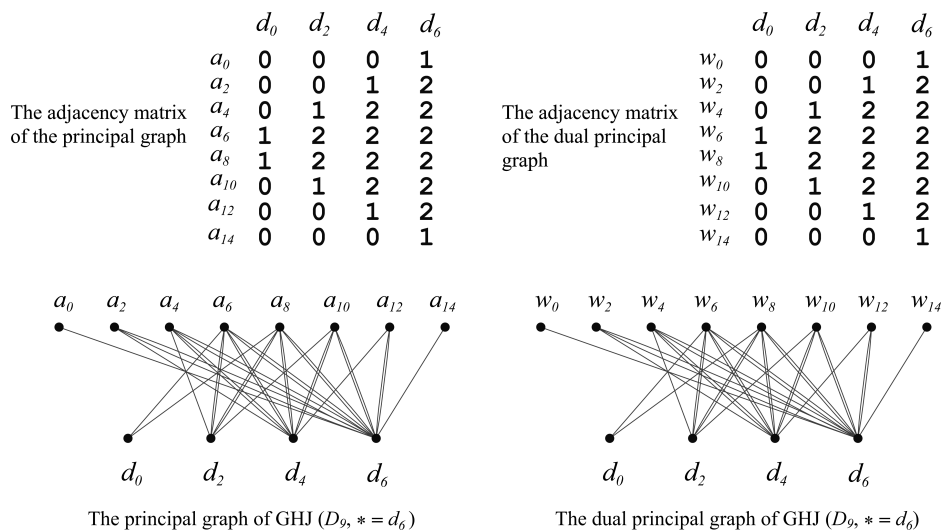


Figure 64. The (dual) principal graph of GHJ($D_9, * = d_6$).

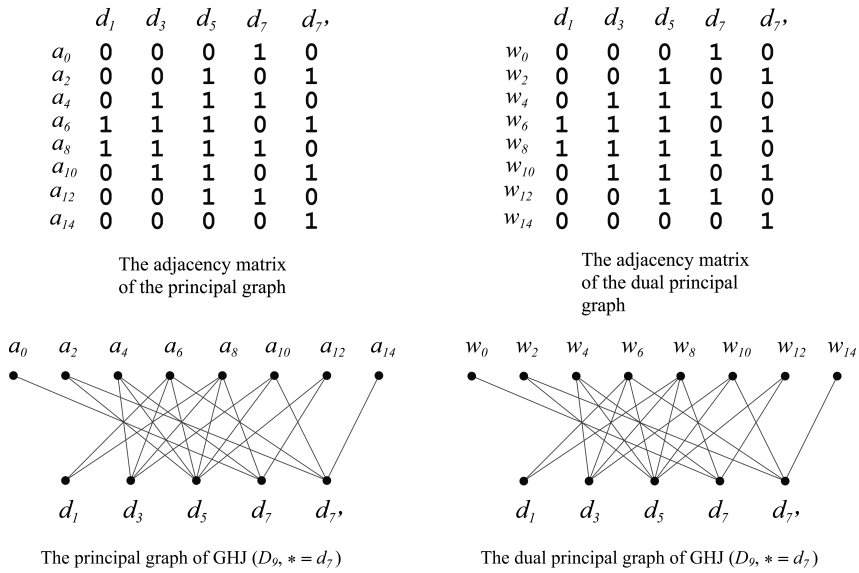


Figure 65. The (dual) principal graph of GHJ($D_9, * = d_7$).

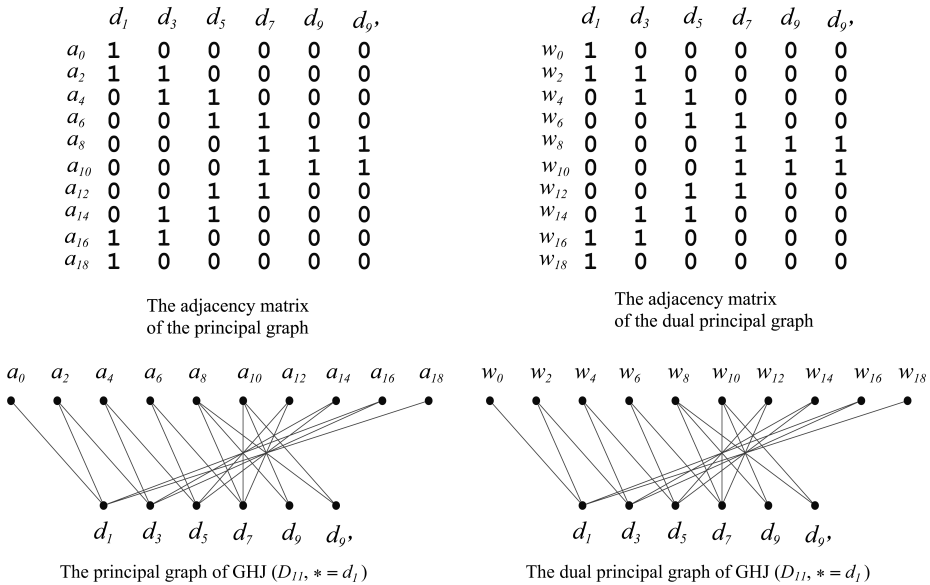


Figure 66. The (dual) principal graph of GHJ($D_{11}, * = d_1$).

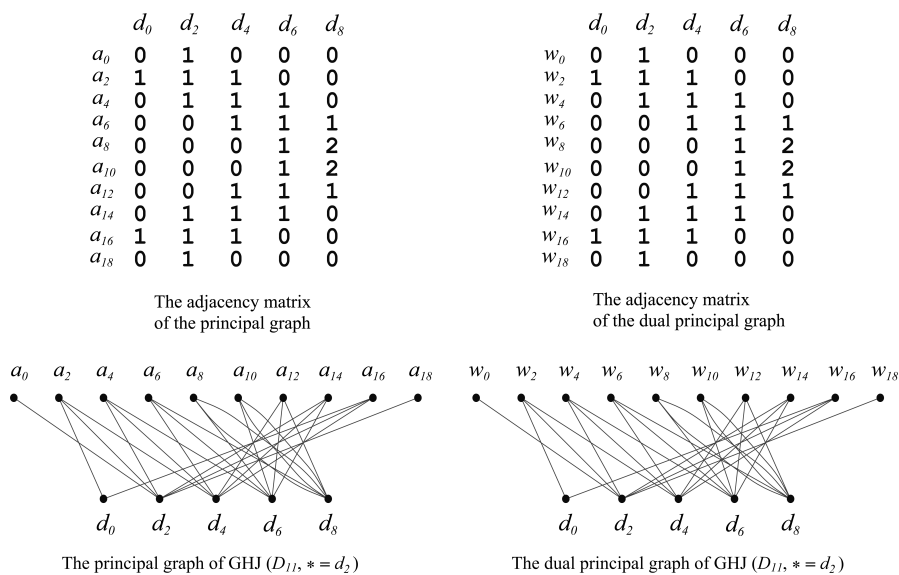


Figure 67. The (dual) principal graph of GHJ($D_{11}, * = d_2$).

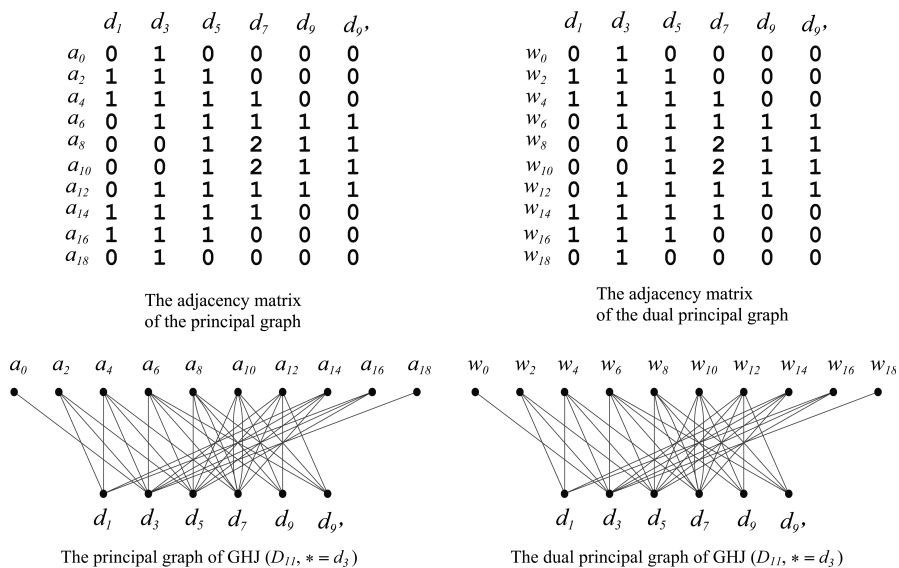


Figure 68. The (dual) principal graph of GHJ($D_{11}, * = d_3$).

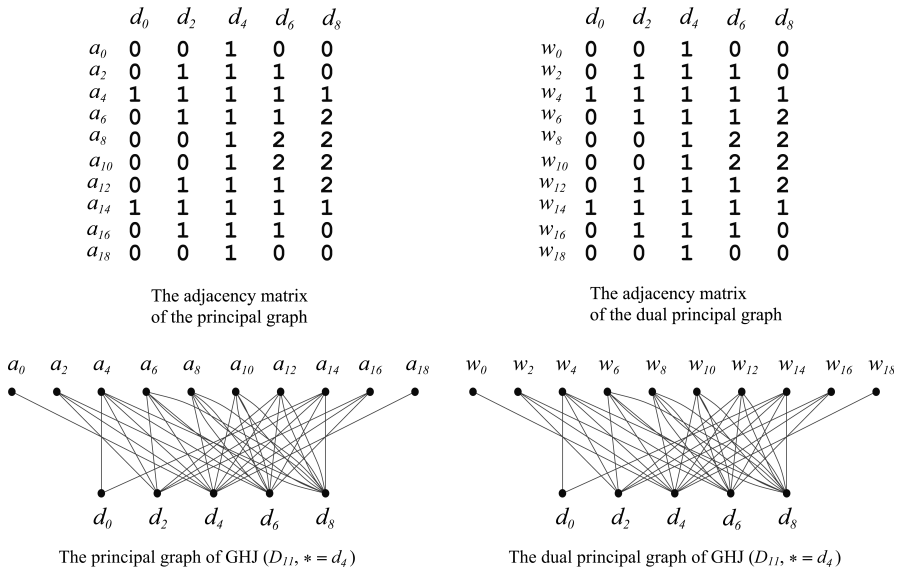


Figure 69. The (dual) principal graph of GHJ($D_{11}, * = d_4$).

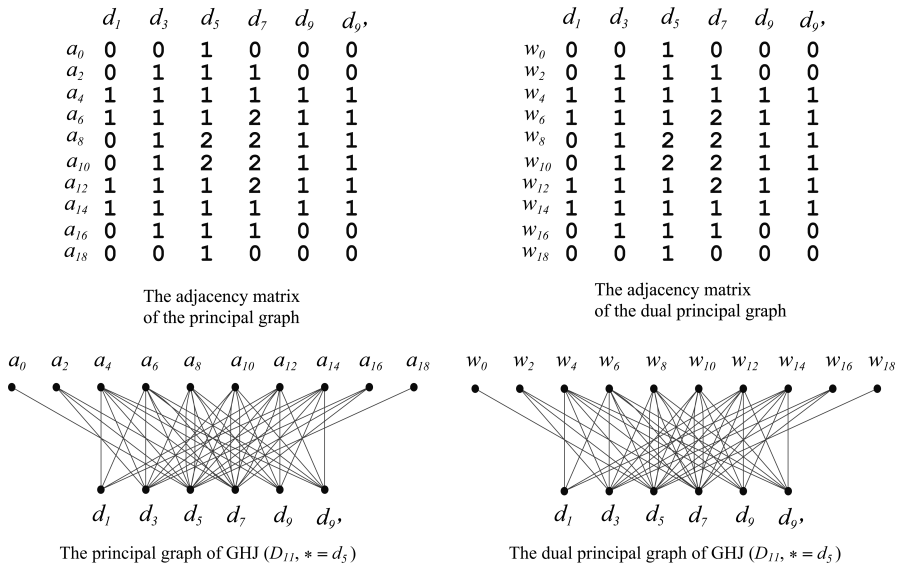


Figure 70. The (dual) principal graph of GHJ($D_{11}, * = d_5$).

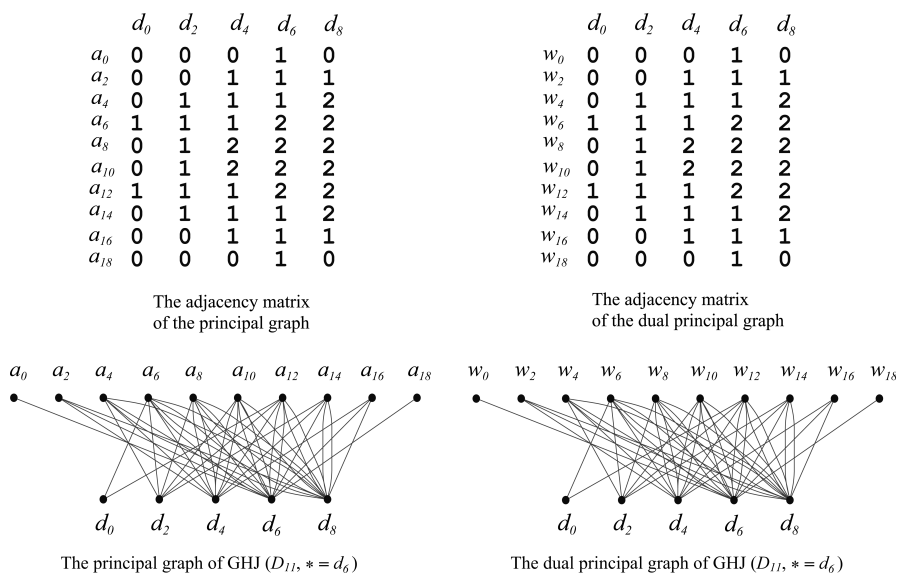


Figure 71. The (dual) principal graph of GHJ($D_{11}, * = d_6$).

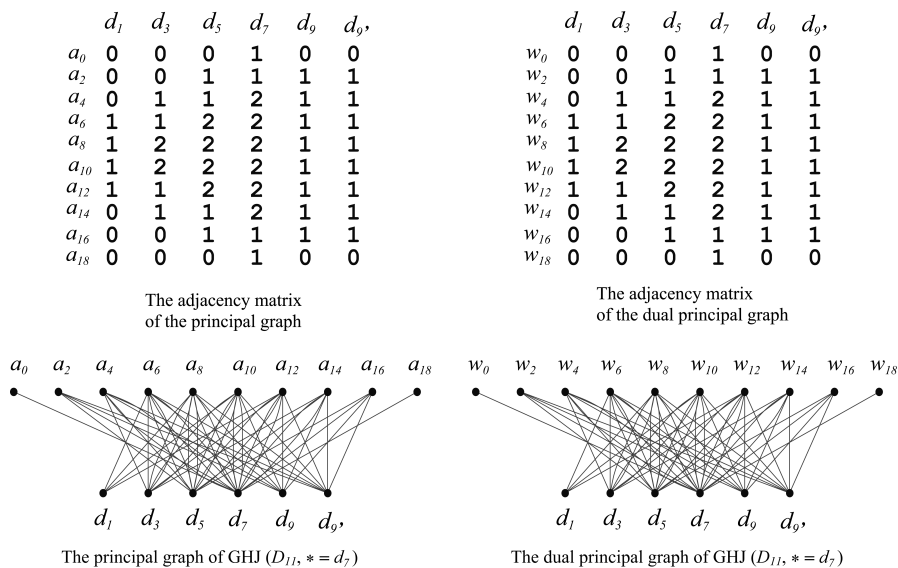


Figure 72. The (dual) principal graph of GHJ($D_{11}, * = d_7$).

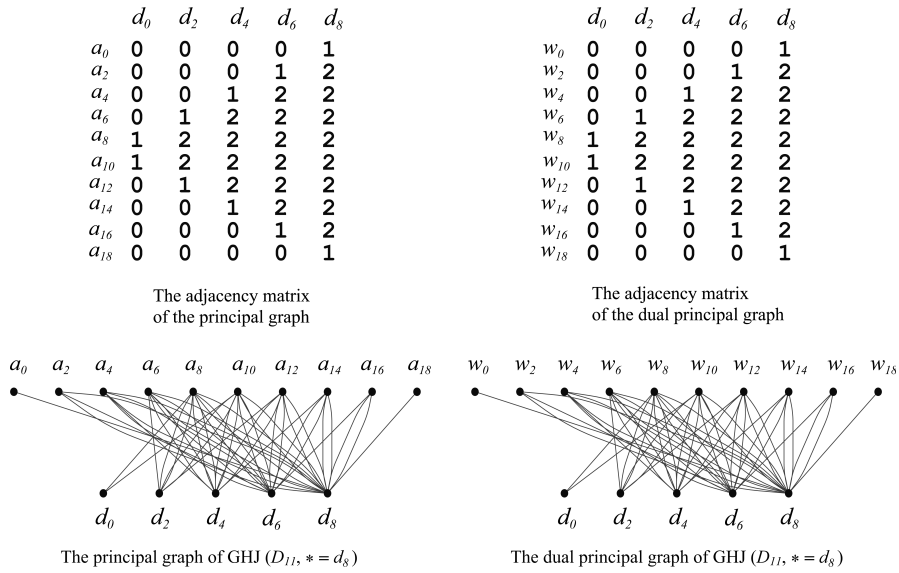


Figure 73. The (dual) principal graph of GHJ($D_{11}, * = d_8$).

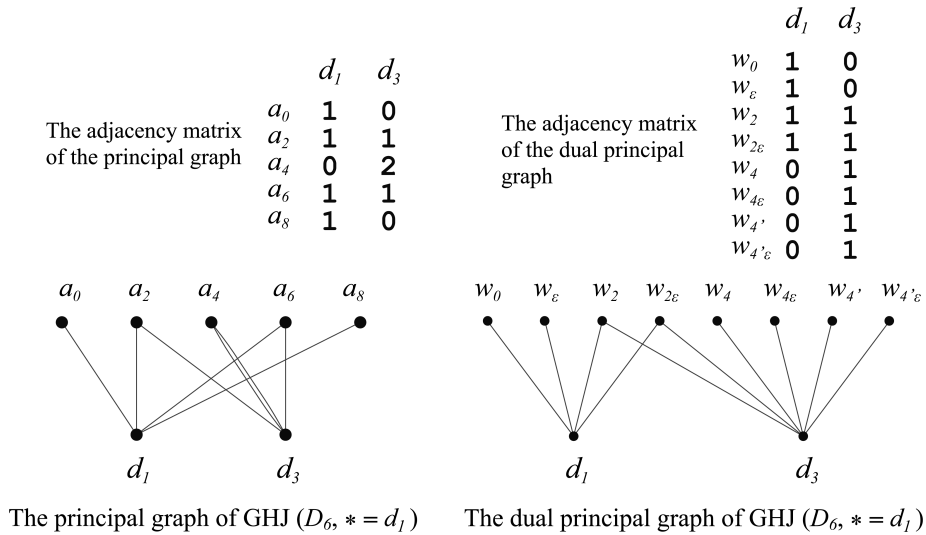


Figure 74. The (dual) principal graph of GHJ($D_6, * = d_1$).

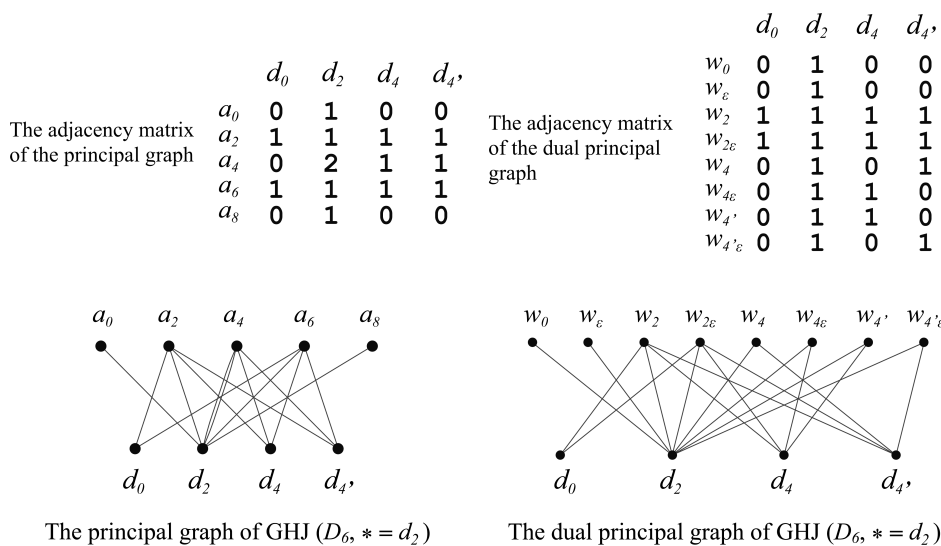


Figure 75. The (dual) principal graph of GHJ($D_6, * = d_2$).

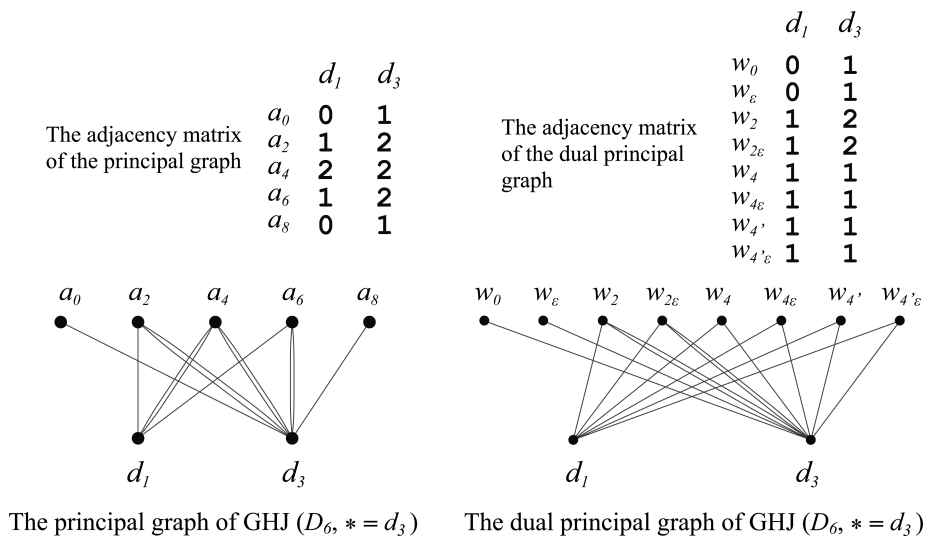


Figure 76. The (dual) principal graph of GHJ($D_6, * = d_3$).

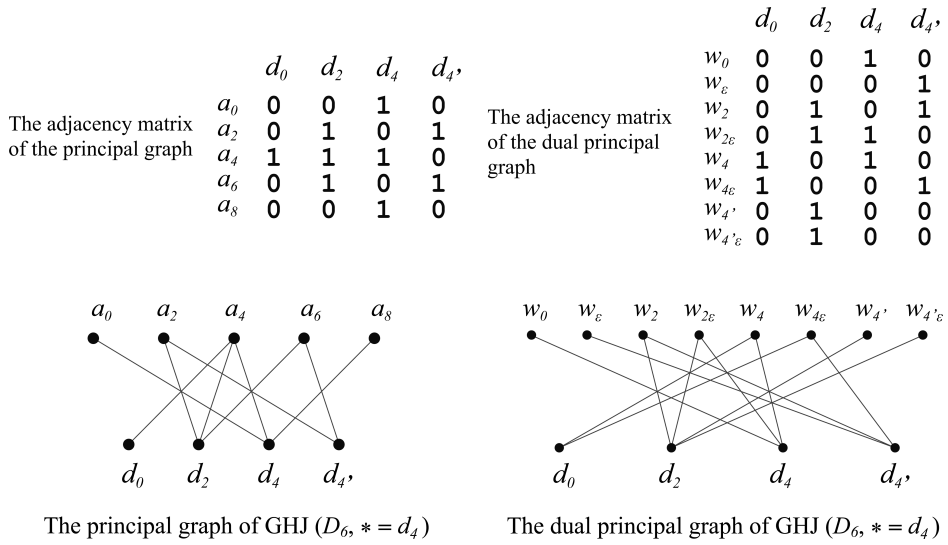
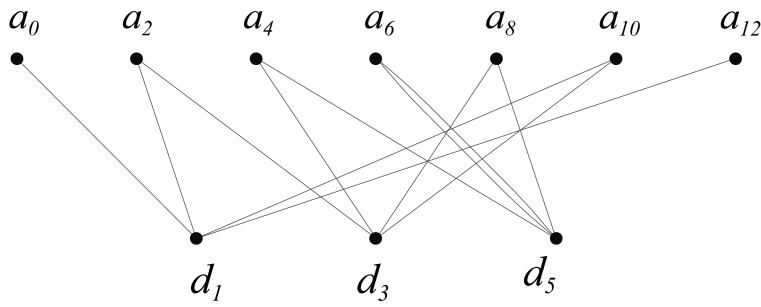


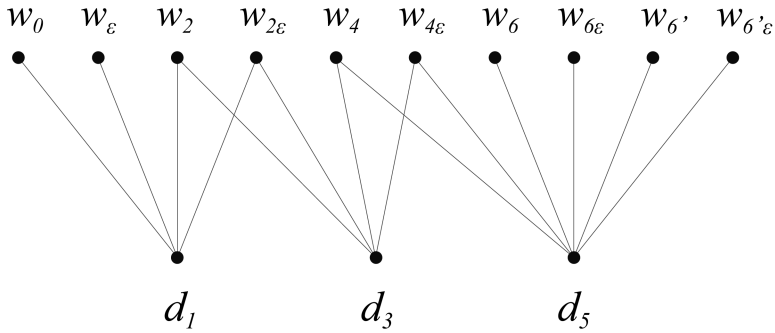
Figure 77. The (dual) principal graph of GHJ($D_6, * = d_4$).

	d_1	d_3	d_5		d_1	d_3	d_5
a_0	1	0	0	The adjacency matrix of the dual principal graph	w_0	1	0
a_2	1	1	0		w_ε	1	0
a_4	0	1	1		w_2	1	1
a_6	0	0	2		$w_{2\varepsilon}$	1	1
a_8	0	1	1		w_4	0	1
a_{10}	1	1	0		$w_{4\varepsilon}$	0	1
a_{12}	1	0	0		w_6	0	0
				$w_{6\varepsilon}$	0	0	
				$w_{6'}$	0	0	
				$w_{6'\varepsilon}$	0	0	

The adjacency matrix of the principal graph



The principal graph of GHJ ($D_8, * = d_1$)



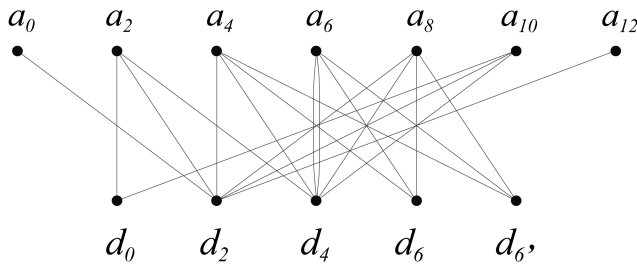
The dual principal graph of GHJ ($D_8, * = d_1$)

Figure 78. The (dual) principal graph of GHJ($D_8, * = d_1$).

	d_0	d_2	d_4	d_6	d_6'
a_0	0	1	0	0	0
a_2	1	1	1	0	0
a_4	0	1	1	1	1
a_6	0	0	2	1	1
a_8	0	1	1	1	1
a_{10}	1	1	1	0	0
a_{12}	0	1	0	0	0

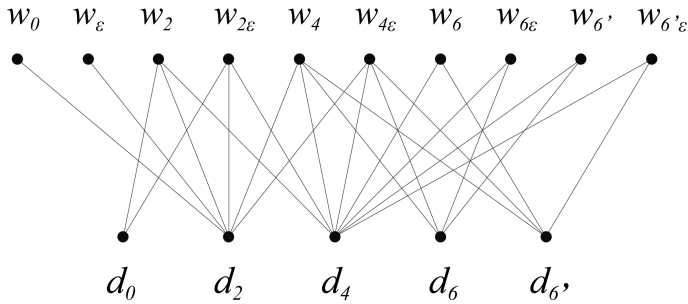
The adjacency matrix of the principal graph

	d_0	d_2	d_4	d_6	d_6'
w_0	0	1	0	0	0
w_ε	0	1	0	0	0
w_2	1	1	1	0	0
$w_{2\varepsilon}$	1	1	1	0	0
w_4	0	1	1	1	1
$w_{4\varepsilon}$	0	1	1	1	1
w_6	0	0	1	0	1
$w_{6\varepsilon}$	0	0	1	1	0
$w_{6'}$	0	0	1	1	0
$w_{6'\varepsilon}$	0	0	1	0	1



The principal graph of GHJ ($D_8, * = d_2$)

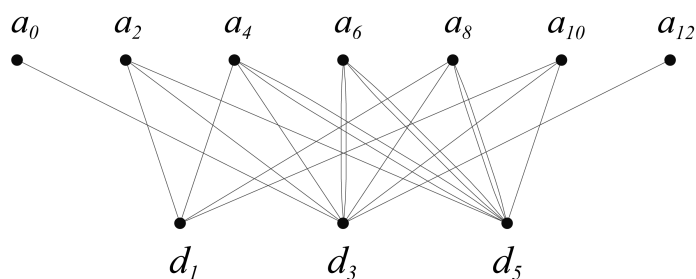
The adjacency matrix of the dual principal graph



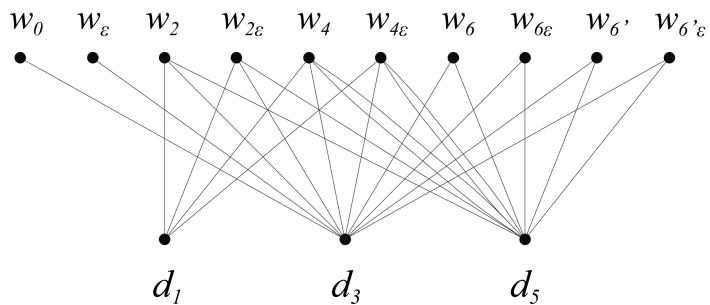
The dual principal graph of GHJ ($D_8, * = d_2$)

Figure 79. The (dual) principal graph of GHJ($D_8, * = d_2$).

	d_1	d_3	d_5		d_1	d_3	d_5	
a_0	0	1	0	The adjacency matrix of the dual principal graph	w_0	0	1	0
a_2	1	1	1		w_ε	0	1	0
a_4	1	1	2		w_2	1	1	1
a_6	0	2	2		$w_{2\varepsilon}$	1	1	1
a_8	1	1	2		w_4	1	1	2
a_{10}	1	1	1		$w_{4\varepsilon}$	1	1	2
a_{12}	0	1	0		w_6	0	1	1
The adjacency matrix of the principal graph				$w_{6\varepsilon}$	0	1	1	
				$w_{6'}$	0	1	1	
				$w_{6'\varepsilon}$	0	1	1	



The principal graph of GHJ ($D_8, * = d_3$)



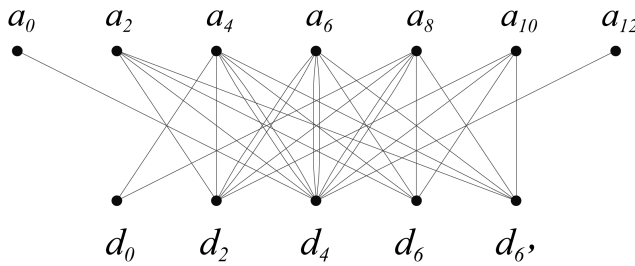
The dual principal graph of GHJ ($D_8, * = d_3$)

Figure 80. The (dual) principal graph of GHJ($D_8, * = d_3$).

	d_0	d_2	d_4	d_6	d_6'
a_0	0	0	1	0	0
a_2	0	1	1	1	1
a_4	1	1	2	1	1
a_6	0	2	2	1	1
a_8	1	1	2	1	1
a_{10}	0	1	1	1	1
a_{12}	0	0	1	0	0

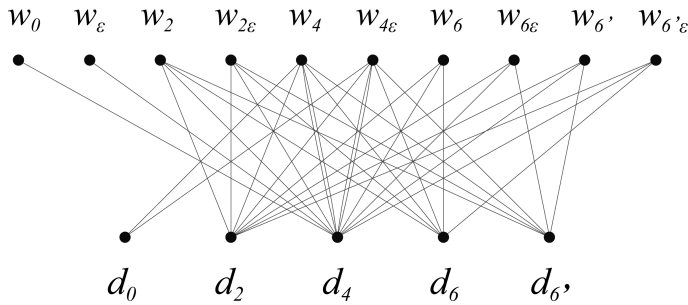
The adjacency matrix of the principal graph

	d_0	d_2	d_4	d_6	d_6'
w_0	0	0	1	0	0
w_ε	0	0	1	0	0
w_2	0	1	1	1	1
$w_{2\varepsilon}$	0	1	1	1	1
w_4	1	1	2	1	1
$w_{4\varepsilon}$	1	1	2	1	1
w_6	0	1	1	1	0
$w_{6\varepsilon}$	0	1	1	0	1
$w_{6'}$	0	1	1	0	1
$w_{6'\varepsilon}$	0	1	1	1	0



The principal graph of GHJ ($D_8, * = d_4$)

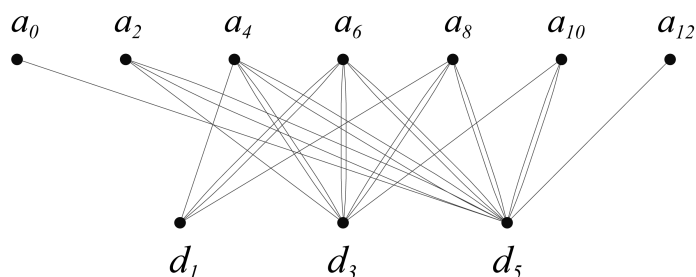
The adjacency matrix of the dual principal graph



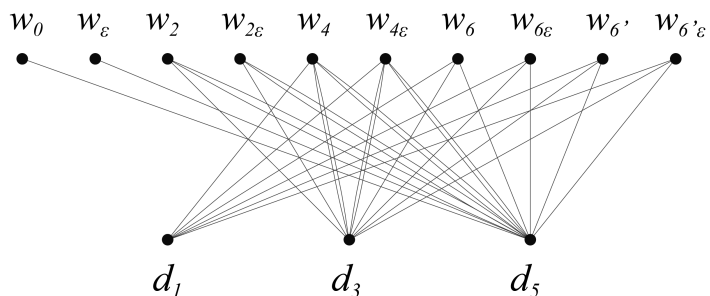
The dual principal graph of GHJ ($D_8, * = d_4$)

Figure 81. The (dual) principal graph of GHJ($D_8, * = d_4$).

	d_1	d_3	d_5		d_1	d_3	d_5
a_0	0	0	1	The adjacency matrix of the dual principal graph	w_0	0	1
a_2	0	1	2		w_ε	0	1
a_4	1	2	2		w_2	0	1
a_6	2	2	2		$w_{2\varepsilon}$	0	1
a_8	1	2	2		w_4	1	2
a_{10}	0	1	2		$w_{4\varepsilon}$	1	2
a_{12}	0	0	1		w_6	1	1
The adjacency matrix of the principal graph				$w_{6\varepsilon}$	1	1	
				$w_{6'}$	1	1	
				$w_{6'\varepsilon}$	1	1	



The principal graph of GHJ ($D_8, * = d_5$)



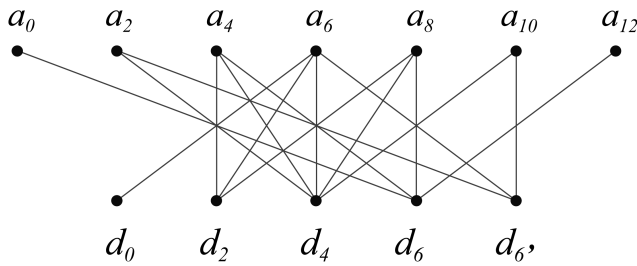
The dual principal graph of GHJ ($D_8, * = d_5$)

Figure 82. The (dual) principal graph of GHJ($D_8, * = d_5$).

	d_0	d_2	d_4	d_6	d_6'
a_0	0	0	0	1	0
a_2	0	0	1	0	1
a_4	0	1	1	1	0
a_6	1	1	1	0	1
a_8	0	1	1	1	0
a_{10}	0	0	1	0	1
a_{12}	0	0	0	1	0

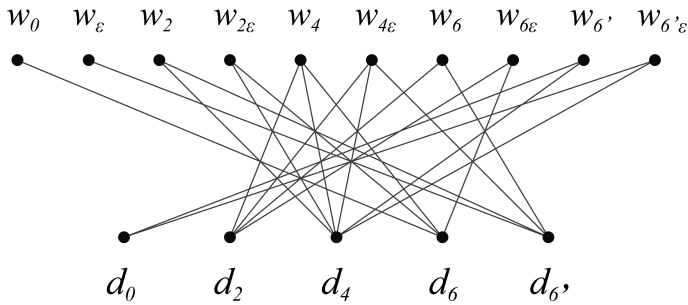
The adjacency matrix of the principal graph

	d_0	d_2	d_4	d_6	d_6'
w_0	0	0	0	1	0
w_ε	0	0	0	0	1
w_2	0	0	1	0	1
$w_{2\varepsilon}$	0	0	1	1	0
w_4	0	1	1	1	0
$w_{4\varepsilon}$	0	1	1	0	1
w_6	0	1	0	0	1
$w_{6\varepsilon}$	0	1	0	1	0
$w_{6'}$	1	0	1	0	0
$w_{6'\varepsilon}$	1	0	1	0	0



The principal graph of GHJ ($D_8, * = d_6$)

The adjacency matrix of the dual principal graph



The dual principal graph of GHJ ($D_8, * = d_6$)

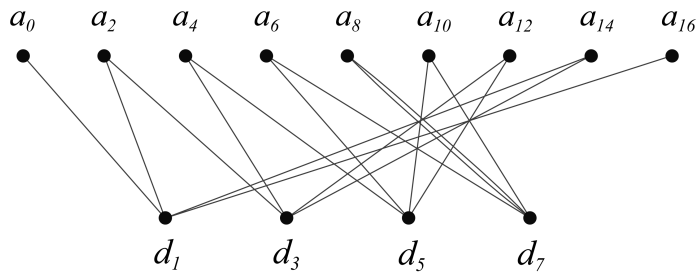
Figure 83. The (dual) principal graph of GHJ($D_8, * = d_6$).

	d_1	d_3	d_5	d_7
a_0	1	0	0	0
a_2	1	1	0	0
a_4	0	1	1	0
a_6	0	0	1	1
a_8	0	0	0	2
a_{10}	0	0	1	1
a_{12}	0	1	1	0
a_{14}	1	1	0	0
a_{16}	1	0	0	0

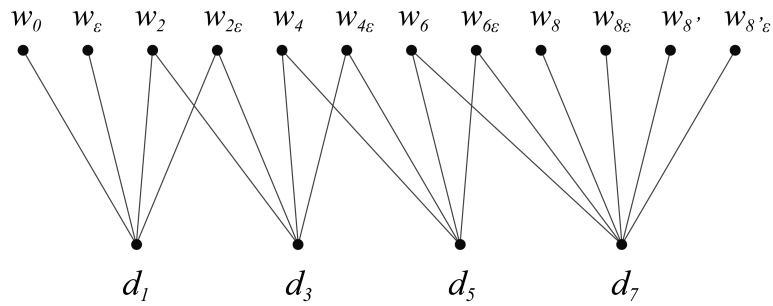
The adjacency matrix of the principal graph

	d_1	d_3	d_5	d_7
w_0	1	0	0	0
w_ε	1	0	0	0
w_2	1	1	0	0
$w_{2\varepsilon}$	1	1	0	0
w_4	0	1	1	0
$w_{4\varepsilon}$	0	1	1	0
w_6	0	0	1	1
$w_{6\varepsilon}$	0	0	1	1
w_8	0	0	0	1
$w_{8\varepsilon}$	0	0	0	1
$w_{8'}$	0	0	0	1
$w_{8'\varepsilon}$	0	0	0	1

The adjacency matrix of the dual principal graph



The principal graph of GHJ ($D_{10}, * = d_1$)



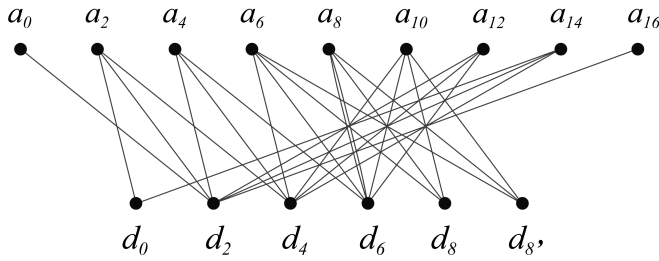
The dual principal graph of GHJ ($D_{10}, * = d_1$)

Figure 84. The (dual) principal graph of GHJ($D_{10}, * = d_1$).

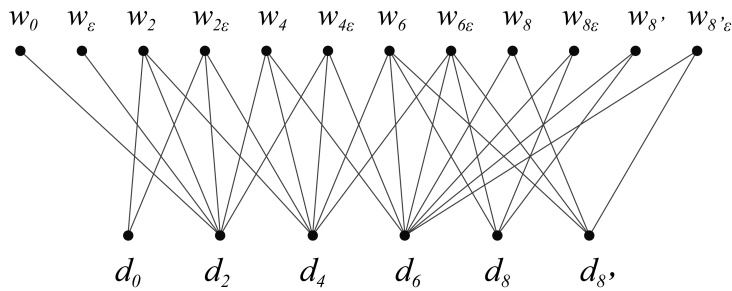
	d_0	d_2	d_4	d_6	d_8	$d_{8'}$		d_0	d_2	d_4	d_6	d_8	$d_{8'}$
a_0	0	1	0	0	0	0	w_0	0	1	0	0	0	0
a_2	1	1	1	0	0	0	w_ε	0	1	0	0	0	0
a_4	0	1	1	1	0	0	w_2	1	1	1	0	0	0
a_6	0	0	1	1	1	1	$w_{2\varepsilon}$	1	1	1	0	0	0
a_8	0	0	0	2	1	1	w_4	0	1	1	1	0	0
a_{10}	0	0	1	1	1	1	$w_{4\varepsilon}$	0	1	1	1	0	0
a_{12}	0	1	1	1	0	0	w_6	0	0	1	1	1	1
a_{14}	1	1	1	0	0	0	$w_{6\varepsilon}$	0	0	1	1	1	1
a_{16}	0	1	0	0	0	0	w_8	0	0	0	1	0	1
							$w_{8\varepsilon}$	0	0	0	1	1	0
							$w_{8'}$	0	0	0	1	1	0
							$w_{8'\varepsilon}$	0	0	0	1	0	1

The adjacency matrix of the principal graph

The adjacency matrix of the dual principal graph



The principal graph of GHJ ($D_{10}, * = d_2$)



The dual principal graph of GHJ ($D_{10}, * = d_2$)

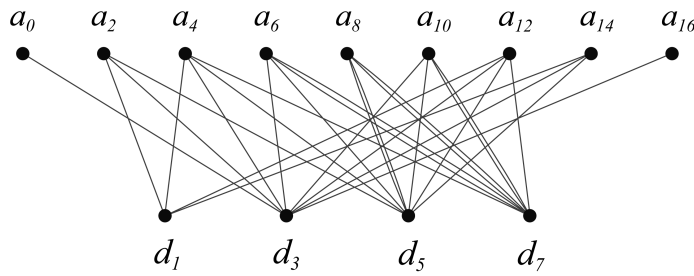
Figure 85. The (dual) principal graph of GHJ($D_{10}, * = d_2$).

	d_1	d_3	d_5	d_7
a_0	0	1	0	0
a_2	1	1	1	0
a_4	1	1	1	1
a_6	0	1	1	2
a_8	0	0	2	2
a_{10}	0	1	1	2
a_{12}	1	1	1	1
a_{14}	1	1	1	0
a_{16}	0	1	0	0

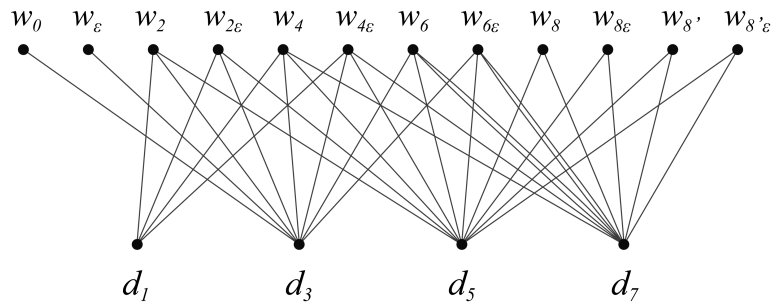
The adjacency matrix of the principal graph

	d_1	d_3	d_5	d_7
w_0	0	1	0	0
w_ε	0	1	0	0
w_2	1	1	1	0
$w_{2\varepsilon}$	1	1	1	0
w_4	1	1	1	1
$w_{4\varepsilon}$	1	1	1	1
w_6	0	1	1	2
$w_{6\varepsilon}$	0	1	1	2
w_8	0	0	1	1
$w_{8\varepsilon}$	0	0	1	1
$w_{8'}$	0	0	1	1
$w_{8'\varepsilon}$	0	0	1	1

The adjacency matrix of the dual principal graph



The principal graph of GHJ ($D_{10}, * = d_3$)



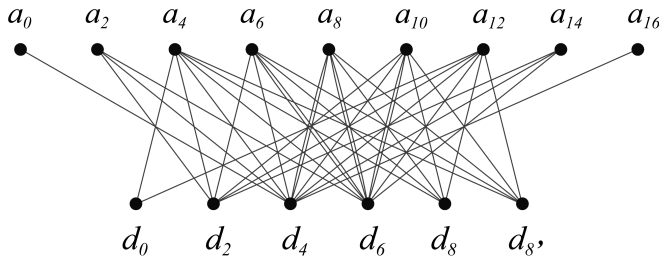
The dual principal graph of GHJ ($D_{10}, * = d_3$)

Figure 86. The (dual) principal graph of GHJ($D_{10}, * = d_3$).

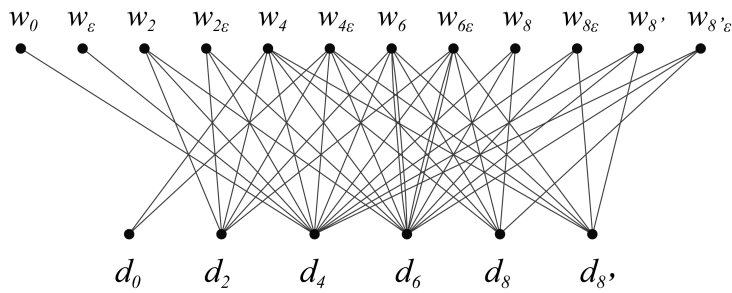
	d_0	d_2	d_4	d_6	d_8	$d_{8'}$		d_0	d_2	d_4	d_6	d_8	$d_{8'}$
a_0	0	0	1	0	0	0	w_0	0	0	1	0	0	0
a_2	0	1	1	1	0	0	w_ε	0	0	1	0	0	0
a_4	1	1	1	1	1	1	w_2	0	1	1	1	0	0
a_6	0	1	1	2	1	1	$w_{2\varepsilon}$	0	1	1	1	0	0
a_8	0	0	2	2	1	1	w_4	1	1	1	1	1	1
a_{10}	0	1	1	2	1	1	$w_{4\varepsilon}$	1	1	1	1	1	1
a_{12}	1	1	1	1	1	1	w_6	0	1	1	2	1	1
a_{14}	0	1	1	1	0	0	$w_{6\varepsilon}$	0	1	1	2	1	1
a_{16}	0	0	1	0	0	0	w_8	0	0	1	1	1	0
							$w_{8\varepsilon}$	0	0	1	1	0	1
							$w_{8'}$	0	0	1	1	0	1
							$w_{8'\varepsilon}$	0	0	1	1	1	0

The adjacency matrix of the principal graph

The adjacency matrix of the dual principal graph



The principal graph of GHJ ($D_{10}, * = d_4$)



The dual principal graph of GHJ ($D_{10}, * = d_4$)

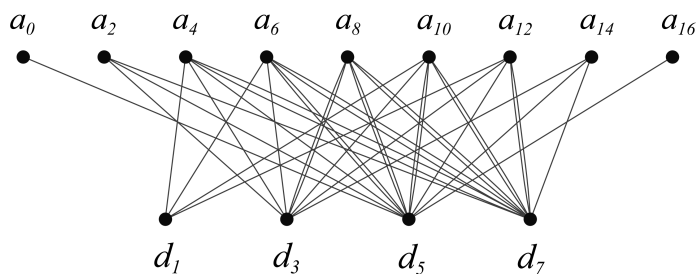
Figure 87. The (dual) principal graph of GHJ($D_{10}, * = d_4$).

	d_1	d_3	d_5	d_7
a_0	0	0	1	0
a_2	0	1	1	1
a_4	1	1	1	2
a_6	1	1	2	2
a_8	0	2	2	2
a_{10}	1	1	2	2
a_{12}	1	1	1	2
a_{14}	0	1	1	1
a_{16}	0	0	1	0

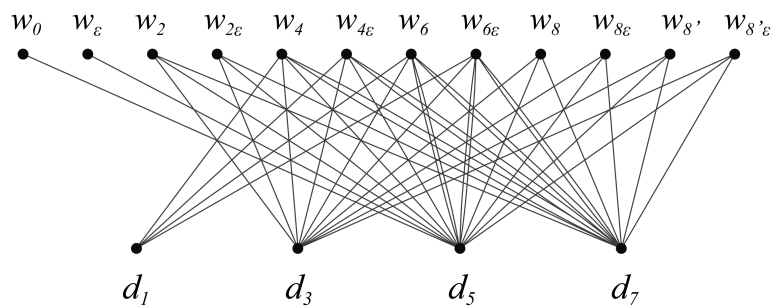
The adjacency matrix of the principal graph

	d_1	d_3	d_5	d_7
w_0	0	0	1	0
w_ε	0	0	1	0
w_2	0	1	1	1
$w_{2\varepsilon}$	0	1	1	1
w_4	1	1	1	2
$w_{4\varepsilon}$	1	1	1	2
w_6	1	1	2	2
$w_{6\varepsilon}$	1	1	2	2
w_8	0	1	1	1
$w_{8\varepsilon}$	0	1	1	1
$w_{8'}$	0	1	1	1
$w_{8'\varepsilon}$	0	1	1	1

The adjacency matrix of the dual principal graph



The principal graph of GHJ ($D_{10}, * = d_5$)



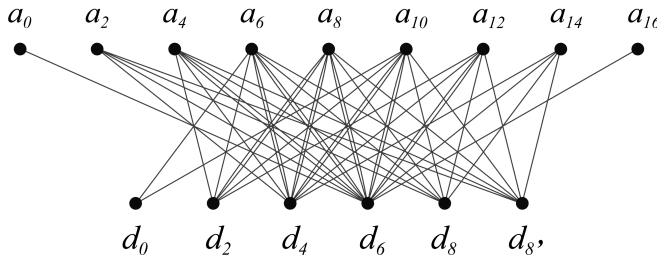
The dual principal graph of GHJ ($D_{10}, * = d_5$)

Figure 88. The (dual) principal graph of GHJ($D_{10}, * = d_5$).

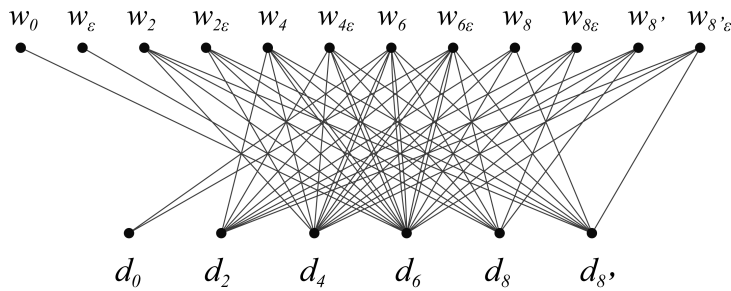
	d_0	d_2	d_4	d_6	d_8	d_8'		d_0	d_2	d_4	d_6	d_8	d_8'
a_0	0	0	0	1	0	0	w_0	0	0	0	1	0	0
a_2	0	0	1	1	1	1	w_ε	0	0	0	1	0	0
a_4	0	1	1	2	1	1	w_2	0	0	1	1	1	1
a_6	1	1	2	2	1	1	$w_{2\varepsilon}$	0	0	1	1	1	1
a_8	0	2	2	2	1	1	w_4	0	1	1	2	1	1
a_{10}	1	1	2	2	1	1	$w_{4\varepsilon}$	0	1	1	2	1	1
a_{12}	0	1	1	2	1	1	w_6	1	1	2	2	1	1
a_{14}	0	0	1	1	1	1	$w_{6\varepsilon}$	1	1	2	2	1	1
a_{16}	0	0	0	1	0	0	w_8	0	1	1	1	0	1
							$w_{8\varepsilon}$	0	1	1	1	1	0
							$w_{8'}$	0	1	1	1	1	0
							$w_{8'\varepsilon}$	0	1	1	1	0	1

The adjacency matrix of the principal graph

The adjacency matrix of the dual principal graph



The principal graph of GHJ ($D_{10}, * = d_6$)



The dual principal graph of GHJ ($D_{10}, * = d_6$)

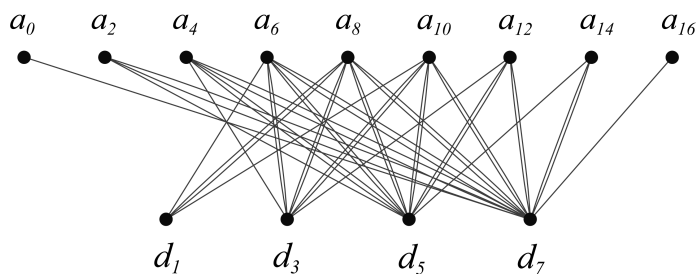
Figure 89. The (dual) principal graph of GHJ($D_{10}, * = d_6$).

	d_1	d_3	d_5	d_7
a_0	0	0	0	1
a_2	0	0	1	2
a_4	0	1	2	2
a_6	1	2	2	2
a_8	2	2	2	2
a_{10}	1	2	2	2
a_{12}	0	1	2	2
a_{14}	0	0	1	2
a_{16}	0	0	0	1

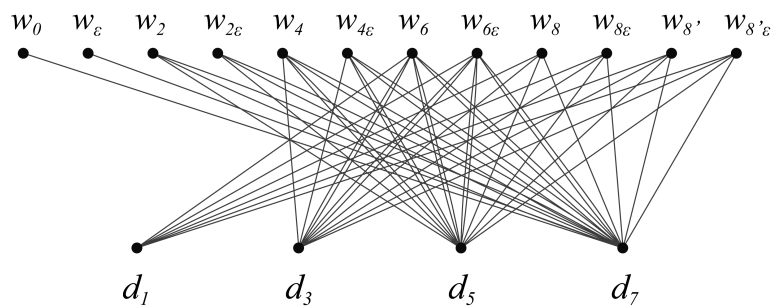
The adjacency matrix of the principal graph

	d_1	d_3	d_5	d_7
w_0	0	0	0	1
w_ε	0	0	0	1
w_2	0	0	1	2
$w_{2\varepsilon}$	0	0	1	2
w_4	0	1	2	2
$w_{4\varepsilon}$	0	1	2	2
w_6	1	2	2	2
$w_{6\varepsilon}$	1	2	2	2
w_8	1	1	1	1
$w_{8\varepsilon}$	1	1	1	1
$w_{8'}$	1	1	1	1
$w_{8'\varepsilon}$	1	1	1	1

The adjacency matrix of the dual principal graph



The principal graph of GHJ ($D_{10}, * = d_7$)



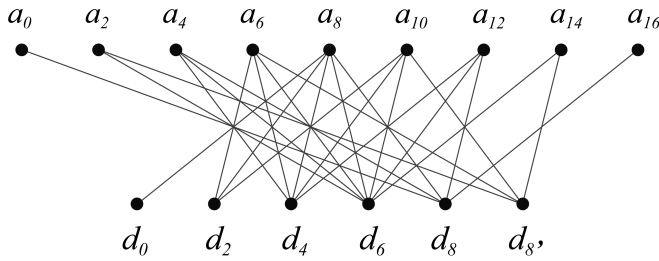
The dual principal graph of GHJ ($D_{10}, * = d_7$)

Figure 90. The (dual) principal graph of GHJ($D_{10}, * = d_7$).

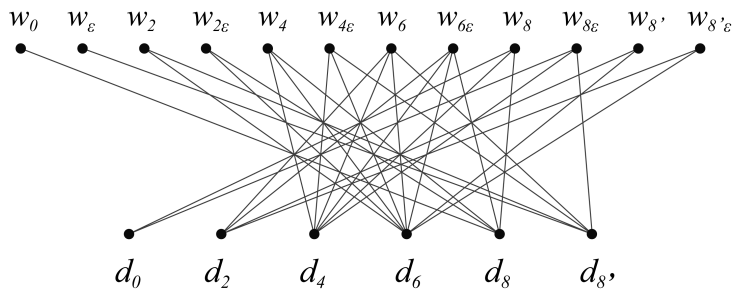
	d_0	d_2	d_4	d_6	d_8	d_8'		d_0	d_2	d_4	d_6	d_8	d_8'
a_0	0	0	0	0	1	0	w_0	0	0	0	0	1	0
a_2	0	0	0	1	0	1	w_ε	0	0	0	0	0	1
a_4	0	0	1	1	1	0	w_2	0	0	0	1	0	1
a_6	0	1	1	1	0	1	$w_{2\varepsilon}$	0	0	0	1	1	0
a_8	1	1	1	1	1	0	w_4	0	0	1	1	1	0
a_{10}	0	1	1	1	0	1	$w_{4\varepsilon}$	0	0	1	1	0	1
a_{12}	0	0	1	1	1	0	w_6	0	1	1	1	0	1
a_{14}	0	0	0	1	0	1	$w_{6\varepsilon}$	0	1	1	1	1	0
a_{16}	0	0	0	0	1	0	w_8	1	0	1	0	1	0
							$w_{8\varepsilon}$	1	0	1	0	0	1
							$w_{8'}$	0	1	0	1	0	0
							$w_{8'\varepsilon}$	0	1	0	1	0	0

The adjacency matrix of the principal graph

The adjacency matrix of the dual principal graph



The principal graph of GHJ ($D_{10}, * = d_8$)



The dual principal graph of GHJ ($D_{10}, * = d_8$)

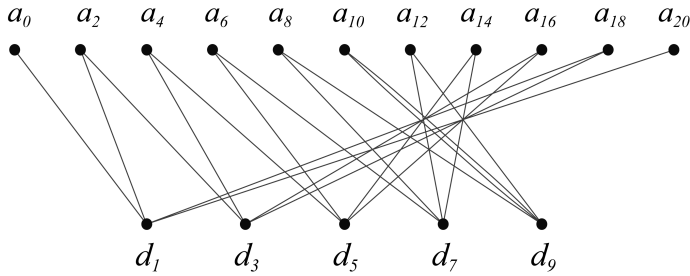
Figure 91. The (dual) principal graph of GHJ($D_{10}, * = d_8$).

	d_1	d_3	d_5	d_7	d_9
a_0	1	0	0	0	0
a_2	1	1	0	0	0
a_4	0	1	1	0	0
a_6	0	0	1	1	0
a_8	0	0	0	1	1
a_{10}	0	0	0	0	2
a_{12}	0	0	0	1	1
a_{14}	0	0	1	1	0
a_{16}	0	1	1	0	0
a_{18}	1	1	0	0	0
a_{20}	1	0	0	0	0

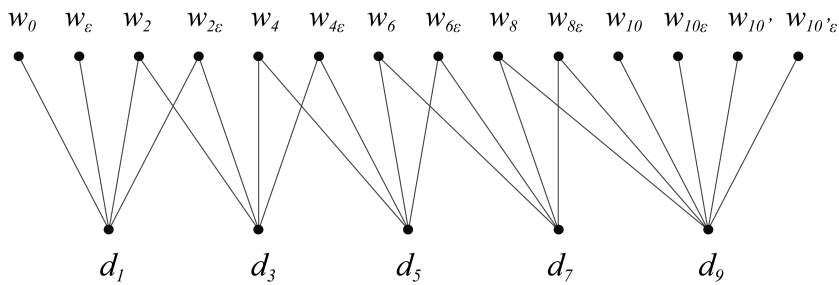
The adjacency matrix of the principal graph

	d_1	d_3	d_5	d_7	d_9
w_0	1	0	0	0	0
w_ε	1	0	0	0	0
w_2	1	1	0	0	0
$w_{2\varepsilon}$	1	1	0	0	0
w_4	0	1	1	0	0
$w_{4\varepsilon}$	0	1	1	0	0
w_6	0	0	1	1	0
$w_{6\varepsilon}$	0	0	1	1	0
w_8	0	0	0	1	1
$w_{8\varepsilon}$	0	0	0	1	1
w_{10}	0	0	0	0	1
$w_{10\varepsilon}$	0	0	0	0	1
$w_{10'}$	0	0	0	0	1
$w_{10'\varepsilon}$	0	0	0	0	1

The adjacency matrix of the dual principal graph



The principal graph of GHJ ($D_{12}, * = d_1$)



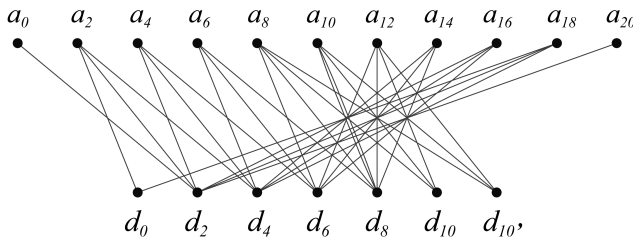
The dual principal graph of GHJ ($D_{12}, * = d_1$)

Figure 92. The (dual) principal graph of GHJ($D_{12}, * = d_1$).

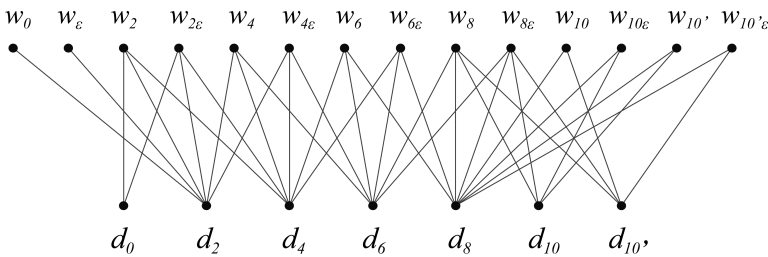
	d_0	d_2	d_4	d_6	d_8	d_{10}	$d_{10'}$		d_0	d_2	d_4	d_6	d_8	d_{10}	$d_{10'}$
a_0	0	1	0	0	0	0	0	w_0	0	1	0	0	0	0	0
a_2	1	1	1	0	0	0	0	w_ε	0	1	0	0	0	0	0
a_4	0	0	1	1	0	0	0	w_2	1	1	1	0	0	0	0
a_6	0	0	0	1	1	0	0	$w_{2\varepsilon}$	1	1	1	0	0	0	0
a_8	0	0	0	0	1	1	1	w_4	0	1	1	1	0	0	0
a_{10}	0	0	0	0	2	1	1	$w_{4\varepsilon}$	0	1	1	1	1	0	0
a_{12}	0	0	0	1	1	1	1	w_6	0	0	1	1	1	0	0
a_{14}	0	0	1	1	1	0	0	$w_{6\varepsilon}$	0	0	1	1	1	0	0
a_{16}	0	1	1	1	0	0	0	w_8	0	0	0	1	1	1	1
a_{18}	1	1	1	0	0	0	0	$w_{8\varepsilon}$	0	0	0	1	1	1	1
a_{20}	0	1	0	0	0	0	0	w_{10}	0	0	0	0	1	0	1
								$w_{10\varepsilon}$	0	0	0	0	1	1	0
								$w_{10'}$	0	0	0	0	1	1	0
								$w_{10'\varepsilon}$	0	0	0	0	1	0	1

The adjacency matrix of the principal graph

The adjacency matrix of the dual principal graph



The principal graph of GHJ ($D_{12}, * = d_2$)



The dual principal graph of GHJ ($D_{12}, * = d_2$)

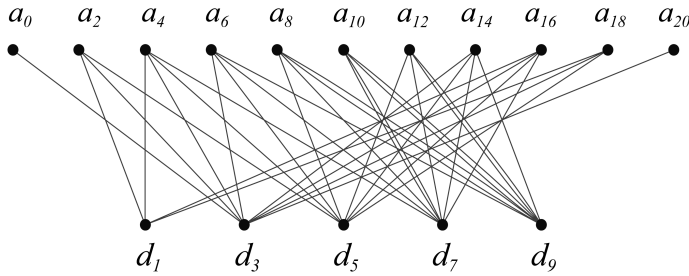
Figure 93. The (dual) principal graph of GHJ($D_{12}, * = d_2$).

	d_1	d_3	d_5	d_7	d_9
a_0	0	1	0	0	0
a_2	1	1	1	0	0
a_4	1	1	1	1	0
a_6	0	1	1	1	1
a_8	0	0	1	1	2
a_{10}	0	0	0	2	2
a_{12}	0	0	1	1	2
a_{14}	0	1	1	1	1
a_{16}	1	1	1	1	0
a_{18}	1	1	1	0	0
a_{20}	0	1	0	0	0

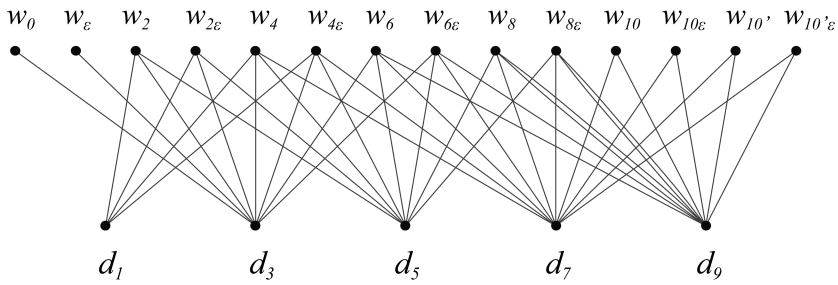
The adjacency matrix of the principal graph

	d_1	d_3	d_5	d_7	d_9
w_0	0	1	0	0	0
w_ε	0	1	0	0	0
w_2	1	1	1	0	0
$w_{2\varepsilon}$	1	1	1	0	0
w_4	1	1	1	1	0
$w_{4\varepsilon}$	1	1	1	1	0
w_6	0	1	1	1	1
$w_{6\varepsilon}$	0	1	1	1	1
w_8	0	0	1	1	2
$w_{8\varepsilon}$	0	0	1	1	2
w_{10}	0	0	0	1	1
$w_{10\varepsilon}$	0	0	0	1	1
$w_{10'}$	0	0	0	1	1
$w_{10'\varepsilon}$	0	0	0	1	1

The adjacency matrix of the dual principal graph



The principal graph of GHJ ($D_{12}, * = d_3$)



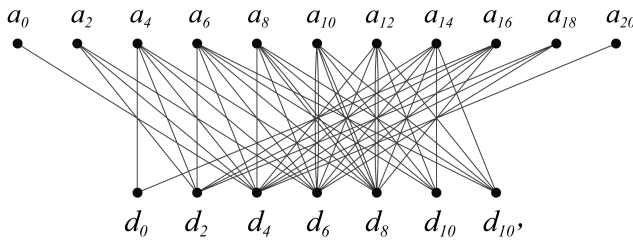
The dual principal graph of GHJ ($D_{12}, * = d_3$)

Figure 94. The (dual) principal graph of GHJ($D_{12}, * = d_3$).

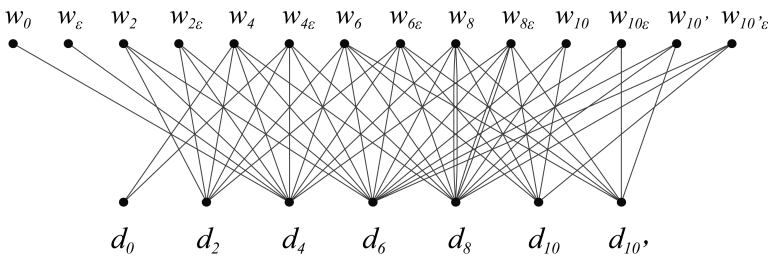
	d_0	d_2	d_4	d_6	d_8	d_{10}	$d_{10'}$		d_0	d_2	d_4	d_6	d_8	d_{10}	$d_{10'}$
a_0	0	0	1	0	0	0	0	w_0	0	0	1	0	0	0	0
a_2	0	1	1	1	0	0	0	w_ε	0	0	1	0	0	0	0
a_4	1	1	1	1	1	0	0	w_2	0	1	1	1	0	0	0
a_6	0	1	1	1	1	1	1	$w_{2\varepsilon}$	0	1	1	1	0	0	0
a_8	0	0	1	1	2	1	1	w_4	1	1	1	1	1	0	0
a_{10}	0	0	0	2	2	1	1	$w_{4\varepsilon}$	1	1	1	1	1	1	1
a_{12}	0	0	1	1	2	1	1	w_6	0	1	1	1	1	1	1
a_{14}	0	1	1	1	1	1	1	$w_{6\varepsilon}$	0	1	1	1	1	1	1
a_{16}	1	1	1	1	1	0	0	w_8	0	0	1	1	2	1	1
a_{18}	0	1	1	1	0	0	0	$w_{8\varepsilon}$	0	0	1	1	2	1	1
a_{20}	0	0	1	0	0	0	0	w_{10}	0	0	0	1	1	1	0
								$w_{10\varepsilon}$	0	0	0	1	1	0	1
								$w_{10'}$	0	0	0	1	1	0	1
								$w_{10'\varepsilon}$	0	0	0	1	1	1	0

The adjacency matrix of the principal graph

The adjacency matrix of the dual principal graph



The principal graph of GHJ ($D_{12}, * = d_4$)



The dual principal graph of GHJ ($D_{12}, * = d_4$)

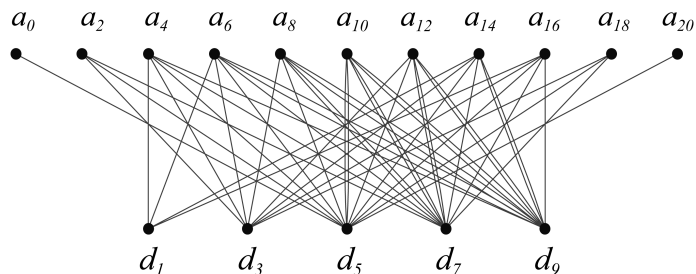
Figure 95. The (dual) principal graph of GHJ($D_{12}, * = d_4$).

	d_1	d_3	d_5	d_7	d_9
a_0	0	0	1	0	0
a_2	0	1	1	1	0
a_4	1	1	1	1	1
a_6	1	1	1	1	2
a_8	0	1	1	2	2
a_{10}	0	0	2	2	2
a_{12}	0	1	1	2	2
a_{14}	1	1	1	1	2
a_{16}	1	1	1	1	1
a_{18}	0	1	1	1	0
a_{20}	0	0	1	0	0

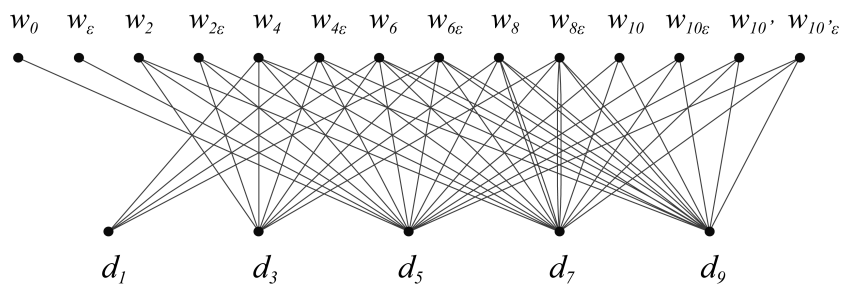
The adjacency matrix of the principal graph

	d_1	d_3	d_5	d_7	d_9
w_0	0	0	1	0	0
w_ε	0	0	1	0	0
w_2	0	1	1	1	0
$w_{2\varepsilon}$	0	1	1	1	0
w_4	1	1	1	1	1
$w_{4\varepsilon}$	1	1	1	1	1
w_6	1	1	1	1	2
$w_{6\varepsilon}$	1	1	1	1	2
w_8	0	1	1	2	2
$w_{8\varepsilon}$	0	1	1	2	2
w_{10}	0	0	1	1	1
$w_{10\varepsilon}$	0	0	1	1	1
$w_{10'}$	0	0	1	1	1
$w_{10'\varepsilon}$	0	0	1	1	1

The adjacency matrix of the dual principal graph



The principal graph of GHJ ($D_{12}, * = d_5$)



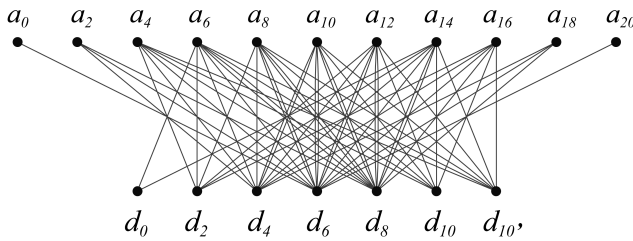
The dual principal graph of GHJ ($D_{12}, * = d_5$)

Figure 96. The (dual) principal graph of GHJ($D_{12}, * = d_5$).

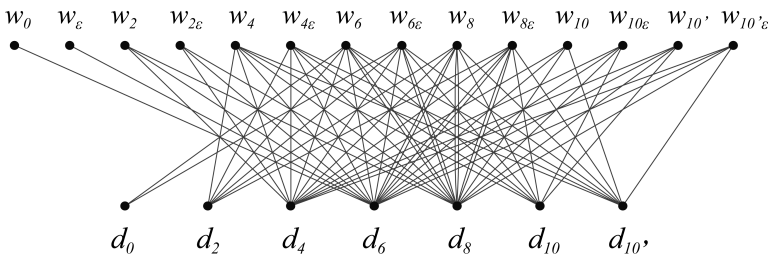
	d_0	d_2	d_4	d_6	d_8	d_{10}	$d_{10'}$		d_0	d_2	d_4	d_6	d_8	d_{10}	$d_{10'}$
a_0	0	0	0	1	0	0	0	w_0	0	0	0	1	0	0	0
a_2	0	0	1	1	1	0	0	w_ε	0	0	0	1	0	0	0
a_4	0	1	1	1	1	1	1	w_2	0	0	1	1	1	0	0
a_6	1	1	1	1	2	1	1	$w_{2\varepsilon}$	0	0	1	1	1	0	0
a_8	0	1	1	2	2	1	1	w_4	0	1	1	1	1	1	1
a_{10}	0	0	2	2	2	1	1	$w_{4\varepsilon}$	0	1	1	1	1	1	1
a_{12}	0	1	1	2	2	1	1	w_6	1	1	1	1	2	1	1
a_{14}	1	1	1	1	2	1	1	$w_{6\varepsilon}$	1	1	1	1	2	1	1
a_{16}	0	1	1	1	1	1	1	w_8	0	1	1	2	2	1	1
a_{18}	0	0	1	1	1	0	0	$w_{8\varepsilon}$	0	1	1	2	2	1	1
a_{20}	0	0	0	1	0	0	0	w_{10}	0	0	1	1	1	0	1
								$w_{10\varepsilon}$	0	0	1	1	1	1	0
								$w_{10'}$	0	0	1	1	1	1	0
								$w_{10'\varepsilon}$	0	0	1	1	1	0	1

The adjacency matrix of the principal graph

The adjacency matrix of the dual principal graph



The principal graph of GHJ ($D_{12}, * = d_6$)



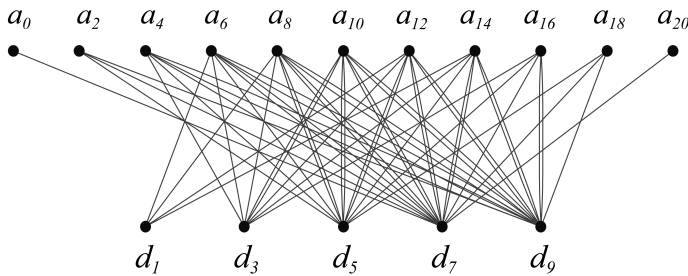
The dual principal graph of GHJ ($D_{12}, * = d_6$)

Figure 97. The (dual) principal graph of GHJ($D_{12}, * = d_6$).

	d_1	d_3	d_5	d_7	d_9
a_0	0	0	0	1	0
a_2	0	0	1	1	1
a_4	0	1	1	1	2
a_6	1	1	1	2	2
a_8	1	1	2	2	2
a_{10}	0	2	2	2	2
a_{12}	1	1	2	2	2
a_{14}	1	1	1	2	2
a_{16}	0	1	1	1	2
a_{18}	0	0	1	1	1
a_{20}	0	0	0	1	0

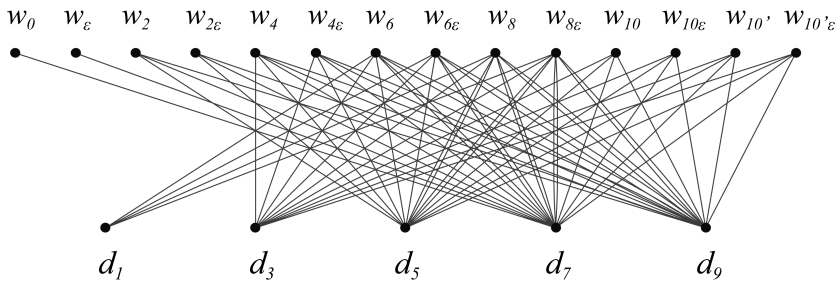
The adjacency matrix of the principal graph

	d_1	d_3	d_5	d_7	d_9
w_0	0	0	0	1	0
w_ε	0	0	0	1	0
w_2	0	0	1	1	1
$w_{2\varepsilon}$	0	0	1	1	1
w_4	0	1	1	1	2
$w_{4\varepsilon}$	0	1	1	1	2
w_6	1	1	1	2	2
$w_{6\varepsilon}$	1	1	1	2	2
w_8	1	1	2	2	2
$w_{8\varepsilon}$	1	1	2	2	2
w_{10}	0	1	1	1	1
$w_{10\varepsilon}$	0	1	1	1	1
$w_{10'}$	0	1	1	1	1
$w_{10'\varepsilon}$	0	1	1	1	1



The principal graph of GHJ ($D_{12}, * = d_7$)

The adjacency matrix of the dual principal graph



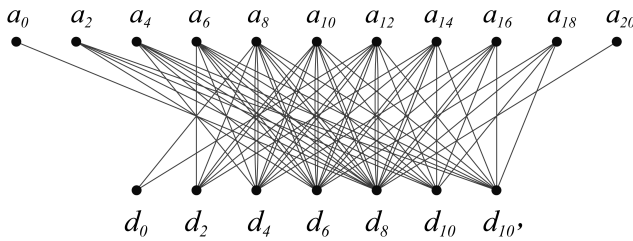
The dual principal graph of GHJ ($D_{12}, * = d_7$)

Figure 98. The (dual) principal graph of GHJ($D_{12}, * = d_7$).

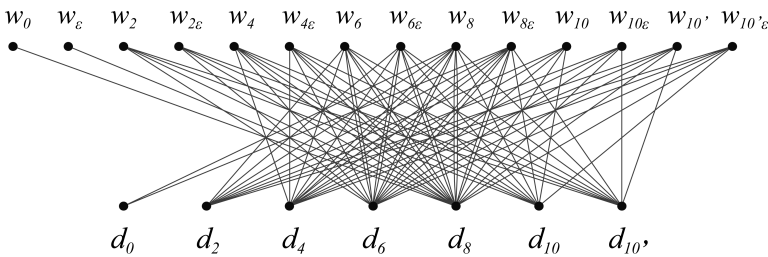
	d_0	d_2	d_4	d_6	d_8	d_{10}	$d_{10'}$		d_0	d_2	d_4	d_6	d_8	d_{10}	$d_{10'}$
a_0	0	0	0	0	1	0	0	w_0	0	0	0	0	1	0	0
a_2	0	0	0	1	1	1	1	w_ε	0	0	0	0	1	0	0
a_4	0	0	1	1	2	1	1	w_2	0	0	0	1	1	1	1
a_6	0	1	1	2	2	1	1	$w_{2\varepsilon}$	0	0	0	1	1	1	1
a_8	1	1	2	2	2	1	1	w_4	0	0	1	1	2	1	1
a_{10}	0	2	2	2	2	1	1	$w_{4\varepsilon}$	0	0	1	1	2	1	1
a_{12}	1	1	2	2	2	1	1	w_6	0	1	1	2	2	1	1
a_{14}	0	1	1	2	2	1	1	$w_{6\varepsilon}$	0	1	1	2	2	1	1
a_{16}	0	0	1	1	2	1	1	w_8	1	1	2	2	2	1	1
a_{18}	0	0	0	1	1	1	1	$w_{8\varepsilon}$	1	1	2	2	2	1	1
a_{20}	0	0	0	0	1	0	0	w_{10}	0	1	1	1	1	1	0
								$w_{10\varepsilon}$	0	1	1	1	1	0	1
								$w_{10'}$	0	1	1	1	1	0	1
								$w_{10'\varepsilon}$	0	1	1	1	1	1	0

The adjacency matrix of the principal graph

The adjacency matrix of the dual principal graph



The principal graph of GHJ ($D_{12}, * = d_8$)



The dual principal graph of GHJ ($D_{12}, * = d_8$)

Figure 99. The (dual) principal graph of GHJ($D_{12}, * = d_8$).

	d_1	d_3	d_5	d_7	d_9
a_0	0	0	0	0	1
a_2	0	0	0	1	2
a_4	0	0	1	2	2
a_6	0	1	2	2	2
a_8	1	2	2	2	2
a_{10}	2	2	2	2	2
a_{12}	1	2	2	2	2
a_{14}	0	1	2	2	2
a_{16}	0	0	1	2	2
a_{18}	0	0	0	1	2
a_{20}	0	0	0	0	1

The adjacency matrix
of the principal graph

	d_1	d_3	d_5	d_7	d_9
w_0	0	0	0	0	1
w_ε	0	0	0	0	1
w_2	0	0	0	1	2
$w_{2\varepsilon}$	0	0	0	1	2
w_4	0	0	1	2	2
$w_{4\varepsilon}$	0	0	1	2	2
w_6	0	1	2	2	2
$w_{6\varepsilon}$	0	1	2	2	2
w_8	1	2	2	2	2
$w_{8\varepsilon}$	1	2	2	2	2
w_{10}	1	1	1	1	1
$w_{10\varepsilon}$	1	1	1	1	1
$w_{10'}$	1	1	1	1	1
$w_{10'\varepsilon}$	1	1	1	1	1

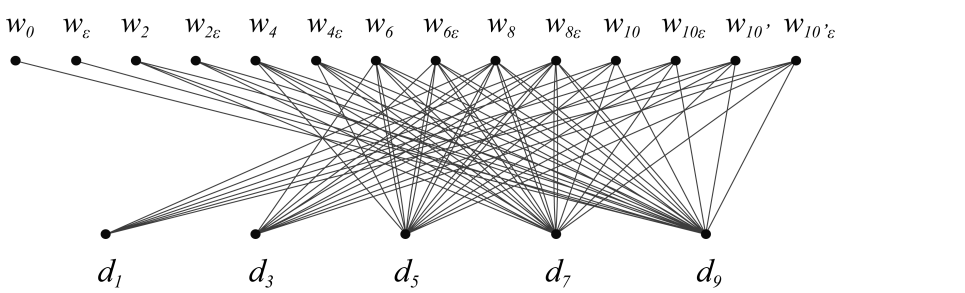
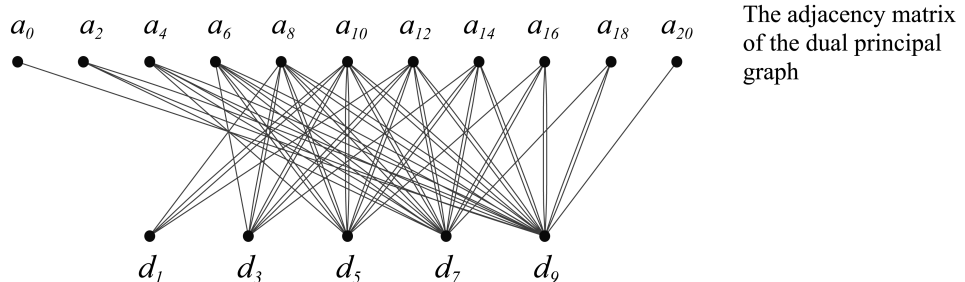
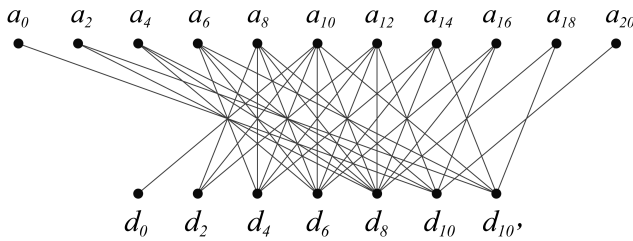


Figure 100. The (dual) principal graph of GHJ($D_{12}, * = d_9$).

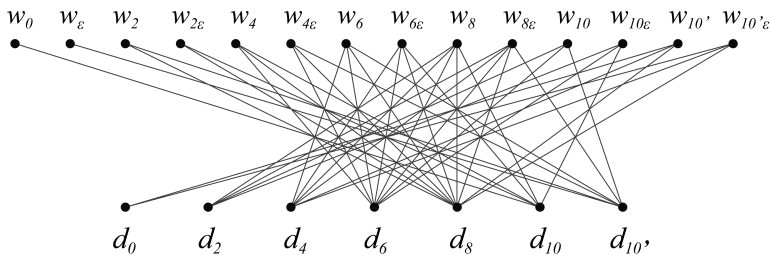
	d_0	d_2	d_4	d_6	d_8	d_{10}	d_{10}'		d_0	d_2	d_4	d_6	d_8	d_{10}	d_{10}'
a_0	0	0	0	0	0	1	0	w_0	0	0	0	0	0	1	0
a_2	0	0	0	0	1	0	1	w_ε	0	0	0	0	0	0	1
a_4	0	0	0	1	1	1	0	w_2	0	0	0	0	1	0	1
a_6	0	0	1	1	1	0	1	$w_{2\varepsilon}$	0	0	0	0	1	1	0
a_8	0	1	1	1	1	1	0	w_4	0	0	0	1	1	1	0
a_{10}	1	1	1	1	1	0	1	$w_{4\varepsilon}$	0	0	0	1	1	0	1
a_{12}	0	1	1	1	1	1	0	w_6	0	0	1	1	1	0	1
a_{14}	0	0	1	1	1	0	1	$w_{6\varepsilon}$	0	0	1	1	1	1	0
a_{16}	0	0	0	1	1	1	0	w_8	0	1	1	1	1	1	0
a_{18}	0	0	0	0	1	0	1	$w_{8\varepsilon}$	0	1	1	1	1	0	1
a_{20}	0	0	0	0	0	1	0	w_{10}	0	1	0	1	0	0	1
								$w_{10\varepsilon}$	0	1	0	1	0	1	0
								$w_{10'}$	1	0	1	0	1	0	0
								$w_{10'\varepsilon}$	1	0	1	0	1	0	0

The adjacency matrix of the principal graph

The adjacency matrix of the dual principal graph



The principal graph of GHJ ($D_{12}, * = d_{10}$)



The dual principal graph of GHJ ($D_{12}, * = d_{10}$)

Figure 101. The (dual) principal graph of GHJ($D_{12}, * = d_{10}$).

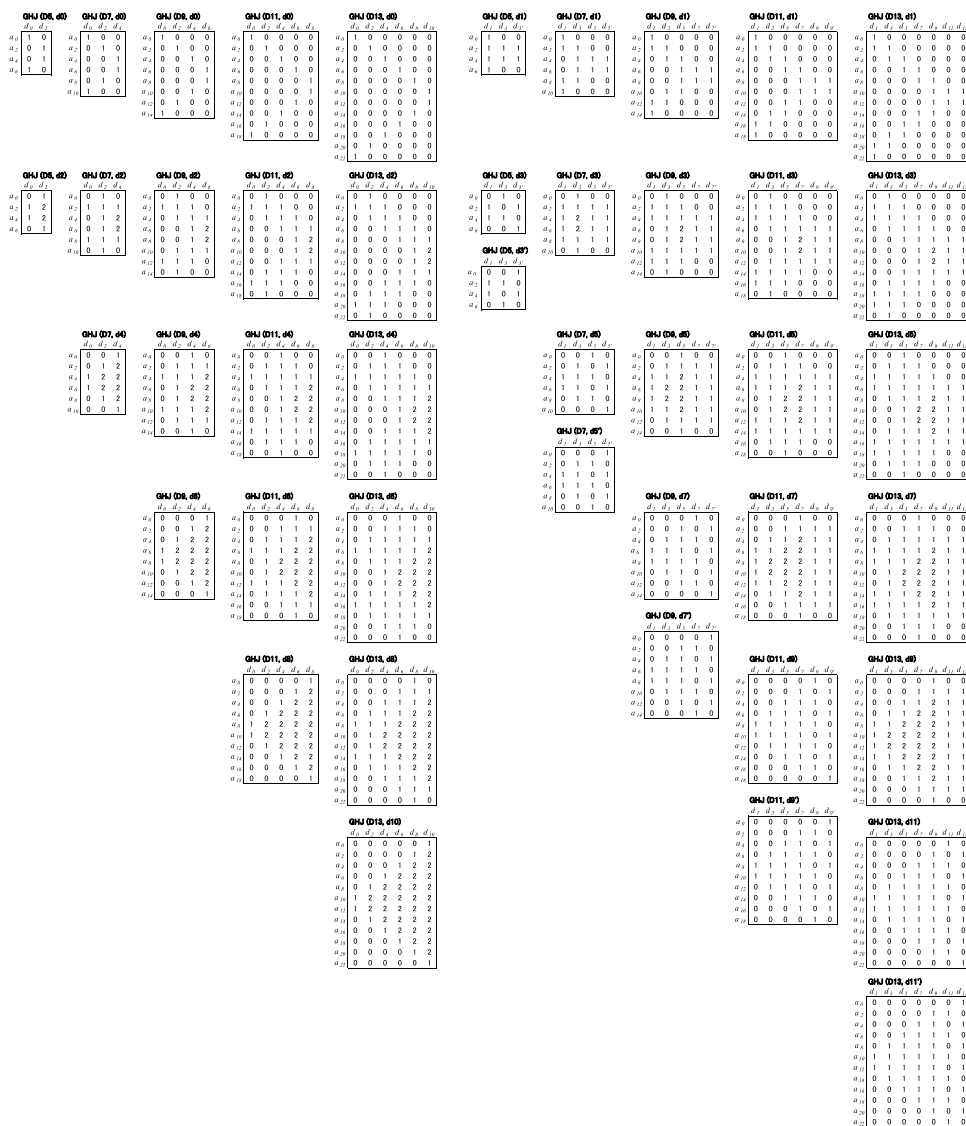


Figure 102. The incidence matrices of the (dual) principal graphs of $GHJ(D_{odd})$.

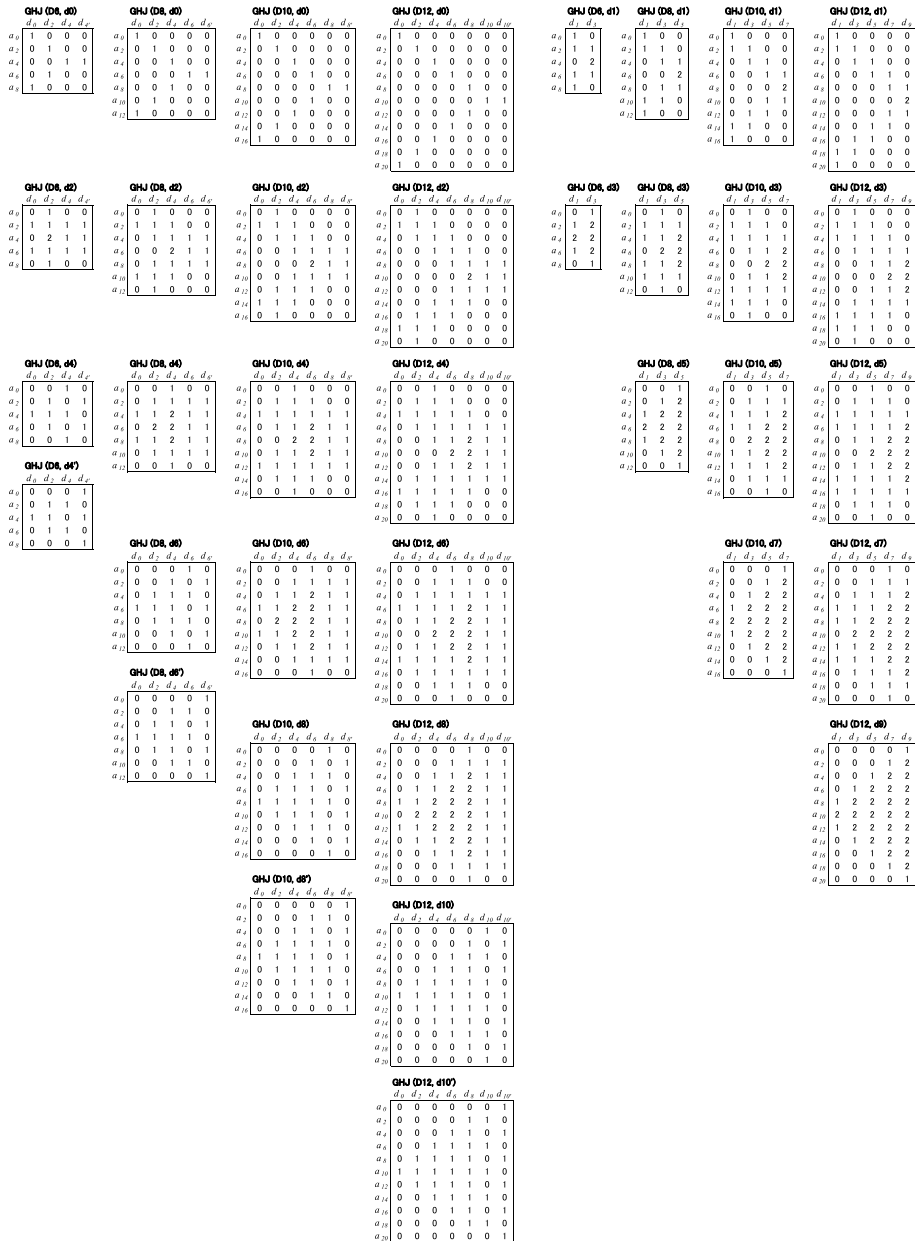


Figure 103. The incidence matrices of the principal graphs of $\text{GHJ}(D_{\text{even}})$.

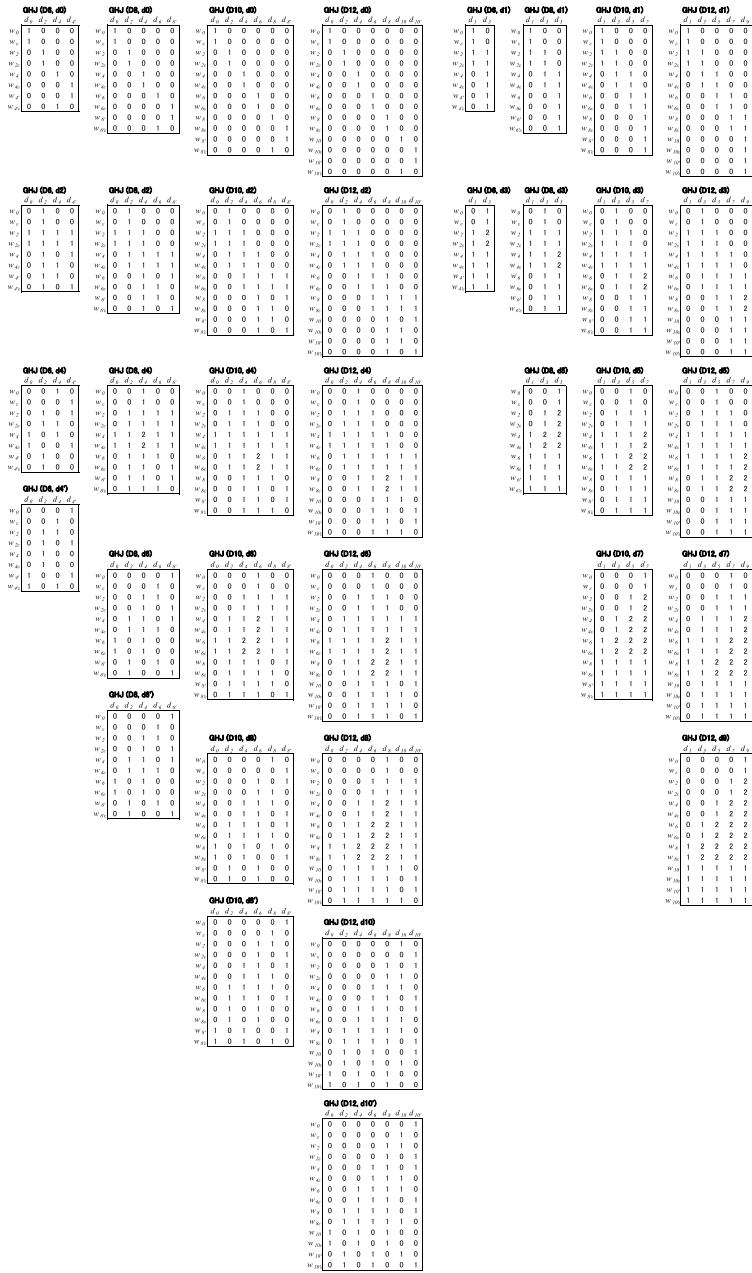


Figure 104. The incidence matrices of the dual principal graphs of $\text{GHJ}(D_{\text{even}})$.

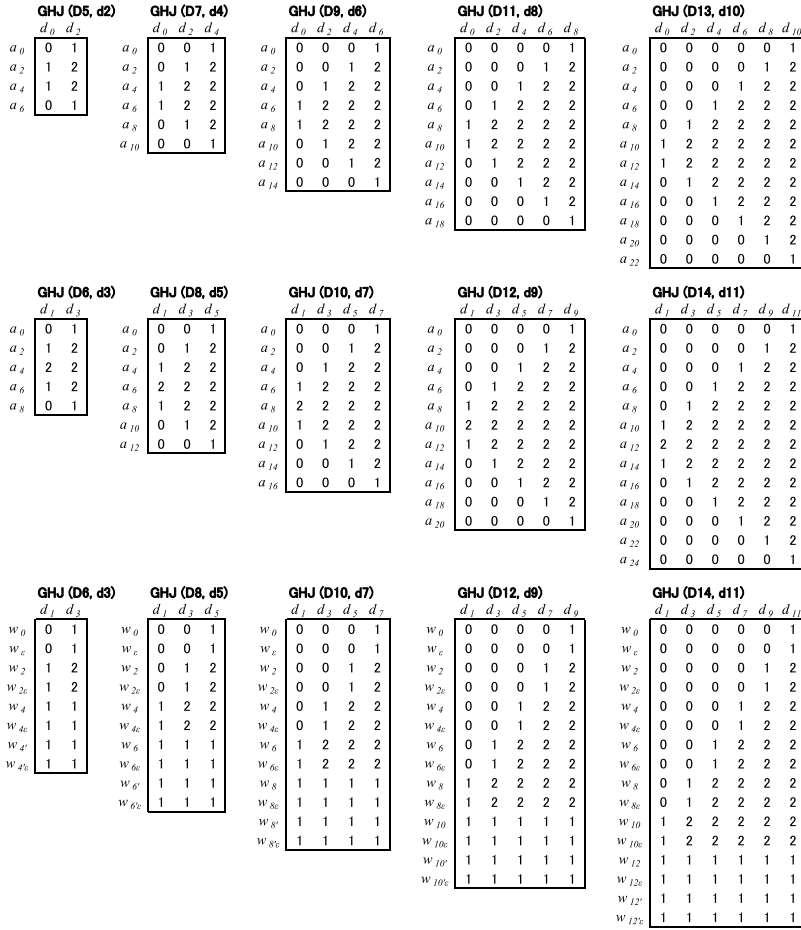


Figure 105. The incidence matrices of the (dual) principal graphs of GHJ(D, * = triple point).

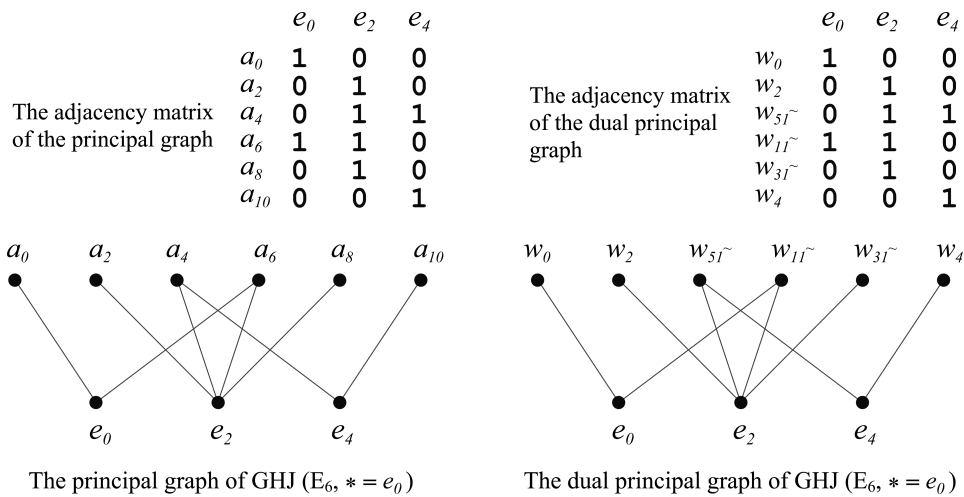


Figure 106. The (dual) principal graph of GHJ($E_6, * = e_0$).

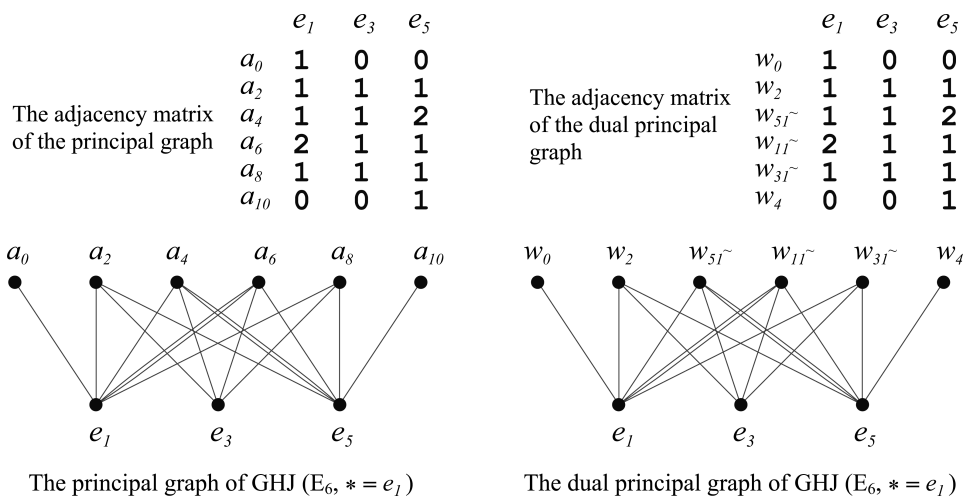


Figure 107. The (dual) principal graph of GHJ($E_6, * = e_1$).

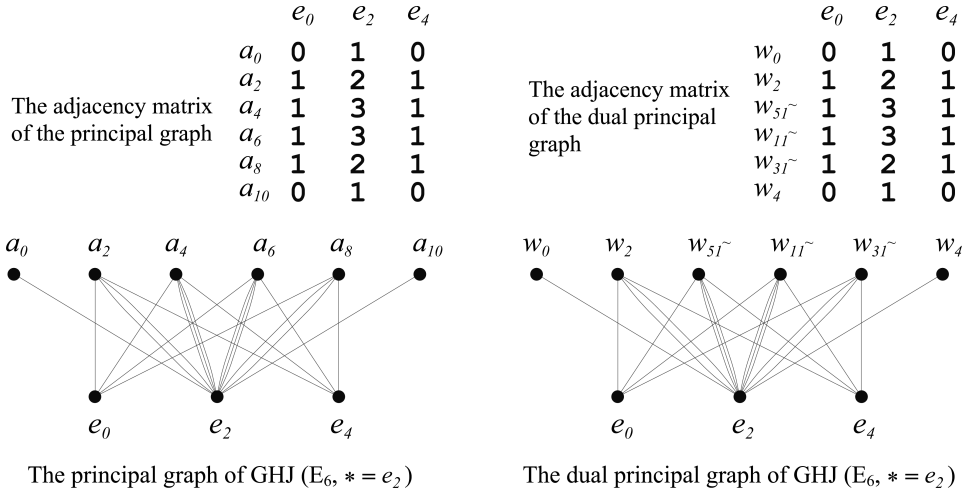


Figure 108. The (dual) principal graph of GHJ($E_6, * = e_2$).

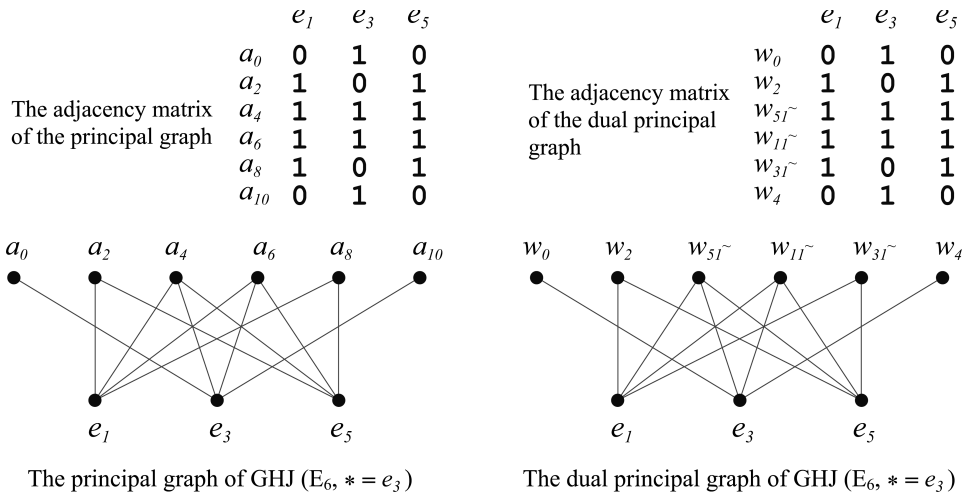
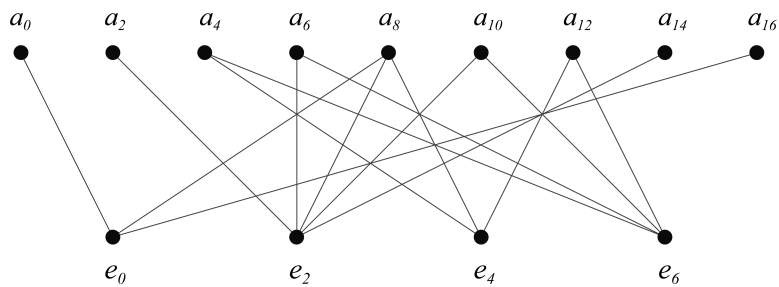
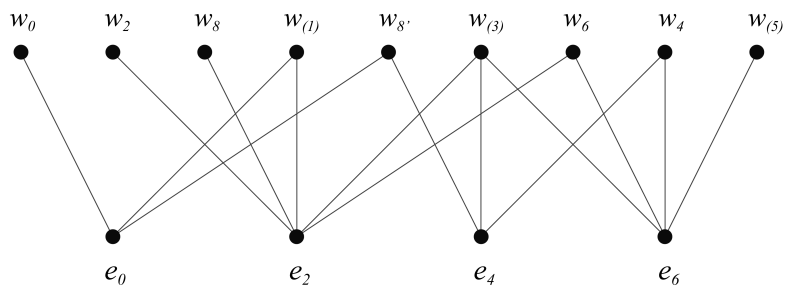


Figure 109. The (dual) principal graph of GHJ($E_6, * = e_3$).

The adjacency matrix of the principal graph					The adjacency matrix of the dual principal graph				
	e_0	e_2	e_4	e_6		e_0	e_2	e_4	e_6
a_0	1	0	0	0	w_0	1	0	0	0
a_2	0	1	0	0	w_2	0	1	0	0
a_4	0	0	1	1	w_8	0	1	0	0
a_6	0	1	0	1	$w_{(1)}$	1	1	0	0
a_8	1	1	1	0	$w_{8'}$	1	0	1	0
a_{10}	0	1	0	1	$w_{(3)}$	0	1	1	1
a_{12}	0	0	1	1	w_6	0	1	0	1
a_{14}	0	1	0	0	w_4	0	0	1	1
a_{16}	1	0	0	0	$w_{(5)}$	0	0	0	1



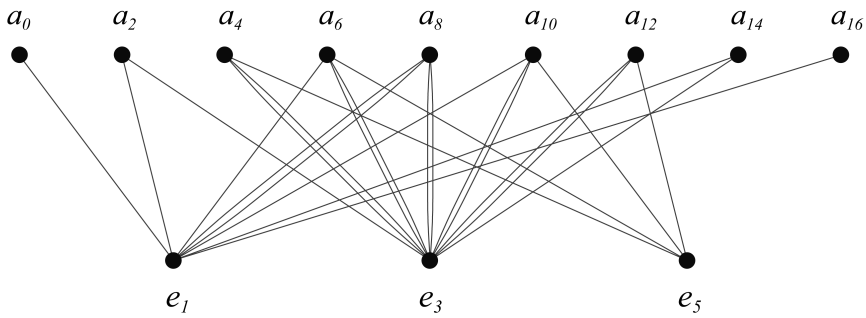
The principal graph of GHJ ($E_7, * = e_0$)



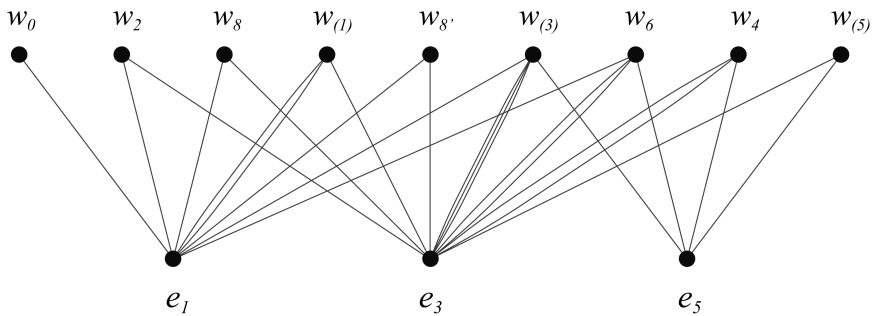
The dual principal graph of GHJ ($E_7, * = e_0$)

Figure 110. The (dual) principal graph of GHJ($E_7, * = e_0$).

	e_1	e_3	e_5		e_1	e_3	e_5			
The adjacency matrix of the principal graph	a_0	1	0	0	The adjacency matrix of the dual principal graph	w_0	1	0	0	
	a_2	1	1	0		w_2	1	1	0	0
	a_4	0	2	1		w_8	1	1	0	0
	a_6	1	2	1		$w_{(1)}$	2	1	0	0
	a_8	2	2	0		$w_{8'}$	1	1	0	0
	a_{10}	1	2	1		$w_{(3)}$	1	3	1	1
	a_{12}	0	2	1		w_6	1	2	1	1
	a_{14}	1	1	0		w_4	0	2	1	1
a_{16}	1	0	0	$w_{(5)}$	0	1	1	1		



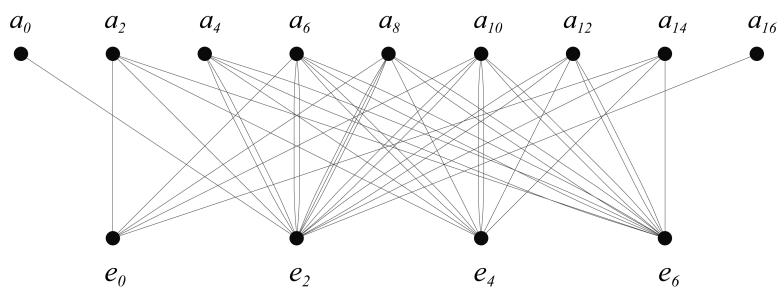
The principal graph of GHJ ($E_7, * = e_1$)



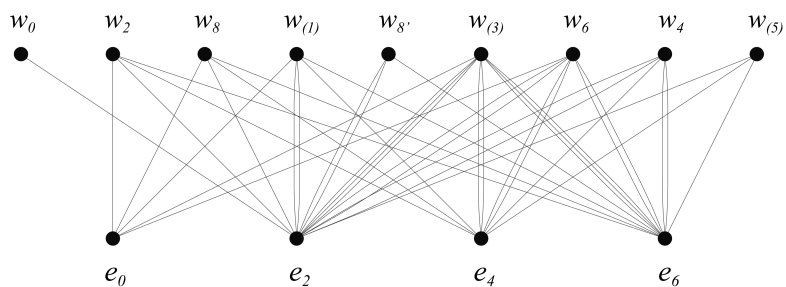
The dual principal graph of GHJ ($E_7, * = e_1$)

Figure 111. The (dual) principal graph of the GHJ subfactor corresponding to $(E_7, * = e_1)$.

	e_0	e_2	e_4	e_6		e_0	e_2	e_4	e_6	
The adjacency matrix of the principal graph	a_0	0	1	0	0	w_0	0	1	0	0
	a_2	1	1	1	1	w_2	1	1	1	1
	a_4	0	2	1	2	w_8	1	1	1	1
	a_6	1	2	2	2	$w_{(1)}$	1	2	1	1
	a_8	1	3	1	2	$w_{8'}$	0	2	0	1
	a_{10}	1	2	2	2	$w_{(3)}$	1	3	2	3
	a_{12}	0	2	1	2	w_6	1	2	2	2
	a_{14}	1	1	1	1	w_4	0	2	1	2
	a_{16}	0	1	0	0	$w_{(5)}$	0	1	1	1



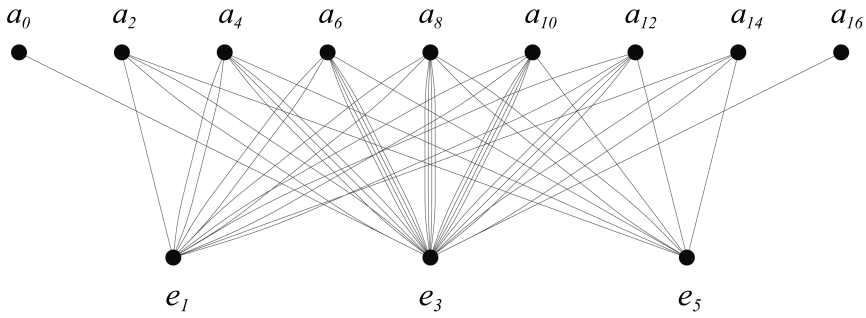
The principal graph of GHJ ($E_7, * = e_2$)



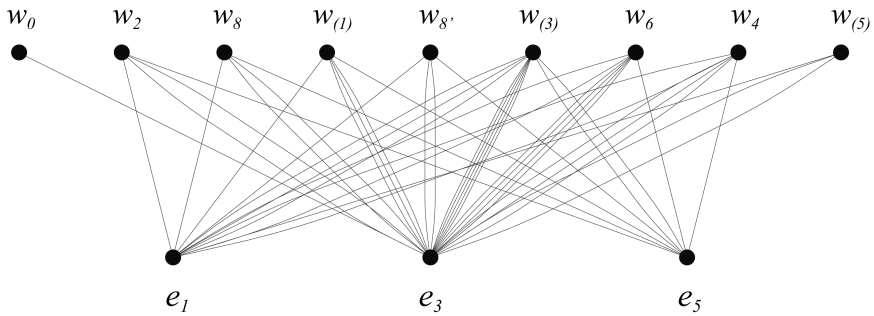
The dual principal graph of GHJ ($E_7, * = e_2$)

Figure 112. The (dual) principal graph of the GHJ subfactor corresponding to $(E_7, * = e_2)$.

		e_1	e_3	e_5			e_1	e_3	e_5
The adjacency matrix of the principal graph	a_0	0	1	0	The adjacency matrix of the dual principal graph	w_0	0	1	0
	a_2	1	2	1		w_2	1	2	1
	a_4	2	3	1		w_8	1	2	1
	a_6	2	4	1		$w_{(1)}$	1	3	1
	a_8	2	4	2		$w_{8'}$	1	2	1
	a_{10}	2	4	1		$w_{(3)}$	3	5	2
	a_{12}	2	3	1		w_6	2	4	1
	a_{14}	1	2	1		w_4	2	3	1
	a_{16}	0	1	0		$w_{(5)}$	1	2	0



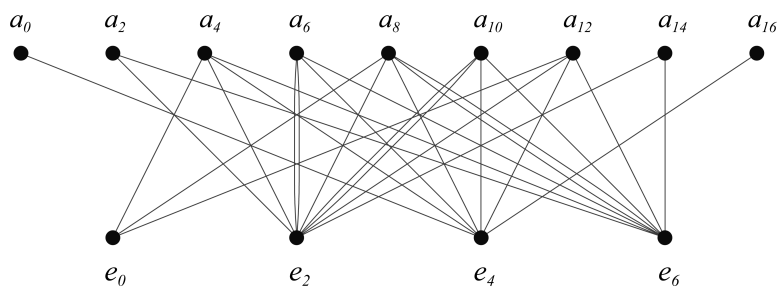
The principal graph of GHJ ($E_7, * = e_3$)



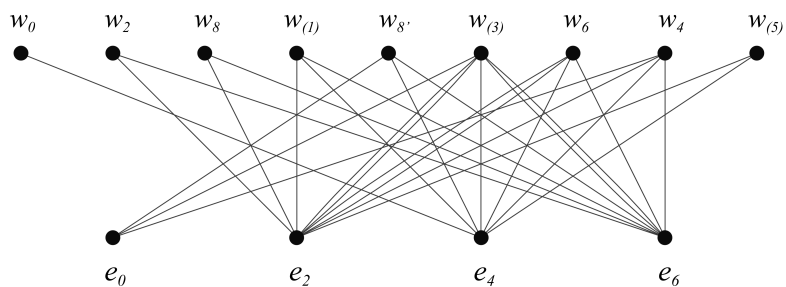
The dual principal graph of GHJ ($E_7, * = e_3$)

Figure 113. The (dual) principal graph of the GHJ subfactor corresponding to $(E_7, * = e_3)$.

	e_0	e_2	e_4	e_6		e_0	e_2	e_4	e_6		
The adjacency matrix of the principal graph	a_0	0	0	1	0	The adjacency matrix of the dual principal graph	w_0	0	0	1	0
	a_2	0	1	0	1		w_2	0	1	0	1
	a_4	1	1	1	1		w_8	0	1	0	1
	a_6	0	2	1	1		$w_{(1)}$	0	1	1	1
	a_8	1	1	1	2		$w_{8'}$	1	0	1	1
	a_{10}	0	2	1	1		$w_{(3)}$	1	2	1	2
	a_{12}	1	1	1	1		w_6	0	2	1	1
	a_{14}	0	1	0	1		w_4	1	1	1	1
	a_{16}	0	0	1	0		$w_{(5)}$	0	1	1	0



The principal graph of GHJ ($E_7, * = e_4$)



The dual principal graph of GHJ ($E_7, * = e_4$)

Figure 114. The (dual) principal graph of the GHJ subfactor corresponding to $(E_7, * = e_4)$.

		e_1	e_3	e_5			e_1	e_3	e_5
The adjacency matrix of the principal graph	a_0	0	0	1	The adjacency matrix of the dual principal graph	w_0	0	0	1
	a_2	0	1	0		w_2	0	1	0
	a_4	1	1	0		w_8	0	1	0
	a_6	1	1	1		$w_{(1)}$	0	1	1
	a_8	0	2	0		$w_{8'}$	0	1	0
	a_{10}	1	1	1		$w_{(3)}$	1	2	0
	a_{12}	1	1	0		w_6	1	1	1
	a_{14}	0	1	0		w_4	1	1	0
a_{16}	0	0	1	$w_{(5)}$	1	0	1		

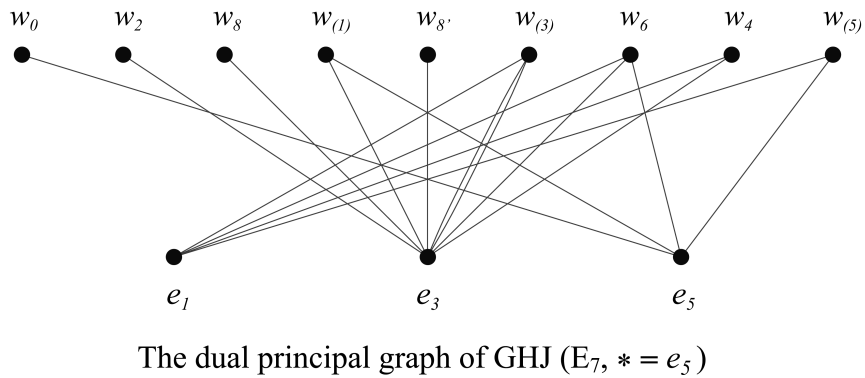
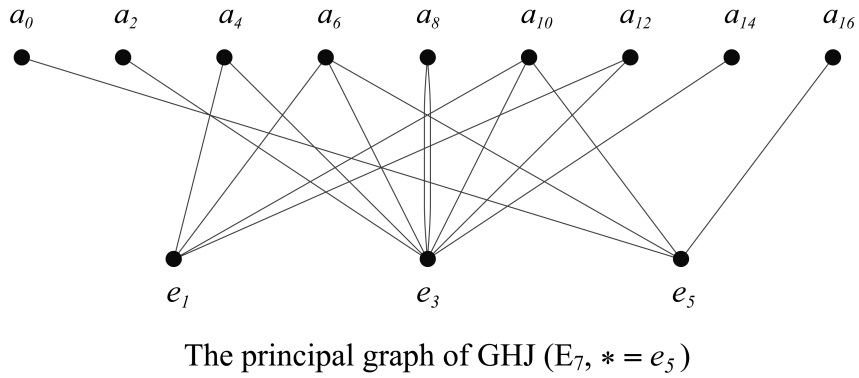
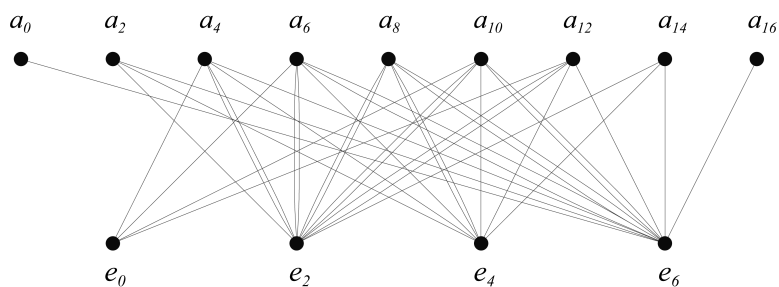
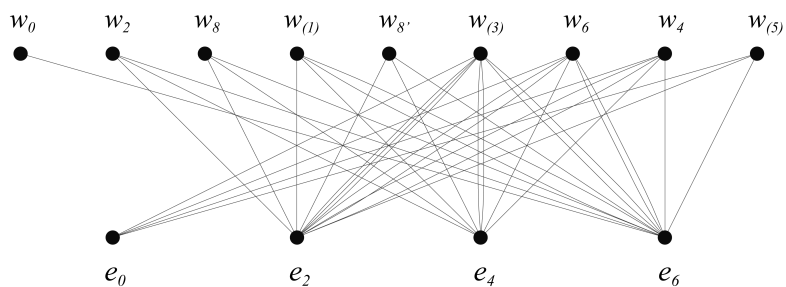


Figure 115. The (dual) principal graph of the GHJ subfactor corresponding to $(E_7, * = e_5)$.

	e_0	e_2	e_4	e_6		e_0	e_2	e_4	e_6		
The adjacency matrix of the principal graph	a_0	0	0	0	1	The adjacency matrix of the dual principal graph	w_0	0	0	0	1
	a_2	0	1	1	1		w_2	0	1	1	1
	a_4	1	2	1	1		w_8	0	1	1	1
	a_6	1	2	1	2		$w_{(1)}$	0	1	1	2
	a_8	0	2	2	2		$w_{8'}$	0	1	1	1
	a_{10}	1	2	1	2		$w_{(3)}$	1	3	2	2
	a_{12}	1	2	1	1		w_6	1	2	1	2
	a_{14}	0	1	1	1		w_4	1	2	1	1
	a_{16}	0	0	0	1		$w_{(5)}$	1	1	0	1



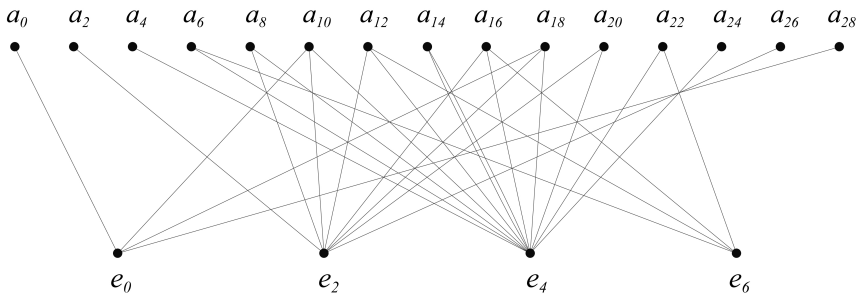
The principal graph of GHJ ($E_7, * = e_6$)



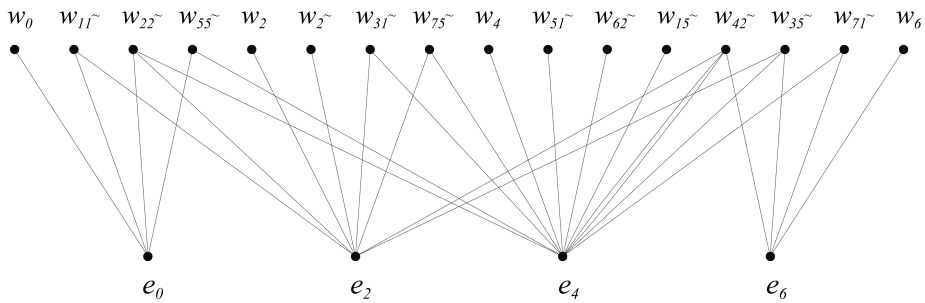
The dual principal graph of GHJ ($E_7, * = e_6$)

Figure 116. The (dual) principal graph of the GHJ subfactor corresponding to $(E_7, * = e_6)$.

		e_0	e_2	e_4	e_6			e_0	e_2	e_4	e_6
The adjacency matrix of the principal graph	a_0	1	0	0	0	The adjacency matrix of the dual principal graph	w_0	1	0	0	0
	a_2	0	1	0	0		w_{11}^{\sim}	1	1	0	0
	a_4	0	0	1	0		w_{22}^{\sim}	1	1	1	0
	a_6	0	0	1	1		w_{55}^{\sim}	1	0	1	0
	a_8	0	1	1	0		w_2	0	1	0	0
	a_{10}	1	1	1	0		w_2^{\sim}	0	1	0	0
	a_{12}	0	1	1	1		w_{31}^{\sim}	0	1	1	0
	a_{14}	0	0	2	0		w_{75}^{\sim}	0	1	1	0
	a_{16}	0	1	1	1		w_4	0	0	1	0
	a_{18}	1	1	1	0		w_{51}^{\sim}	0	0	1	0
	a_{20}	0	1	1	0		w_{62}^{\sim}	0	0	1	0
	a_{22}	0	0	1	1		w_{15}^{\sim}	0	0	1	0
	a_{24}	0	0	1	0		w_{42}^{\sim}	0	1	2	1
	a_{26}	0	1	0	0		w_{35}^{\sim}	0	1	1	1
a_{28}	1	0	0	0	w_{71}^{\sim}	0	0	1	1		
						w_6	0	0	0	1	



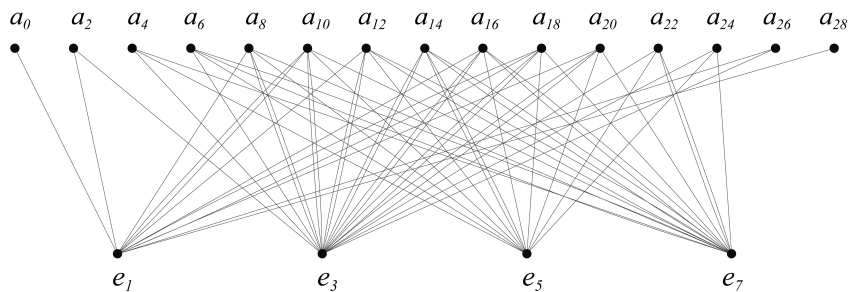
The principal graph of GHJ ($E_8, * = e_0$)



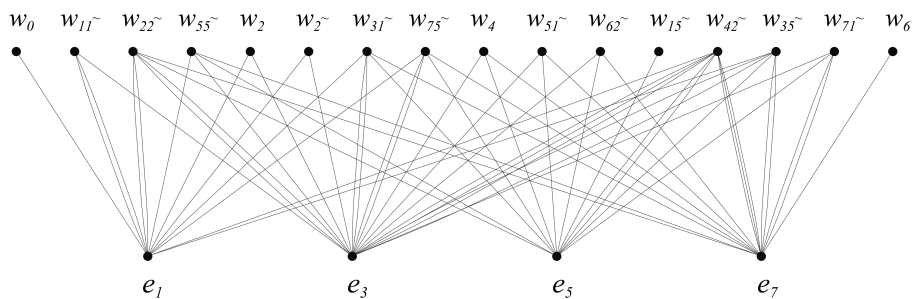
The dual principal graph of GHJ ($E_8, * = e_0$)

Figure 117. The (dual) principal graph of the GHJ subfactor corresponding to $(E_8, * = e_0)$.

The adjacency matrix of the principal graph					The adjacency matrix of the dual principal graph				
	e_1	e_3	e_5	e_7		e_1	e_3	e_5	e_7
a_0	1	0	0	0	w_0	1	0	0	0
a_2	1	1	0	0	$w_{11\sim}$	2	1	0	0
a_4	0	1	1	1	$w_{22\sim}$	2	2	1	1
a_6	0	1	1	2	$w_{35\sim}$	1	1	1	1
a_8	1	2	1	1	w_2	1	1	0	0
a_{10}	2	2	1	1	$w_{2\sim}$	1	1	0	0
a_{12}	1	2	1	2	$w_{31\sim}$	1	2	1	1
a_{14}	0	2	2	2	$w_{75\sim}$	1	2	1	1
a_{16}	1	2	1	2	w_4	0	1	1	1
a_{18}	2	2	1	1	$w_{51\sim}$	0	1	1	1
a_{20}	1	2	1	1	$w_{62\sim}$	0	1	1	1
a_{22}	0	1	1	2	$w_{15\sim}$	0	0	1	0
a_{24}	0	1	1	1	$w_{42\sim}$	1	3	2	3
a_{26}	1	1	0	0	$w_{35\sim}$	1	2	1	2
a_{28}	1	0	0	0	$w_{71\sim}$	0	1	1	2
					w_6	0	0	0	1



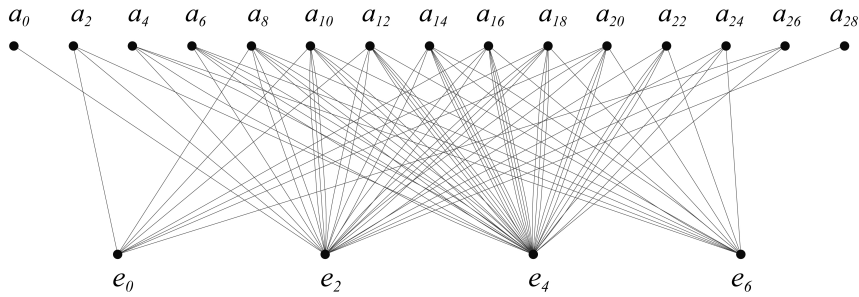
The principal graph of GHJ ($E_8, * = e_1$)



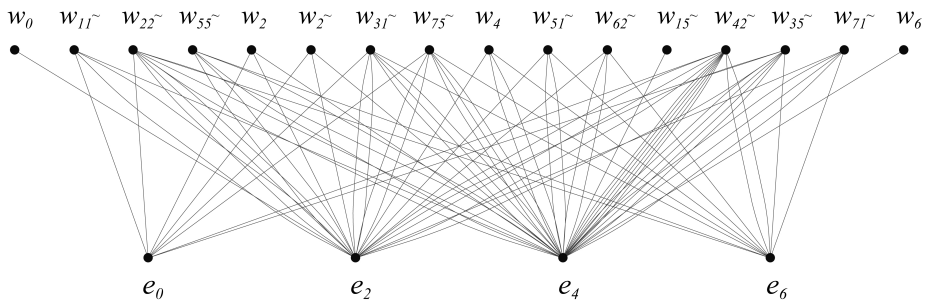
The dual principal graph of GHJ ($E_8, * = e_1$)

Figure 118. The (dual) principal graph of the GHJ subfactor corresponding to $(E_8, * = e_1)$.

		e_0	e_2	e_4	e_6			e_0	e_2	e_4	e_6
The adjacency matrix of the principal graph	a_0	0	1	0	0	The adjacency matrix of the dual principal graph	w_0	0	1	0	0
	a_2	1	1	1	0		w_{11}^{\sim}	1	2	1	0
	a_4	0	1	2	1		w_{22}^{\sim}	1	3	3	1
	a_6	0	1	3	1		w_{55}^{\sim}	0	2	2	1
	a_8	1	2	3	1		w_2	1	1	1	0
	a_{10}	1	3	3	1		w_2^{\sim}	1	1	1	0
	a_{12}	1	2	4	1		w_{31}^{\sim}	1	2	3	1
	a_{14}	0	2	4	2		w_{75}^{\sim}	1	2	3	1
	a_{16}	1	2	4	1		w_4	0	1	2	1
	a_{18}	1	3	3	1		w_{51}^{\sim}	0	1	2	1
	a_{20}	1	2	3	1		w_{62}^{\sim}	0	1	2	1
	a_{22}	0	1	3	1		w_{15}^{\sim}	0	0	1	0
	a_{24}	0	1	2	1		w_{42}^{\sim}	1	3	6	2
	a_{26}	1	1	1	0		w_{35}^{\sim}	1	2	4	1
a_{28}	0	1	0	0	w_{71}^{\sim}	0	1	3	1		
						w_6	0	0	1	0	



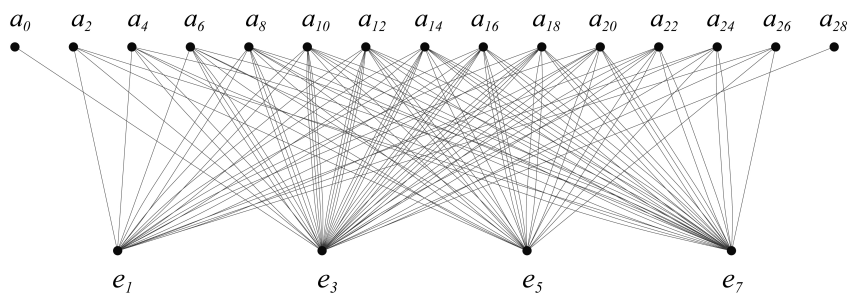
The principal graph of GHJ ($E_8, * = e_2$)



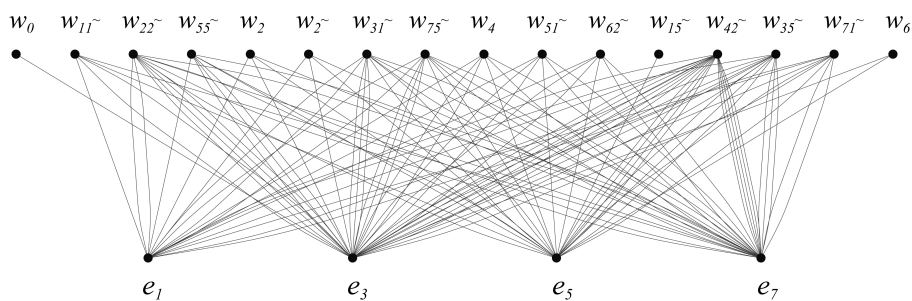
The dual principal graph of GHJ ($E_8, * = e_2$)

Figure 119. The (dual) principal graph of the GHJ subfactor corresponding to $(E_8, * = e_2)$.

The adjacency matrix of the principal graph					The adjacency matrix of the dual principal graph				
	e_1	e_3	e_5	e_7		e_1	e_3	e_5	e_7
a_0	0	1	0	0	w_0	0	1	0	0
a_2	1	1	1	1	w_{11}^-	1	2	1	1
a_4	1	2	1	2	w_{22}^-	2	4	2	3
a_6	1	3	2	2	w_{35}^-	1	3	1	2
a_8	2	3	2	3	w_2	1	1	1	1
a_{10}	2	4	2	3	w_2^-	1	1	1	1
a_{12}	2	4	3	3	w_{31}^-	2	3	2	3
a_{14}	2	4	2	4	w_{75}^-	2	3	2	3
a_{16}	2	4	3	3	w_4	1	2	1	2
a_{18}	2	4	2	3	w_{51}^-	1	2	1	2
a_{20}	2	3	2	3	w_{62}^-	1	2	1	2
a_{22}	1	3	2	2	w_{15}^-	0	0	1	0
a_{24}	1	2	1	2	w_{42}^-	3	6	4	5
a_{26}	1	1	1	1	w_{35}^-	2	4	3	3
a_{28}	0	1	0	0	w_{71}^-	1	3	2	2
					w_6	0	1	1	0



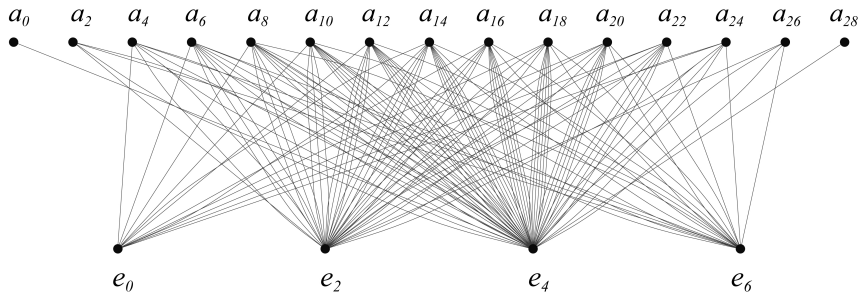
The principal graph of GHJ ($E_8, * = e_3$)



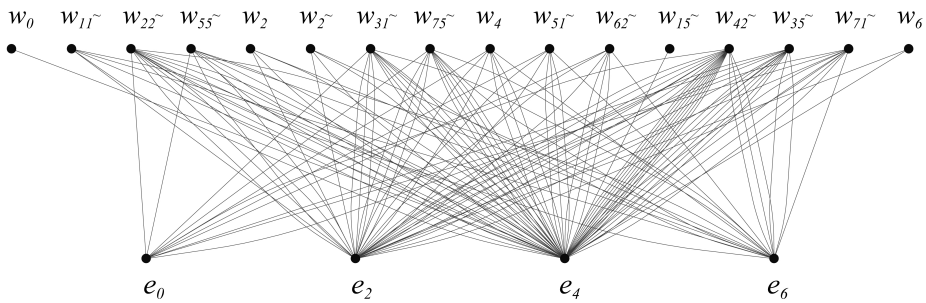
The dual principal graph of GHJ ($E_8, * = e_3$)

Figure 120. The (dual) principal graph of the GHJ subfactor corresponding to $(E_8, * = e_3)$.

The adjacency matrix of the principal graph					The adjacency matrix of the dual principal graph				
	e_0	e_2	e_4	e_6		e_0	e_2	e_4	e_6
a_0	0	0	1	0	w_0	0	0	1	0
a_2	0	1	2	1	w_{11}^{\sim}	0	1	3	1
a_4	1	2	3	1	w_{22}^{\sim}	1	3	6	2
a_6	1	3	4	1	w_{55}^{\sim}	1	2	4	1
a_8	1	3	5	2	w_2	0	1	2	1
a_{10}	1	3	6	2	w_2^{\sim}	0	1	2	1
a_{12}	1	4	6	2	w_{31}^{\sim}	1	3	5	2
a_{14}	2	4	6	2	w_{75}^{\sim}	1	3	5	2
a_{16}	1	4	6	2	w_4	1	2	3	1
a_{18}	1	3	6	2	w_{51}^{\sim}	1	2	3	1
a_{20}	1	3	5	2	w_{62}^{\sim}	1	2	3	1
a_{22}	1	3	4	1	w_{15}^{\sim}	0	0	1	0
a_{24}	1	2	3	1	w_{42}^{\sim}	2	6	9	3
a_{26}	0	1	2	1	w_{35}^{\sim}	1	4	6	2
a_{28}	0	0	1	0	w_{71}^{\sim}	1	3	4	1
					w_6	0	1	1	0



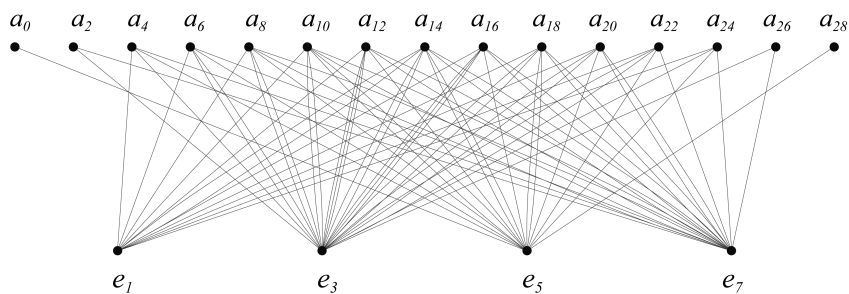
The principal graph of GHJ ($E_8, * = e_4$)



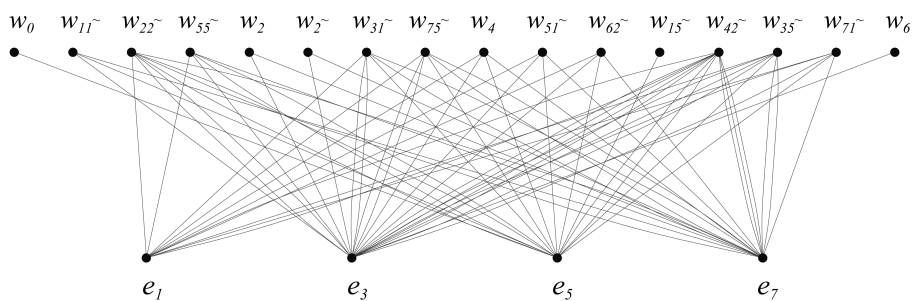
The dual principal graph of GHJ ($E_8, * = e_4$)

Figure 121. The (dual) principal graph of the GHJ subfactor corresponding to $(E_8, * = e_4)$.

The adjacency matrix of the principal graph					The adjacency matrix of the dual principal graph				
	e_1	e_3	e_5	e_7		e_1	e_3	e_5	e_7
a_0	0	0	1	0	w_0	0	0	1	0
a_2	0	1	0	1	w_{11}^-	0	1	1	1
a_4	1	1	1	1	w_{22}^-	1	2	2	2
a_6	1	2	1	1	w_{35}^-	1	1	2	1
a_8	1	2	1	2	w_2	0	1	0	1
a_{10}	1	2	2	2	w_2^-	0	1	0	1
a_{12}	1	3	1	2	w_{31}^-	1	2	1	2
a_{14}	2	2	2	2	w_{75}^-	1	2	1	2
a_{16}	1	3	1	2	w_4	1	1	1	1
a_{18}	1	2	2	2	w_{51}^-	1	1	1	1
a_{20}	1	2	1	2	w_{62}^-	1	1	1	1
a_{22}	1	2	1	1	w_{15}^-	0	0	1	0
a_{24}	1	1	1	1	w_{42}^-	2	4	2	3
a_{26}	0	1	0	1	w_{35}^-	1	3	1	2
a_{28}	0	0	1	0	w_{71}^-	1	2	1	1
					w_6	0	1	0	0



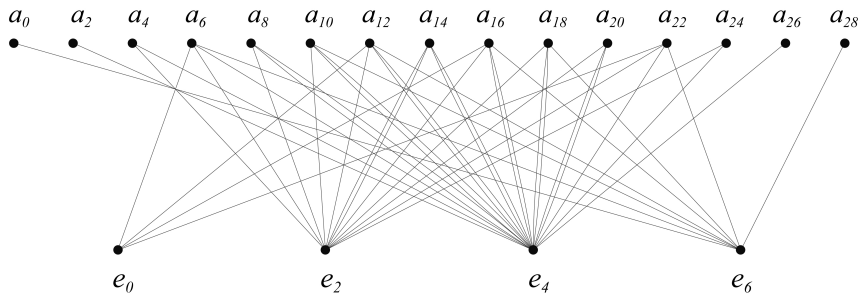
The principal graph of GHJ ($E_8, * = e_5$)



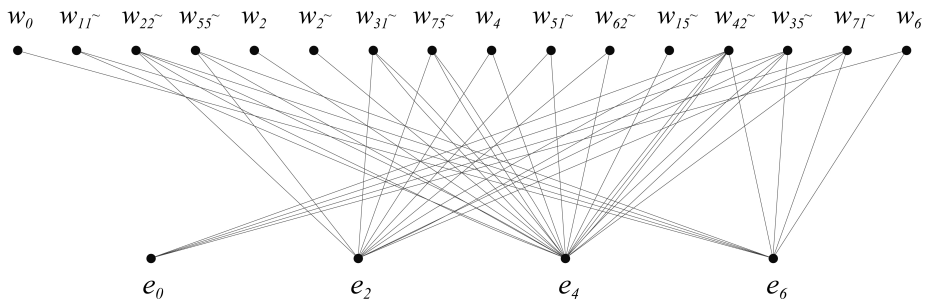
The dual principal graph of GHJ ($E_8, * = e_5$)

Figure 122. The (dual) principal graph of the GHJ subfactor corresponding to $(E_8, * = e_5)$.

	e_0	e_2	e_4	e_6		e_0	e_2	e_4	e_6		
The adjacency matrix of the principal graph	a_0	0	0	0	1	The adjacency matrix of the dual principal graph	w_0	0	0	0	1
	a_2	0	0	1	0		$w_{11\sim}$	0	0	1	1
	a_4	0	1	1	0		$w_{22\sim}$	0	1	2	1
	a_6	1	1	1	1		$w_{55\sim}$	0	1	1	1
	a_8	0	1	2	0		w_2	0	0	1	0
	a_{10}	0	1	2	1		$w_{2\sim}$	0	0	1	0
	a_{12}	1	1	2	1		$w_{31\sim}$	0	1	2	0
	a_{14}	0	2	2	0		$w_{75\sim}$	0	1	2	0
	a_{16}	1	1	2	1		w_4	0	1	1	0
	a_{18}	0	1	2	1		$w_{51\sim}$	0	1	1	0
	a_{20}	0	1	2	0		$w_{62\sim}$	0	1	1	0
	a_{22}	1	1	1	1		$w_{15\sim}$	0	0	1	0
	a_{24}	0	1	1	0		$w_{42\sim}$	1	2	3	1
	a_{26}	0	0	1	0		$w_{35\sim}$	1	1	2	1
a_{28}	0	0	0	1	$w_{71\sim}$	1	1	1	1		
					w_6	1	0	0	1		



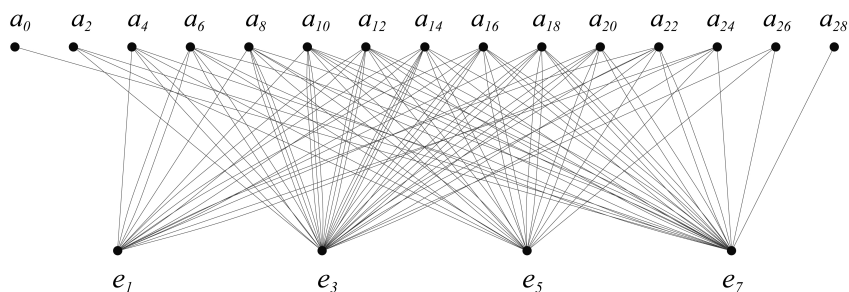
The principal graph of GHJ ($E_8, * = e_6$)



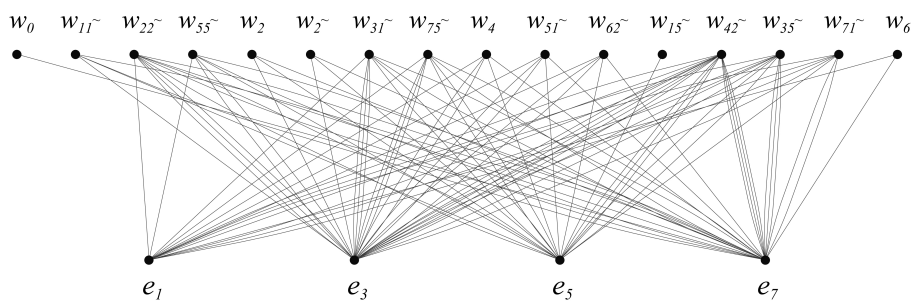
The dual principal graph of GHJ ($E_8, * = e_6$)

Figure 123. The (dual) principal graph of the GHJ subfactor corresponding to $(E_8, * = e_6)$.

The adjacency matrix of the principal graph					The adjacency matrix of the dual principal graph				
	e_1	e_3	e_5	e_7		e_1	e_3	e_5	e_7
a_0	0	0	0	1	w_0	0	0	0	1
a_2	0	1	1	1	w_{11}^-	0	1	1	2
a_4	1	2	1	1	w_{22}^-	1	3	2	3
a_6	2	2	1	2	w_{35}^-	1	2	1	2
a_8	1	3	2	2	w_2	0	1	1	1
a_{10}	1	3	2	3	w_2^-	0	1	1	1
a_{12}	2	3	2	3	w_{31}^-	1	3	2	2
a_{14}	2	4	2	2	w_{75}^-	1	3	2	2
a_{16}	2	3	2	3	w_4	1	2	1	1
a_{18}	1	3	2	3	w_{51}^-	1	2	1	1
a_{20}	1	3	2	2	w_{62}^-	1	2	1	1
a_{22}	2	2	1	2	w_{15}^-	0	0	1	0
a_{24}	1	2	1	1	w_{42}^-	3	5	3	4
a_{26}	0	1	1	1	w_{35}^-	2	3	2	3
a_{28}	0	0	0	1	w_{71}^-	2	2	1	2
					w_6	1	0	0	1



The principal graph of GHJ ($E_8, * = e_7$)



The dual principal graph of GHJ ($E_8, * = e_7$)

Figure 124. The (dual) principal graph of the GHJ subfactor corresponding to $(E_8, * = e_7)$.

References

- [1] Asaeda, M. and U. Haagerup, Exotic subfactors of finite depth with Jones indices $(5 + \sqrt{13})/2$ and $(5 + \sqrt{17})/2$, *Comm. Math. Phys.* **202** (1999), 1–63.
- [2] Bion-Nadal, J., Subfactor of the hyperfinite II_1 factor with Coxeter graph E_6 as invariant, *J. Operator Theory* **28** (1992), 27–50.
- [3] Bisch, D., Principal graphs of subfactors with small Jones index, *Math. Ann.* **311** (1998), 223–231.
- [4] Bisch, D., On the existence of central sequences in subfactors, *Trans. Amer. Math. Soc.* **321** (1990), 117–128.
- [5] Böckenhauer, J. and D. E. Evans, Modular Invariants, Graphs and α -Induction for Nets of Subfactors I, *Comm. Math. Phys.* **197** (1998), 361–386.
- [6] Böckenhauer, J. and D. E. Evans, Modular Invariants, Graphs and α -Induction for Nets of Subfactors II, *Comm. Math. Phys.* **200** (1999), 57–103.
- [7] Böckenhauer, J. and D. E. Evans, Modular Invariants, Graphs and α -Induction for Nets of Subfactors III, *Comm. Math. Phys.* **205** (1999), 183–228.
- [8] Böckenhauer, J., Evans, D. E. and Y. Kawahigashi, *Chiral structure of modular invariants for subfactors*, *Comm. Math. Phys.* **210** (2000), 733–784.
- [9] Evans, D. E. and Y. Kawahigashi, *Quantum symmetries on operator algebras*, Oxford University Press, Oxford, 1998.
- [10] Cappelli, A., Itzykson C. and J.-B. Zuber, The A - D - E classification of minimal and $A_1^{(1)}$ conformal invariant theories, *Comm. Math. Phys.* **113** (1987), 1–26.
- [11] Goodman, F., de la Harpe, P. and V. F. R. Jones, *Coxeter graphs and towers of algebras*, MSRI Publications, 14, Springer, Berlin, 1989.
- [12] Goto, S., On Ocneanu’s theory of double triangle algebras for subfactors and classification of irreducible connections on the Dynkin diagrams, *Expos. Math.* **28** (2010), 218–253.
- [13] Izumi, M., Application of fusion rules to classification of subfactors, *Publ. Res. Inst. Math. Sci.* **27** (1991), 953–994.
- [14] Izumi, M., On flatness of the Coxeter graph E_8 , *Pacific J. Math.* **166** (1994), 305–327.
- [15] Jones, V. F. R., Index for subfactors, *Invent. Math.* **72** (1983), 1–15.
- [16] Kawahigashi, Y., On flatness of Ocneanu’s connections on the Dynkin diagrams and classification of subfactors, *J. Funct. Anal.* **127** (1995), 63–107.
- [17] Kawahigashi, Y., Classification of paragroup actions on subfactors, *Publ. Res. Inst. Math. Sci.* **31** (1995), 481–517.
- [18] Ocneanu, A., Quantized group string algebras and Galois theory for algebras, in “Operator algebras and applications, Vol. 2 (Warwick, 1987),” London

- Math. Soc. Lect. Note Series Vol. 136, Cambridge University Press, (1988), 119–172.
- [19] Ocneanu, A., Paths on Coxeter diagrams: from Platonic solids and singularities to minimal models and subfactors, (Notes recorded by S. Goto), in *Lectures on operator theory*, (ed. B. V. Rajarama Bhat *et al.*), The Fields Institute Monographs, Providence, Rhode Island: AMS Publications. (2000), 243–323.
- [20] Okamoto, S., Invariants for subfactors arising from Coxeter graphs, *Current Topics in Operator Algebras*, World Scientific Publishing, (1991), 84–103.
- [21] Sunder, V. S. and A. K. Vijayarajan, On the non-occurrence of the Coxeter graphs β_{2n+1} , E_7 , D_{2n+1} as principal graphs of an inclusion of II_1 factors, *Pacific J. Math.* **161** (1993), 185–200.
- [22] Xu, F., New braided endomorphisms from conformal inclusions, *Comm. Math. Phys.* **192** (1998), 349–403.

(Received March 4, 2009)

(Revised November 2, 2012)

Department of Information and
Communication Sciences
Sophia University
Kioicho, Chiyoda-ku
Tokyo 102-8554, Japan
E-mail: s-goto@sophia.ac.jp